

AUTOMATED NON-INVASIVE BLOOD PRESSURE MONITORING UNDER STRESS CONDITIONS

GRADUATION REPORT

By

MAX WESSELS

19/6/2016



Submitted to Hanze University of Applied Science Groningen

In partial fulfilment of the requirements of fulltime Honours Bachelor Advanced Sensor Applications

AUTOMATED NON-INVASIVE BLOOD PRESSURE MONITORING UNDER STRESS CONDITIONS

By

MAX WESSELS

19/6/2016

ABSTRACT

This report presents an innovative method for non-invasively measuring blood pressure under stress conditions. Using advanced signal processing, the adaptive Korotkoff sound detection algorithm was validated to be able to function in noisy conditions. Furthermore, the digital filter was measured to reduce the spread of noise by 65% compared to 27% in signal of interest. Results show promising agreement with theoretical predictions formulated during literature research. The work presented here has profound implications for future studies of cardiovascular research and may one day be helpful in reducing the global cardiovascular disease incidence [1].

DECLARATION

I hereby certify that this report constitutes my own product, that where the language of others is set forth, quotation marks so indicate, and that appropriate credit is given where I have used the language, ideas, expressions or writings of another.

I declare that the report describes original work that has not previously been presented for the award of any other degree of any institution.

Signed,

Max Wessels

A handwritten signature in blue ink that reads "Max Wessels". The signature is written in a cursive style with a large, looping initial "M" and a long horizontal stroke extending to the right.

PREFACE

This report describes the results of a five month graduation period at Lode B.V. Furthermore, it is the completion of the HBO-study Advanced Sensor Application. This graduation project interests me because of its biomedical background. With this project I have set up the fundamentals for the development of a blood pressure monitoring system capable of being used under stress conditions. This was a challenging process as there are many different aspects to the project such as literature research, applied research in the domains of electronics and signal processing as well as human anatomy, physiology and biomedical engineering.

I would like to express my sincere gratitude to all people involved in this project. Jan Reinder Fransens was my company supervisor at Lode B.V. He was an excellent coach and helped me with time management, resources and integration into Lode B.V. Secondly, I would like to thank Jan Zijlstra, my first assessor. His knowledge on biomedical engineering helped me think critically. Thirdly, I would like to thank Bryan Williams for helping me orientate on the topic of digital filtering at the start of this project. Furthermore, I would like to thank Ronald de Wild for taking the time to discuss signal processing topics not included in my studies curriculum. Finally, I would like to show my gratitude to all colleagues at the Lode B.V. R&D department for all their support and sociability.

SUMMARY

Although automatic blood pressure monitors have been commercially available for over 20 years, measuring under stress conditions is still a challenge [2]. Noisy signals, population variations and homeostatic mechanisms maintaining blood pressure are some of factors causing difficulty. Lode B.V. assigned me to develop a non-invasive blood pressure monitor capable of measuring under stress conditions. The blood pressure monitor should be capable of functioning under stress conditions with medical grade accuracy. The central research question in this project is formulated as follows:

“How can blood pressure be monitored automatically whilst the patient is under stress conditions on a bicycle ergometer using non-invasive techniques?”

Based on literature research the auscultatory method was selected as a basis for the to be developed blood pressure monitor. The auscultatory method utilizes as pressurized cuff in combination with a piezo microphone to detect the presence of K-sounds. These K-sounds are vibrations caused by turbulent blood flow and occur when the pressurized cuff its pressure is between systolic and diastolic blood pressure. Start and end time of the K-sounds in combination with the cuff pressure can be used to obtain blood pressure.

To obtain measured signals a data acquisition system was developed. Existing hardware was used to inflate and deflate the cuff. Signals were obtained during rest and increasing stress conditions. Using time-frequency analysis tools like the Fast Fourier Transform and the Wavelet transform the obtained signals were analysed.

An experimental procedure was formulated to quantify the performance of digital filters. By shifting cut-off frequencies of filters and using the experimental procedure to quantify the performance, optimal cut-off frequencies were obtained. The resulting band-pass filter was measured to reduce the spread of noise by 65% compared to 27% in signal of interest. To determine the start and end time of the K-sounds an algorithm was developed. The algorithm utilizes peak detection to identify K-sounds and a periodicity check to filter out false positive detections.

Suggestions for future work include: the creation of a database of K-sound with as many population groups as possible, the implementation of the K-sound detection algorithm into an embedded environment and the development of an automatically adjusting programmable gain.

The work presented here is a solid first step towards the development of a non-invasive BP monitoring system for usage under stress conditions. The most challenging topics have been addressed. Literature research provided a clear outcome: the auscultatory method was the most viable method. The applied research conducted was extensive, providing insight into the complexity of the task. An effective digital filter was realized via time-frequency analysis of measured signals. Furthermore, the basis of a robust peak detection algorithm is ready for testing on a larger dataset.

TABLE OF CONTENTS

TABLE OF CONTENTS.....	6
LIST OF FIGURES	8
LIST OF TABLES.....	11
ABBREVIATIONS	12
DEFINITIONS.....	12
1 RATIONALE.....	13
2 SITUATIONAL ANALYSIS	14
2.1 Strengths	14
2.2 Weaknesses.....	14
2.3 Opportunities.....	15
2.4 Threats.....	15
3 THEORETICAL ANALYSIS	16
3.1 Blood pressure	16
3.2 Disturbed homeostasis	17
3.3 Manual blood pressure monitors.....	17
3.4 Stress testing	21
3.5 Medical device directive	22
4 RESEARCH DESIGN	23
4.1 Research question	23
4.2 Success factors	24
4.3 Requirements	25
5 LITERATURE RESEARCH	26
5.1 Automated blood pressure monitors	26
5.2 Conclusion	31
6 CONCEPTUAL MODEL.....	32
7 APPLIED RESEARCH	33
7.1 System as a whole.....	33
7.2 Signal acquisition.....	34
7.3 Filter cut-off frequencies.....	37
7.4 Band-pass filter design with optimal passband.....	41
7.5 Final filter design	42
7.6 Korotkoff detection algorithm	43
8 CONCLUSIONS.....	48
8.1 Sub-questions answered.....	48

8.2	Research question answered	49
8.3	Developed system	49
8.4	Success factors	50
8.5	Meeting the requirements.....	50
8.6	Final conclusion	50
9	DISCUSSION	51
9.1	Literature & Applied research.....	51
9.2	Method of collecting data	51
9.3	Calibration of peak detection parameters.....	52
9.4	Digital filter.....	52
10	FUTURE RECOMMENDATIONS	53
10.1	Improvements	53
10.2	Proceedings	55
10.3	Final product design.....	56
10.4	Requirements	57
	BIBLIOGRAPHY	58
	APPENDIX A: BLOOD VESSELS AND PRESSURE REGULATION	63
	APPENDIX B: COMPONENT VALIDATION	66
	APPENDIX C: KOROTKOFF SIGNALS	75
	APPENDIX D: FILTER COEFFICIENTS STANDARD DEVIATION TEST RESULTS	79
	APPENDIX E: ADC SOFTWARE FLOW CHARTS	82
	APPENDIX F: ANTI-ALIASING FILTER DESIGN.....	85
	APPENDIX G: RESULTING SIGNALS	89
	APPENDIX H: DAQ SIGNALS	99

LIST OF FIGURES

Figure 1: Systemic blood pressure variation throughout the cardiovascular system [62].....	16
Figure 2: Mercury column sphygmomanometer [66]	17
Figure 3: Auscultatory method of blood pressure measurement using a sphygmomanometer [63]	18
Figure 4: Korotkoff sounds [5]	19
Figure 5: Simplified view of pressure in cuff over time during oscillometric measurement [12]	20
Figure 6: SBP and DBP during exercise [24]	22
Figure 7: Auscultatory VS Oscillometric [38]	27
Figure 8: Possible configuration of Applanation tonometry used in the BPro [67].....	29
Figure 9: Basic principle of ultrasound Doppler imaging [70]	30
Figure 10: Flow chart demonstrating the conceptual model.....	32
Figure 11: Dataflow of the designed non-invasive BP monitoring system.....	33
Figure 12: Time series of piezo microphone during BP-measurement whilst cycling at a load of 50 Watt for test person A.....	36
Figure 13: Scaled attenuation ratio of baseline over K-sounds for various HP-filters	39
Figure 14: Scaled attenuation ratio of baseline over K-sound for various BP-filters	40
Figure 15: Band-pass filter design with optimal amplitude response	41
Figure 16: Band-pass filter design with balanced amplitude and phase response	42
Figure 17: Time series of cycling at a load of 50 Watt filtered with the high and low order band-pass filters, adjusted for phase shift	42
Figure 18: Initialize function of Korotkoff detection algorithm	44
Figure 19: Main function of Korotkoff detection algorithm	45
Figure 20: Filtered microphone signal after peak detection.....	46
Figure 21: Periodicity check via a forward and backward expanding window, over which the standard deviation is calculated and only allow to decrease	46
Figure 22: Periodicity check of Korotkoff detection algorithm.....	47
Figure 23: Possible configuration of the finalized BP monitor.....	56
Figure 24: Summary of blood vessel anatomy [64]	64
Figure 25: Baroreceptor reflexes that help maintain blood pressure homeostasis [65]	64
Figure 26: Major factors enhancing CO [54].....	65
Figure 27: Exploded view of piezo microphone developed by Lode B.V.....	67

Figure 28: Test setup impulse response piezo microphone, configuration B under	68
Figure 29: Impulse response of a piezo microphone for a drop height of 3 mm	69
Figure 30: Impulse response of a piezo microphone for a drop height of 5 mm	69
Figure 31: Impulse response of a piezo microphone for a drop height of 10 mm	69
Figure 32: Schematic instrumentation amplifier.....	70
Figure 33: Function generator on instrumentation amplifier	71
Figure 34: Function generator at different frequencies sampled with Teensy ADC	72
Figure 35: Function generator at different frequencies on anti-aliasing filter	74
Figure 36: Time series of piezo microphone during BP-measurement whilst in rest for test person A	76
Figure 37: Time series of piezo microphone during BP-measurement whilst cycling at a load of 200 Watt for test person A.....	76
Figure 38: Time series of piezo microphone during BP-measurement whilst cycling during recovery at a load of 50 Watt for test person A	76
Figure 39: Smoothed FFT on K-sounds, inversed baseline and the K-sounds–baseline during rest	77
Figure 40: Smoothed FFT on K-sounds, inversed baseline and the K-sounds–baseline whilst cycling at a load of 200 Watt.....	77
Figure 41: Smoothed FFT on K-sounds, inversed baseline and the K-sounds–baseline during recovery whilst cycling at a load of 50 Watt	77
Figure 42: Interpolated continuous wavelet transform with Morlet wavelet of K-sounds during rest .	78
Figure 43: Interpolated continuous wavelet transform with Morlet wavelet of K-sounds whilst cycling at a load 200.....	78
Figure 44: Interpolated continuous wavelet transform with Morlet wavelet of K-sounds during recovery whilst cycling at a load 50	78
Figure 45: Main function of ADC algorithm.....	83
Figure 46: timer callback function of ADC algorithm.....	84
Figure 47: Write ADC function of teensy algorithm	84
Figure 48: Check StartStop function of the ADC algorithm.....	84
Figure 49: Circuit design of 3 rd order Butterworth filter.....	86
Figure 50: Magnitude response of 3 rd order Butterworth filter	87
Figure 51: Phase delay of 3 rd order Butterworth filter	87
Figure 52: Step response of 3 rd order Butterworth filter	88
Figure 53: Unfiltered and filtered signals before and after peak detection and periodicity check, obtained whilst test person A was in rest conditions	90

Figure 54: Unfiltered and filtered signals before and after peak detection and periodicity check, obtained whilst test person B was in rest conditions	91
Figure 55: Unfiltered and filtered signals before and after peak detection and periodicity check, obtained whilst test person C was in rest conditions	92
Figure 56: Unfiltered and filtered signals before and after peak detection and periodicity check, obtained whilst test person A cycling at a load of 200 Watt	93
Figure 57: Unfiltered and filtered signals before and after peak detection and periodicity check, obtained whilst test person B was cycling at a load of 200 Watt	94
Figure 58: Unfiltered and filtered signals before and after peak detection and periodicity check, obtained whilst test person C was cycling at a load of 200 Watt	95
Figure 59: Unfiltered and filtered signals before and after peak detection and periodicity check, obtained whilst test person A was cycling at a load of 50 during recovery. Note that in the unfiltered situation only three peaks are detected, which make the periodicity check fail due to the assumption that the minimum amount of K-sounds is 9.....	96
Figure 60: Unfiltered and filtered signals before and after peak detection and periodicity check, obtained whilst test person B cycling at a load of 50 Watt during recovery	97
Figure 61: Unfiltered and filtered signals before and after peak detection and periodicity check, obtained whilst test person C was cycling at a load of 50 Watt during recovery	98
Figure 62: Time series whilst cycling at a load of 50 Watt with data skipping	100
Figure 63: Time series whilst cycling at a load of 50 Watt with high frequent noise.....	100

LIST OF TABLES

Table 1: Overview of the SWOT analysis	15
Table 2: Requirements of the to be developed non-invasive BP monitoring system	25
Table 3: Overview of comparison between methods of NIBP monitoring.....	31
Table 4: Standard deviation decrease ratios for a high order high-pass filter with different cut-off frequencies, applied to a signal obtained during rest conditions.....	38
Table 5: Average decrease percentages for signals rest, load 200 and recovery of various HP-filters	39
Table 6: Average decrease percentages for signals rest, load 200 and recovery of various HP-filters	40
Table 7: Average decrease percentages for signals rest, load200 and recovery for the low order BP-filter	43
Table 8: Requirements of the to be developed non-invasive BP monitoring system	57
Table 9: Most important characteristics of popular anti-aliasing filter designs rated according to the requirements [60].....	73
Table 10: Standard deviation decrease ratios for a high order high-pass filter with different cut-off frequencies, applied to a signal obtained during rest	80
Table 11: Standard deviation decrease ratios for a high order high-pass filter with different cut-off frequencies, applied to a signal obtained during cycling at a load of 200 Watt.....	80
Table 12: Standard deviation decrease ratios for a high order high-pass filter with different cut-off frequencies, applied to a signal obtained during recovery whilst cycling at a load of 50 Watt.....	80
Table 13: Standard deviation decrease ratios for a high order low-pass filter with different cut-off frequencies, applied to a signal obtained during rest	80
Table 14: Standard deviation decrease ratios for a high order low-pass filter with different cut-off frequencies, applied to a signal obtained during cycling at a load of 200 Watt.....	81
Table 15: Standard deviation decrease ratios for a high order low-pass filter with different cut-off frequencies, applied to a signal obtained during recovery whilst cycling at a load of 50 Watt.....	81
Table 16: Standard deviation decrease ratios for a high order band-pass filter with different cut-off frequencies, applied to a signal obtained during rest	81
Table 17: Standard deviation decrease ratios for a high order band-pass filter with different cut-off frequencies, applied to a signal obtained whilst cycling at a load of 200 Watt	81
Table 18: Standard deviation decrease ratios for a high order band-pass filter with different cut-off frequencies, applied to a signal obtained during recovery whilst cycling at a load of 50 Watt.....	81

ABBREVIATIONS

Below, a list of abbreviations is given for the convenience of the reader. Hopefully, this will allow a practical reading experience.

- **Non-invasive (NI):** without penetration of the body
- **Blood pressure (BP):** force per unit area exerted on a vessel wall by the contained blood
- **Systolic blood pressure (SBP):** systemic arterial pressure during systole
- **Diastolic blood pressure (DBP):** systemic arterial pressure during diastole
- **Mean arterial pressure (MAP):** average blood pressure over an cardiac cycle
- **Systemic arterial pressure (SAP):** arterial pressure in the systemic circulation, without reference this is usually meant with blood pressure
- **Heart rate (HR):** the speed of the beating of the heart, denoted in beats per minute (BPM)
- **Millimeters of mercury (mm Hg):** unit in which blood pressure is measured
- **Cardiac output (CO):** volume of blood pump by the heart per unit time
- **Total peripheral resistance (TPR):** resistance that must be overcome to push blood through the circulatory system to create flow, mainly caused by blood viscosity, vessel length and vessel diameter
- **Photoplethysmogram (PPG):** an optically obtained plethysmogram, a volumetric measurement of an organ
- **Peripheral capillary oxygen saturation (SpO₂):** the percentage of oxygenated haemoglobin

DEFINITIONS

A list of definitions is given below, this will aid in understanding the information presented throughout this report.

- **Systemic venous pressure:** venous pressure in the systemic circulation
- **Pulmonary pressure:** pressure in the pulmonary artery
- **Pulse pressure:** difference between systolic and diastolic pressure
- **Systole:** part of the cardiac cycle when the ventricles contract
- **Diastole:** part of the cardiac cycle when the heart refills with blood
- **Baroreceptors:** pressure sensors located in the blood vessels of all vertebrate animals
- **Vasoconstriction:** narrowing of the blood vessels resulting from contraction of the muscular wall of the vessels, in particular the large arteries and small arterioles
- **Vasodilation:** widening of blood vessels resulting from relaxation of muscular wall of vessels
- **Vagal withdraw:** withdraw of the vagal tone, in combination with activation of sympathetic nerves, causes heart rate to increase above intrinsic rate
- **Frank–Starling law:** stroke volume of the heart increases in response to an increase in the volume of blood filling the heart (the end diastolic volume) when all other factors remain constant
- **Standard atmosphere (atm):** is a unit of pressure defined as pressure at sea level
- **Gauge pressure:** pressure measured against 1 atm
- **Transducer:** a device that converts one form of energy to another, usually to convert a signal
- **Cardiovascular system:** organ system that permits blood to circulate and transport nutrients, oxygen, carbon dioxide and hormones

1

RATIONALE

Lode B.V. was founded in 1952 and started in the market of cardiology and pulmonary function. The first products of Lode B.V. were electro-magnetic cycle ergometers. Since then, Lode B.V. has become a specialist in the complete spectrum of medical ergometry. The Lode product range varies from bicycle ergometers and treadmills to recumbent, arm and supine ergometers and ergometry software.

At Lode B.V. ergometers are available for cardiac and pulmonary assessment. Ergometers can optionally be equipped with a non-invasive (NI) blood pressure (BP) monitoring system. These NIBP monitoring systems are unique due to their usability during stress conditions. NIBP monitoring systems are provided by an external manufacturer SunTech. However, SunTech will cease producing the NIBP monitoring system Lode B.V. uses in their ergometers due to changes in medical legislation. The newer versions of NIBP monitoring systems SunTech produces will result in the total loss of profit margin on bicycle ergometers due to its higher price. Furthermore, the newer versions provided by SunTech require an ECG-trigger. This means that a BP-measurement can only be done if an ECG signal is available.

By researching into the topic of NIBP monitoring themselves, Lode B.V. wishes to develop a NIBP monitor that can be used in combination with their bicycle ergometers for the purpose of stress testing. Not only will this result in a larger profit margin on the bicycle ergometers, it will also reduce the dependency on external manufacturing by SunTech. Moreover, it will increase the company knowledge of Lode B.V. making the company more valuable.

My task will be to research into technologies which can be used to monitor BP under stress conditions using NI techniques. If research suggests a new technology can be used, a prototype will be built as a proof of concept. However, if research suggests that the conventional auscultatory technology looks most promising, the focus will be to evaluate and solve problems encountered in BP monitoring during stress conditions. The central research question in this project is formulated as follows:

“How can blood pressure be monitored automatically whilst the patient is under stress conditions on a bicycle ergometer using non-invasive techniques?”

This report starts with the Research design, which provides a description of the ‘where’, ‘what’ and ‘how’. The chapter Situational and Theoretical analysis shows relevant literature to help answer research questions. After that the Conceptual model will graphically demonstrate the interaction of involved variables. Numerical and analytical data from experiments conducted will be presented in the Research results. This is followed by Conclusions in which data from the previous chapter will be interpreted and reflected on the project as a whole. Finally, in the Recommendations chapter the acquired knowledge will be used to provide future recommendations.

2

SITUATIONAL ANALYSIS

As an aid for conducting the situational analysis, a SWOT analysis was used. A SWOT analysis is used to evaluate strong and weak points for a situation, both internal and external. SWOT stands for: Strengths, Weaknesses, Opportunities and Threats. The results of this analysis are presented below and summarized in Table 1.

2.1 Strengths

In a project like this, when a product has to be designed from scratch, many aspects have to be taken into account. Having an interdisciplinary educational background provides insight into more of these aspects than most other educations. A strength of this project is its collaboration with both Lode B.V. and Hanzehogeschool. Due to years of experience Lode B.V. has expertise knowledge on designing and manufacturing. Hanzehogeschool also employs many experts in a wide variety of topics. This knowledge can be used to help the progress and quality of the end result.

- + Interdisciplinary educational background
- + Resources of Lode B.V.
- + Experts on variety of disciplines

2.2 Weaknesses

A weakness of this project is the complexity of the task ahead. Blood pressure measurements are difficult even in rest conditions, during stress conditions the task becomes more complex. Some of these difficulties are caused by motion artefacts, some by internal mechanisms that ensure homeostasis. Furthermore, the project is a very large assignment meaning that many aspects will have to be taken into account.

- Complexity of project
- Many aspects to be taken into account

2.3 Opportunities

The opportunities in this project are for Lode B.V. to become independent of SunTech. Furthermore, a larger profit margin on the ergometers can be created.

- + Independency of SunTech
- + Larger profit margin on ergometers
- + Increased company knowledge

2.4 Threats

A threat of this project is the fact that there already are products with the same functionality on the market. There are only a few companies capable of producing these systems with medical grade precision [3] [4].

- Existing technology
- Lacking marketing and competitor research

Table 1: Overview of the SWOT analysis

<p>Strengths</p> <ul style="list-style-type: none"> • Interdisciplinary educational background • Resources of Lode BV • Experts on variety of disciplines 	<p>S</p>	<p>W</p>	<p>Weaknesses</p> <ul style="list-style-type: none"> • Complexity of project • Many aspects to be taken into account
<p>Opportunities</p> <ul style="list-style-type: none"> • Independency of SunTech • Larger profit margin on ergometers • Increased company knowledge 	<p>O</p>	<p>T</p>	<p>Threats</p> <ul style="list-style-type: none"> • Existing technology • Lacking marketing and competitor research

3

THEORETICAL ANALYSIS

In this chapter the theoretical background of this project is presented. All fundamental knowledge collected is summarized here. This will provide the reader with enough background information to draw his own conclusion on the interpretation of information presented in chapter 5, literature research. Furthermore, this knowledge was used to strive for an analytical approach in the project.

3.1 Blood pressure

Fundamentally, pressure is force per unit area. Pressure is denoted in many different units, such as atm, PSI and mm Hg. However, these represent the same physical property. When looking into the pressure of fluids, a famous principle is that of Pascal's law: "pressure applied to an enclosed fluid is transmitted undiminished to every portion of the fluid and the walls of the containing vessel" [5]. Pascal his law holds approximately true in hydrodynamic systems in which flow is non-turbulent and vessel lumen is small, as is the case in blood vessels. Blood flow is mainly laminar, except around valves [6].

As said before, pressure is force per unit area. The heart is the main pump of the body, creating flow of blood in the cardiovascular system. When this flow is opposed by resistance in the form of friction the result is pressure. BP is one of the vital signs along with respiratory rate, heart rate (HR), oxygen saturation, and body temperature. Normal resting BP in an adult is approximately 120/80 mm Hg [7].

As Figure 1 depicts, the BP in the arteries is pulsatile, especially in the elastic arteries near the heart. This is caused by the pumping mechanism of the heart, which forces blood out of its ventricles at regular intervals. From arterial pressure two things can be deduced: how much the elastic arteries close to the heart can stretch, compliance and distensibility, and the volume of blood entering and leaving the elastic arteries [7].

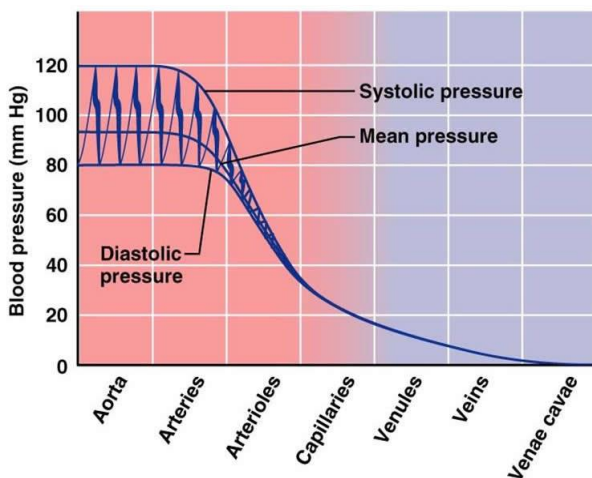


Figure 1: Systemic blood pressure variation throughout the cardiovascular system [62]

The heart is not the only mechanism that ensures blood flow, there are also the muscular and respiratory pump. The muscular pump consist of skeletal muscle activity. These muscles surround deep arteries and as they contract and relax, they ‘milk’ blood towards the heart. Valves in the blood vessels prevent backflow. The respiratory pump moves blood up towards the heart via pressure changes in the ventral body cavity during breathing. As we inhale, abdominal pressure increases, squeezing local veins and forcing blood towards the heart. At the same instance, the pressure in the thorax decreases, allowing thoracic veins to expand and speed blood entry into the right atrium [7].

3.2 Disturbed homeostasis

Normal BP for resting adults is 120/80 mm Hg. Transient elevations in BP which are normal for one person, might be extreme or even lethal for another. Chronically elevated BP is called hypertension. Hypertension is characterized by a systolic blood pressure (SBP) above 140 mm Hg or a diastolic blood pressure (DBP) above 90 mm Hg. There is a distinction between primary and secondary hypertension. About 90% of the hypertensive people have primary hypertension. Factors that might cause primary hypertension are: heredity, diet, obesity, age, stress and smoking. Secondary hypertension is caused by an identifiable condition, such as renal arteries, kidney disease and endocrine disorders [7]. Different studies show that high blood pressure is related to coronary heart disease. The relative risk that coronary heart disease results in fatality rose by 28% if an increase of 10 mm Hg in systolic blood pressure was detected. An increase of 5 mm Hg in diastolic BP had a similar effect [8].

Hypotension is a too low BP, namely below 90/60 mm Hg. Hypotension is often associated with long life and old age without cardiovascular disease. In most cases it is no reason for concern, however, in some cases it is a sign for a serious underlying condition [7].

3.3 Manual blood pressure monitors

The earliest recorded attempt at measuring BP was in 1773 by Stephen Hales. He inserted an open ended tube directly into the artery of a horse. He observed the blood rising in the tube, until it reached equilibrium with the pressure inside the artery and pulsed with the same frequency as the HR of the horse [6].

Ever since this experiment, the method of measuring BP has been refined. The biggest improvement was when the method became non-invasive (NI). The first NI method was a mercury column sphygmomanometer, as depicted in Figure 2. However, invasive BP measurements are still used. A saline-filled needle or catheter is inserted into the patient his artery. There usually is a pressure transducer at the end of the needle or catheter [9].

However, as it is stated in my research question it is required to develop a NI technique. This is mainly due to patient comfort and ease of use. Therefore, no further research will be presented into invasive BP measurements.



Figure 2: Mercury column sphygmomanometer [66]

3.3.1 Palpation

The method named palpation is fairly simple. It uses a cuff, just like a sphygmomanometer, which is inflated around the upper arm. The pressure is released slowly until the pulse becomes palpable, or able to be felt, in the radial artery. This is monitored by placing the index and middle finger on the wrist above the radial artery. When the first pulse is noticed, the pressure indicated by the sphygmomanometer is considered the SBP.

3.3.2 Flush

This method requires two operators and two cuffs. The cuffs are placed on the upper and lower arm and are inflated. The blood in the section between the two cuffs is massaged out, leaving the lower arm pale and blanched. The pressure in the upper cuff is then released slowly. The point in time at which a sudden red flush is noticed, the pressure is recorded and this is considered to be the MAP. Although this method is uncommon, it is used on infants.

3.3.3 Auscultatory

The auscultatory method uses a sphygmomanometer and a stethoscope. The inflatable cuff is placed on the upper arm of the patient and the stethoscope usually over the brachial artery, as depicted in Figure 3. By deflating the cuff slowly whilst listening to the presence or absence of Korotkoff sounds, the SBP and DBP can be determined. Korotkoff sounds are part of a broader range of arterial vibrations, namely the Korotkoff vibrations, which are caused by turbulent flow in the blood vessels. The amplitude of the Korotkoff sounds is a measure of the Korotkoff vibrations [10].

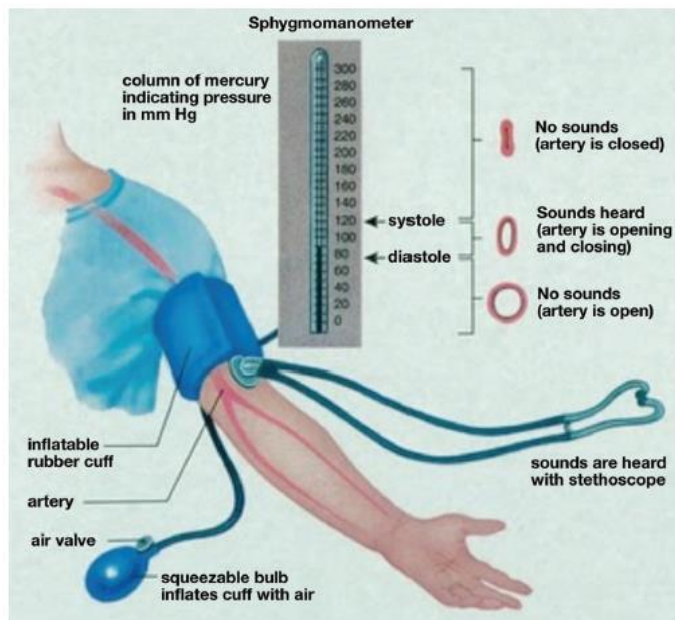


Figure 3: Auscultatory method of blood pressure measurement using a sphygmomanometer [63]

There are five categories of Korotkoff sounds, namely:

1. The first Korotkoff sound is the snapping sound first heard at the systolic pressure. Clear tapping, repetitive sounds for at least two consecutive beats is considered the systolic pressure
2. The second sounds are the murmurs heard for most of the area between the systolic and diastolic pressures
3. The third sound was described as a loud, crisp tapping sound
4. The fourth sound, at pressures within 10 mm Hg above the diastolic blood pressure, was described as "thumping" and "muting"
5. The fifth Korotkoff sound is silent as the cuff pressure drops below the diastolic blood pressure. The disappearance of sound is considered diastolic blood pressure – 2 mm Hg below the last sound heard [11]

The frequencies present in K-sounds change per phase. From phase 1 to 2 there is an increase in high frequencies, from 224 to 275 Hz. There is a significant decrease in frequency of the highest amplitude frequency from phase 3 to 4 with a decrease from 262 to 95 Hz [12]. Furthermore, there is more 60 Hz signal amplitude in K-Vibrations 1, 4 and 5. There is less in 2 and 3 [10]. However, in practice these frequencies will vary per person and measurement equipment making it difficult to obtain definite bounds.

A detailed description of this method is provided by the book Medical Equipment Technology by Carr & Brown and is presented below [6].

The cuff is wrapped around the patient his upper arm at a point about midway between the elbow and shoulder. The stethoscope is placed over an artery distal to the cuff. This is preferred because the brachial artery comes close to the surface near the antecubital space and so is easily accessible.

The cuff is inflated so that the pressure inside the inflated bladder is increased to a point greater than the anticipated systolic pressure. This pressure compresses the artery against the underlying bone, causing an occlusion that shuts off the flow of blood in the vessel.

The operator then slowly releases the pressure in the cuff. About 3 mm Hg per second is usually deemed best. When the systolic pressure first exceeds the cuff pressure, the operator begins to hear some crashing, snapping sounds in the stethoscope that are caused by the first jets of blood pushing through the occlusion. These sounds, called Korotkoff sounds, continue as the cuff pressure diminishes, becoming less loud as the blood flow through the occlusion becomes smoother. Korotkoff sounds disappear or become muffled when the cuff pressure drops below the patient his diastolic pressure. At the point the Korotkoff sounds appear, the operator notes the systolic pressure. When the Korotkoff sounds disappear or get muffled, the operator notes the diastolic pressure. These are usually notes as ratio of systolic over diastolic (i.e., 120/80 mm Hg). This principle is depicted in Figure 4 [6].

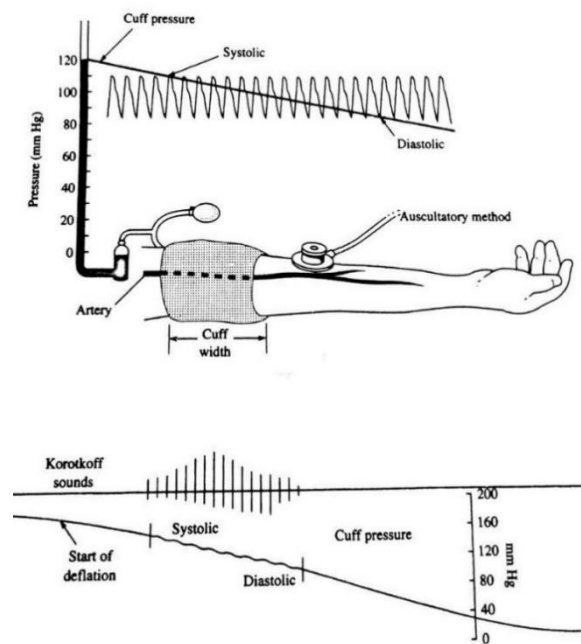


Figure 4: Korotkoff sounds [5]

Variation between direct and indirect measurements is proven to be less than 10 mm Hg. Furthermore, it has been shown that diastolic pressures are less in error if the reading is taken at the point where the Korotkoff sounds (K-sounds) disappear instead of when they are muffled. Limitations of the manual auscultatory method include the hearing and gauge pressure reading capability of the operator. Furthermore, K-sounds contain a lot of 200 Hz signal, a range where the human hearing is not very accurate [6].

3.3.4 Oscillometric

Oscillometric BP measurements are similar to sphygmomanometry in many ways. However, it does not measure BP directly. The oscillometric method measures small pressure differences present in the cuff partially caused by turbulent flow of the blood between systolic and diastolic pressure [6]. The differences in pressure will vary periodically in synchrony with the cyclic vasoconstriction and vasodilation of the brachial artery [13].

To demonstrate the method of obtaining SBP, DBP and MAP from an oscillometric measurement, Figure 5 depicts a simplified view of how pressure in the cuff varies over time. The highest pulse wave is shown to be the MAP. The determination of the systolic and diastolic pressure is done by evaluation of the amplitudes in the envelope. However, as this is an approximation, the calculation differs from manufacturer to manufacturer. The systolic pressure is shown to be a point in time before the MAP, where the amplitude is 55% of the amplitude of the MAP. The diastolic pressure is shown to be a point in time after the MAP, where the amplitude is 85% of the amplitude of the MAP according to Dr. Neil Townsend in 2001 [14]. However, in 2012, another article by Babbs claims that the systolic point is at about 50% and the diastolic point is at about 70% [15]. The reality is that values used by large companies are closely guarded trade secrets and the exact determination of these values remain to be a problem in biomedical engineering. Studies show that it is possible to determine the stiffness of the artery segment from the shape of the envelope [15].

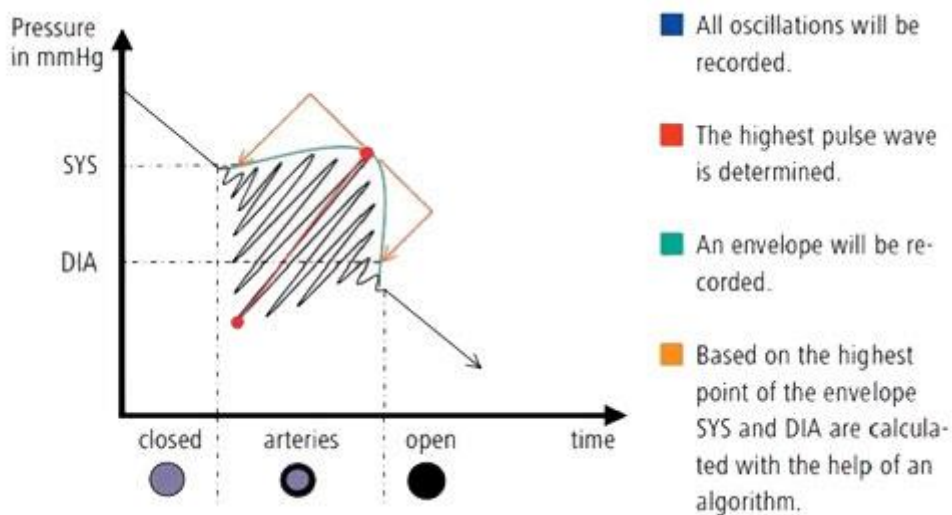


Figure 5: Simplified view of pressure in cuff over time during oscillometric measurement [13]

3.4 Stress testing

Stress testing is a cardiac test where physical stress is exerted on the body whilst vital signs are monitored. Usually physical stress is exerted by placing the patient on a treadmill or bicycle. However, in some cases, like MRI and CT scan, the patient is required to lay still. In these cases a chemical stress inhibitor like for instance adenosine is used [16]. These tests are used to determine functional capacity and extent of coronary disease. It can also be used to determine the chance of heart attacks [17]. Furthermore, it is used in rehabilitation to monitor the effects of therapy [18].

The American Heart Association and the British Hypertension Society recommend that clinicians allow a patient to sit still without talking for at least five minutes prior to measurement [19]. For most patients, it is likely that the first measurement will be higher than the second regardless of the resting interval [20].

Measuring blood pressure during stress conditions is mostly used for cardiac stress testing. A cardiac stress test (or cardiac diagnostic test) is a cardiological test that measures the hearts ability to respond [21]. Some of the parameters often recorded are ECG-waveforms, oxygen saturation and blood pressure [22].

During a stress test, some patients K-sounds may continue to a very low pressure, or in some cases, all the way to 0 mm Hg. This is due to increased arterial compliance, occurring as arteries dilate in response to exercise. When this occurs, there is usually a point where the K-sound amplitude drops off sharply, continuing at a reduced level [23].

An article by David Akinpelu named ‘Treadmill Stress Testing’ describes the relevant changes in the body during dynamic exercise [18]. His findings are summarized point-wise below. The overall hemodynamic response depends on the amount of muscle mass involved, exercise efficiency, conditioning and exercise intensity. The initiation of dynamic exercise results in:

- *Increase in HR, stroke volume and cardiac output (CO) as a result of vagal withdrawal and sympathetic stimulation*
- *Increase in alveolar ventilation and venous return as a consequence of sympathetic vasoconstriction of veins*
- *Initial increase in CO is due to Frank-Starling law and HR*
- *Latter increase in CO is primarily due to increase in ventricular rate*
- *Initial TPR increases due to generalized vasoconstriction, except in vital organs, due to maximal sympathetic discharge and withdraw parasympathetic stimulation*
- *Latter TPR decreases due to vasodilation causing skeletal muscle blood flow to increase*
- *Rise in ventricular contractility due to release of venous and arterial plasma noradrenaline*
- *Oxygen extraction increases as much as 3-fold*
- *Peripheral resistance decreases*
- *SBP, MAP and pulse pressure usually increase*
- *DBP remains unchanged or increases/decreases approximately 10 mm Hg*
- *Pulmonary vascular bed can accommodate as much as a 6-fold increase in CO with only modest increases in pulmonary blood pressure, this is not a limiting determinant of peak exercise capacity in healthy subjects*

During cardiovascular stress testing, a close eye should be kept on the SBP. During stress the SBP should only increase, a decrease in SBP should always lead to the termination of the stress test. An increased SBP up to 225 mm Hg is normal in young adults. DBP increases less, a pressure of 110 mm Hg is considered high. When the DBP approaches 130 mm Hg the stress test should also be terminated [24]. The increase in BP during exercise is depicted in Figure 6.

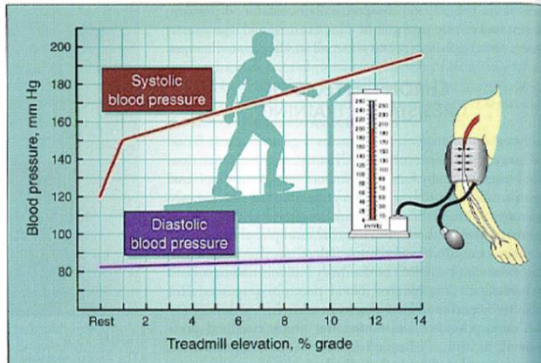


Figure 6: SBP and DBP during exercise [25]

3.5 Medical device directive

When automating a medical product one must always take great care for patient safety. Life threatening decisions might be based on the output of the product, unless specifically stated otherwise. For example in automated BP monitors a pressurized cuff can potentially harm the patient if the pressure becomes too high or stays high too long. It is these kind of factors that determine the classification of medical products. For instance, the Kadenz Original Equipment Manufacturer (OEM) BP monitor, which is currently used in Lode their ergometers, is classified as a Class IIa device [26].

Accuracy of medical devices is tested using standardized procedures, like AAMI and ANSI. There are labels which can be given to devices to indicate accuracy and precision. The acceptable boundaries on these labels can change over time, therefore the year of the label should also be provided. For instance the AAMI/SP10 provides accuracy boundaries for sphygmomanometers. The AAMI/SP10 1993 states that the mean difference should be less than 5 mm Hg and the standard deviation less than 8 mm Hg [27].

4

RESEARCH DESIGN

My task was to research into technologies which can be used to monitor NIBP under stress. This task was carried out at the R&D department of Lode B.V. There are experts on hardware, both electrical and mechanical, and software development available for consultation. The first phase of the project consisted of literature research. If this research suggested that a new technology could be used, a prototype would have been built as a proof of concept. However, if research suggested that the conventional auscultatory technology looks most promising, the aim would have been to evaluate and solve problems posed by measuring under stress conditions.

4.1 Research question

The central research question used to guide this project was:

“How can blood pressure be monitored automatically whilst the patient is under stress conditions on a bicycle ergometer using non-invasive techniques?”

Some of the underlying questions were:

1. What methods can be applied to measure blood pressure?
2. How resilient to motion artefacts are these methods compared to the mostly used oscillometric methods?
3. Can these methods be used to obtain medical grade precision according to ANSI/AAMI standards?
4. What causes motion to induce noise in auscultatory NIBP monitoring?
5. How can artefacts be filtered in an auscultatory NIBP monitoring system?
 - What type of filters are able to do so?
 - What type of filters are used in existing products?
 - How can these filters be implemented into an embedded system?

4.2 Success factors

If research suggested a new technology could have been used to satisfy the research question, the critical success factors were the following:

- The development of a prototype as proof on concept
- Estimation of pricing of the final product lower than those of SunTech
- Testing of the prototype on patients whom are in movement to analyse the artefacts caused by motion

Optional factors would have been the following:

- Compare test results to a conventional auscultatory system
- Evaluation of motion resilience of the new prototype compared to the auscultatory system by evaluating measured world signals

If research suggested that the auscultatory method was most promising to fulfil the research question, the critical success factors would have been the following:

- Extensive analysis of motion artefacts using an existing NIBP monitoring system
- Development of a filter which is able to filter measured signals
- Development of a detection algorithm capable of determining the presence of K-sounds

Optional factors would have been the following:

- Implementation of an embedded system capable of filtering BP signals real-time

4.3 Requirements

The requirements for the to be developed non-invasive BP monitoring system are presented in Table 2 below. These requirements were formulated in consultation with Miriam Does, product expert at Lode B.V. To sum up, the desired system should be capable of measuring systolic and diastolic BP, whilst the patient is under stress conditions, automatically using non-invasive techniques. The resulting output should be aimed at providing medical grade precision for all population groups and ages, under rest and stress conditions.

Table 2: Requirements of the to be developed non-invasive BP monitoring system

Property	Requirement	Reasoning
SBP Range (mm Hg)	40 - 250	Minimum to be expected is 40, maximum to be expected is 250 [28]
DBP Range (mm Hg)	20 - 150	Diastolic readings can continue to around zero mm Hg during stress test [29]
Patient Safety	Cuff inflation limited to less than 50 seconds	Preventing prolonged blocking of blood stream
Measurement time	Duration of BP reading limited to 160 seconds	Able take frequent readings during stress test
Clinical Accuracy	ANSI/AAMI SP10:2002 (mean difference (SD) ≤ 5 (8) mm Hg)	Reliable output for research, medical procedures and rehabilitation

The mentioned specifications in Table 2 are for a whole BP monitoring system. However, this project aims to develop only part of a BP monitoring system. These requirements are presented to be able to provide future recommendations. For instance, to achieve clinical accuracy according to ANSI/AAMI standards, the entire product will have to be validated to provide accurate results on all population groups [30]. However, within the timeframe and scope of this project, only a part of the entire product will be developed. Therefore, the goal is to prove that the validated part of the product does not exclude the possibility of reaching these requirements.

5

LITERATURE RESEARCH

In the following chapter, findings based on literature research will be presented. Based on these findings, a method for measuring BP was selected. The developed system was based on the selected method. An evaluation of all investigated methods, based on the requirements, can be found at the end of the chapter in Table 3: Overview of comparison between methods of NIBP monitoring.

5.1 Automated blood pressure monitors

Oscillometric BP monitors are the most broadly used followed by auscultatory BP monitors [10]. Automated BP monitors in general are not only desirable for their ease of use but also for their accuracy. However, there are products available that apply different methods, such as arterial unloading and pulse wave velocity. Some advantages of automated blood pressure monitors in general are: the ability to filter environmental noise, the elimination of observer bias and an increase in patient focus [22]. Chapters 5.1.1 5.1.8 describe the different methods of NIBP monitoring.

5.1.1 Auscultatory

The auscultatory BP monitoring method is automated by replacing the stethoscope with a sensor able to transduce vibrations caused by turbulent blood flow. This is usually done using a piezoelectric microphone or a speaker/microphone combination. The piezo crystal microphone is basically a pressure transducer able to detect the Korotkoff vibrations caused by turbulent flow. A speaker/microphone combination can be used to emit ultrasonic waves and detect phase shifts, with which the turbulent flow can be deduced according to the Doppler principle [31]. From the detection of blood flow and the pressure readings in the cuff, SBP and DBP can be determined [6].

The auscultatory method has been the standard for measuring BP for over 100 years. It is considered to be accurate, precise and have excellent repeatability [32]. It does not require calibration as it is measured in the upper left arm, where the arterial pressure is assumed to be equal to the systemic arterial pressure. The processing required mainly consists of the determination of the start and end time of the K-sounds. The start and end time of the K-sounds should be cross references with the cuff pressure on a time scale to arrive at SBP and DBP. The motion tolerance of this method is mostly determined by proper cuff placement, filtering and analysis of the microphone signal. The usability during stress testing of this method is excellent, mainly due to the fact that the relevant part of the signal is not influenced by external pressure variations in the cuff as much as other methods. A popular auscultatory BP monitor used for bicycle ergometric is the SunTech Cycle, which uses a piezoelectric microphone [33].

5.1.2 Oscillometric

In order to automate the oscillometric method of obtaining BP, a pressure transducer has to be implemented into the cuff. The pressure transducer should be selected to maximize variations in pressure rather than read the static pressure heads. The determination of parameters like systolic, diastolic and mean arterial pressure can be deduced in the same way as the manual mode of operation [6]. However, another mode of operation is the volume-oscillometric method, which attempts to maintain a cuff pressure equal to the MAP and measure arterial volume oscillations [10].

The oscillometric method has been widely implemented into automated blood pressure monitors and has successfully fulfilled the validation protocols from international organizations [34]. Although its repeatability is almost as good as the auscultatory method, it is shown that it consistently gives higher readings [32]. This difference falls within acceptable boundaries and is determined to be around 5 mm Hg at most [35] [36]. The difference between the auscultatory and oscillometric methods is visualized in Figure 7. The oscillometric method mostly does not require calibration as it is generally measured in the upper left arm, where the arterial pressure is considered to be equal to the systemic arterial pressure. The processing required consists of the logging of pressure transducer data, peak detection to arrive at MAP and SBP and calculations to arrive at DBP [15]. Its output signal is not influenced much by small displacements of the cuff, making it usable measurements during transport. However, the usability during stress testing is poor as the oscillometric method is sensitive to pressure variations due to arm movement [37]. A popular oscillometric BP monitor used for challenging transport condition is the SunTech Advantage A+, which utilizes an ECG signal for R-wave gating [38].

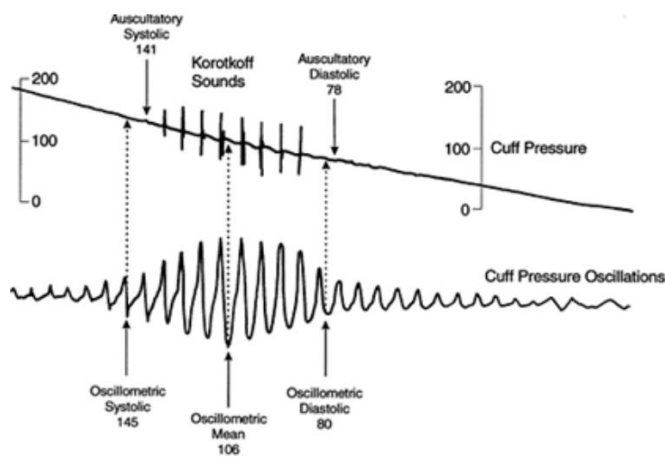


Figure 7: Auscultatory VS Oscillometric [39]

5.1.3 Pulse wave

A relatively new method for obtaining blood pressure is based on the pulse wave characteristics of BP. These characteristics are quantified with at least two pulse transducers placed at different locations [40]. It should be noted that an ECG lead can also be used, where the primary location of the systolic pulse will be near the aortic valve. By measuring the time difference between the arrival of the systolic pulse at two points, BP can be determined using mathematical modelling. This modelling can be done by calibrating the system for each individual or by obtaining population averages and estimating BP accordingly.

The accuracy and precision of pulse wave based methods are poor as its output is determined by an approximation, instead of a direct measurement of pressure. It is influenced greatly by changes in the measurement setting such as placement of the sensor and position of the arm, which makes for poor repeatability sometimes leading to poor accuracy. Information on which variable of BP the method actually measures, SBP/DBP/MAP, is lacking. However, the measured value can be modelled or calibrated to any of those variables. The processing is straightforward as it only requires to determine blood velocity by timing pulse intervals and calculating the corresponding blood pressure with a calibration or modelled equation. The placement of the sensor is critical, causing poor motion tolerance. As said before, pulse wave based methods are greatly influenced by location of the arm and are therefore not suitable for stress testing [41]. A fairly new product which utilizes pulse wave velocity via a pressure transducer in combination with a heart rate (HR) signal is the Maisense Freescan [42].

5.1.4 Cuff and pulse

The cuff and pulse method utilizes a cuff with pressure transducer around the wrist and a pulse transducer on the finger. The cuff will inflate until above SBP, after which it is slowly deflated until a pulse is detected in the finger. When a pulse is detected the cuff pressure will be close to the SBP. The DBP can be deduced from either a pulse time delay or a pulse amplitude difference method [41].

The cuff and pulse method is similar to the way SBP is determined in the auscultatory method, only the cuff and flow transducers have been moved down the arm. Furthermore, the flow transducers is only able to detect flow and are not able to distinguish laminar and turbulent flow, meaning the cuff and pulse method is only able to detect systole. Diastole can be determined but it will be an approximation. These properties make for poor accuracy and precision when considering both SBP and DBP. The processing involved consists the logging of pressure and flow measurements to determine SBP, combined with either the pulse time delay or pulse amplitude difference method for the determination of the DBP [41]. The cuff and pulse method is not usable in transport or stress testing due to its extreme sensitivity to body position [43]. The sensitivity to body position is mainly caused by the facts that the wrist should be held at heart level.

5.1.5 Modified applanation tonometry

The method of modified applanation tonometry is based on the principle that to flatten a closed circuit containing fluids, the pressure required to flatten the container is approximately equal to the pressure inside the closed circuit. By compressing the artery onto a bone, pulse pressures inside the vessel can be obtained [19]. By applying pressure using an actuator and measuring the applied pressure with a transducer, the blood pressure inside the vessel can be determined using Fourier transformations [41].



Figure 8: Possible configuration of Applanation tonometry used in the BPro [67]

The performance of modified applanation tonometry is up to medical standards, if the device is calibrated properly [44]. However, it is advised to perform multiple measurements to obtain accurate data. Calibration is required to obtain the systemic arterial pressure (SAP). Modified applanation tonometry requires a lot of processing, however it is possible to acquire a continuous signal. Modified applanation tonometry has poor motion tolerance, making it necessary to sit down before taking a measurement. Furthermore, it is advised to rest at least 2-3 minutes before taking a reading, leading to the conclusion that modified applanation tonometry has poor usability performance during stress testing [44]. A portable BP monitoring system is the BPro, which is the size of a bulky watch, as shown in Figure 8.

5.1.6 Ultrasound imaging

Ultrasound imaging can be used to obtain blood flow velocity in large arteries. It does so by measuring the Doppler shift of ultrasound waves being reflected by the blood, as depicted in Figure 9. By plugging the Doppler shift and vessel dimensions into a mathematical model, the blood pressure at the exact place of the artery can be determined. The model involves converting the distension waveforms, also measured using imaging techniques, into pressure waveforms using the velocity and vessel diameter measured by Doppler detection [45].

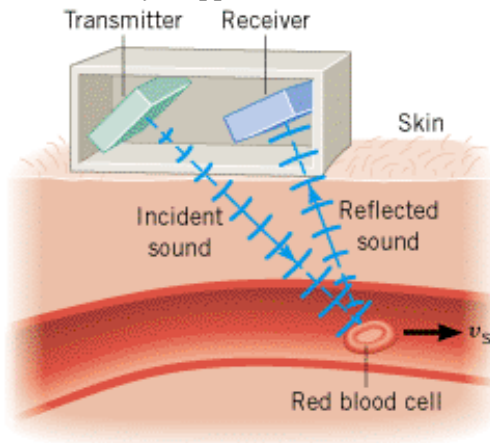


Figure 9: Basic principle of ultrasound Doppler imaging [70]

Ultrasound imaging techniques can accurately and precisely determine blood flow velocity, however when translating ultrasound information into BP the accuracy decreases as variation per individual will not perfectly be reflected in the model. By calculating pulse gradients, systolic and diastolic values can be determined as pressure variation can be determined. Ultrasound imaging does not require calibration but it does require a modelling. The processing required is significant, as it already takes a lot of computing to arrive at velocity imaging, which then still has to be translated to pressure. The motion tolerance and usability during stress testing of ultrasound imaging is very bad as a slight change in the positioning of the probe with respect to the artery will most likely result in a total loss of signal.

5.1.7 Finger cuff

Using two cuffs on two fingers and a photoplethysmogram (PPG) sensor, the finger cuff method works on the principle of the “unloaded artery wall”. It tracks changes in blood flow with the PPG sensor and inflates/deflates the cuff in such a way that the flow is uninterrupted. The desired situation is such that the pressure of the cuffs is equal to the pressure inside the arteries. Reaching equal pressures requires the cuff to follow the pulsations found in these arteries [46].

The finger cuff method is not able to measure absolute blood pressure accurately. It is capable of performing precise measurement but requires calibration or advanced processing to arrive at SAP. It does track changes in systolic and diastolic pressures very accurately. The finger cuff method can be used during transport and stress testing, making it usable in a wide variety of disciplines. A product that utilizes the finger cuff technology is the Portapres from Finapres [4].

5.1.8 Other

There are some other methods that might be used to arrive at BP. However, these will not be taken into consideration as they do not meet the requirements states in chapter 0. Some worth mentioning are: electric manometry and relative oxygen saturation.

Electric manometry is probably one of the most motion resilient measurement techniques. However, it uses a catheter that is introduced into a blood vessel by using a cannula. Penetrating body tissue makes it an invasive techniques and therefore it does not meet the requirements.

Relative oxygen saturation, also called SpO₂, can be used to determine the presence of blood flow. However, the shape characteristics of SpO₂ graphs can be used as an indication of systolic blood pressure. In a study performed by Mohammad Golparvar, it was shown that there was a significant strong-negative correlation between changes in SBP and delta-down changes in SpO₂ [47]. SpO₂ measurements can also be used to detect the presence of blood flow, making it able to detect the SBP in an auscultatory setup [48].

5.2 Conclusion

Many methods for monitoring blood pressure were presented in chapter 5.1. However, as this project aims to develop a BP monitor the purpose of stress testing, many methods show indications of being unqualified. All methods resented in in chapter 5.1 were evaluating according to the requirements as stated in chapter 4.3, Table 2. In Table 3, a qualitative representation of the usability of each method is shown. These ratings are based on their physically properties, descriptions of popular products and intuition.

Table 3: Overview of comparison between methods of NIBP monitoring.

Characteristic Method	Accuracy	Precision	SBP / DBP	Calibration	Processing required	Motion tolerance	Useability during stress testing
Auscultatory	++	++	✓/✓	×	+	+	++
Oscillometric	+	++	✓/✓	×	+	++	-
Finger cuff	+/-	++	✓/✓	✓	-	+	+
Applanation tonometry	+	++	✓/✓	✓	--	-	-
Cuff and pulse	--	+/-	✓/×	×	+/-	--	--
Ultrasound imaging	-	++	✓/✓	✓	--	--	--
Pulse wave velocity	--	-	?/?	✓	++	--	--

From Table 3 it can be concluded that the auscultatory method is the most viable option, scoring best on each property except motion tolerance. Based upon these results the auscultatory method was selected as a basis for the to be developed product. The aforementioned is in agreement with the requirements.

6

CONCEPTUAL MODEL

A conceptual model was created for a non-invasive BP monitor that is usable under stress conditions, which utilized the auscultatory method. Stress conditions are limited to bicycle ergometry. Figure 10 depicts the most important steps and parameters involved. All flowcharts, including Figure 10, were made in Gliffy [49].

To exert physical stress on the patient in the form of exercise, the patient has to be in motion. Motion introduces noise in the form of motion artefacts, which an undesired side effect. As said before, exercise exerts physical stress on the patient. Stress causes a rise in CO and a decrease in TPR, the main factors regulating BP. These changes are what is desired to be accumulated.

In order to accumulate a usable signal using the auscultatory method, a cuff has to be placed on the upper arm. The cuff has to be inflated to a pressure higher than the SBP, which will increase during exercise, meaning that the inflation pressure has to increase as well. Once the cuff pressure is higher than the SBP and the blood vessels in the arm are closed off, the cuff has to be deflated slowly. During the deflation of the cuff, the signal can be accumulated. However, the hardware required to inflate/deflate the cuff and the cuff itself are not within the scope of the project. The development of the pumping and deflation mechanisms are seen as 'standard development' by Lode B.V. They do not expect major issues here.

The accumulated signal will consist of two parts, one desired and one undesired. Therefore, the signal has to be filtered to get rid of as much of the undesired signal as possible, whilst leaving the desired signal intact. From the filtered signal, the start and end time of the K-sounds have to be determined. Once the start and end times are known, they have to be cross referenced with the stored pressure values their timestamps to arrive at the SBP and DBP. Once SBP and DBP are known, the automated BP measurement is done.

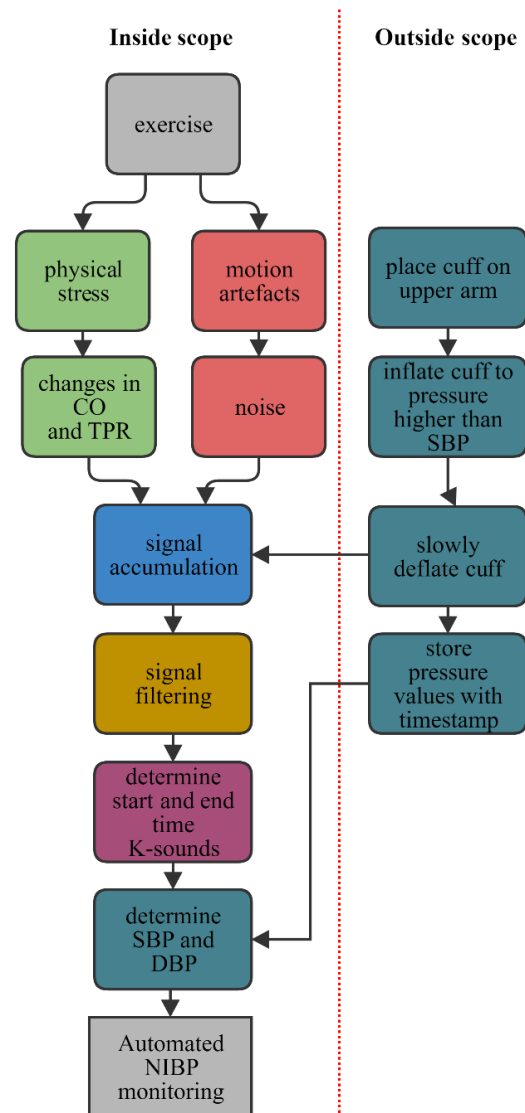


Figure 10: Flow chart demonstrating the conceptual model

7

APPLIED RESEARCH

In this chapter the structure of the developed system is presented, as well as experiments conducted to validate the proper functioning of the system. The adequate functioning of the system was evaluated by testing the system on a component level. Most tests consisted of providing the component with a controlled input and carefully examining the output.

7.1 System as a whole

The data flow of the newly designed non-invasive BP monitoring system is depicted in Figure 11. The system is optimized for usage during stress conditions. It utilizes a piezo microphone that contains two piezo crystals, both of which are fed into an instrumentation amplifier after which a single channel signal is obtained.

The resulting signal is filtered by an analogue low-pass filter to remove high frequencies for the purpose of anti-aliasing. Once filtered, the signal is fed into a 16-bit precision analogue-to-digital (ADC) converter running at a sampling speed of 2500 Hz. The digital signal is band-pass filtered with stop-frequencies of 8 and 292 Hz, attenuated to -60 and -100 dB respectively, and pass-frequencies of 30 and 270 Hz. The filtered signal is fed into a Korotkoff detection algorithm, which determines starting and end time of the K-sounds. The algorithm contains a periodicity check, in which false detections are cancelled out.

The upper four layers in Figure 11 represent hardware which together formed the data acquisition (DAQ) system. Each individual block was validated in a controlled environment. These tests and results as well as detailed description of the components are presented in appendix B. The last two layers in Figure 11 represent a digital environment and consist of software. Both blocks were developed and tested in Matlab 2016a.

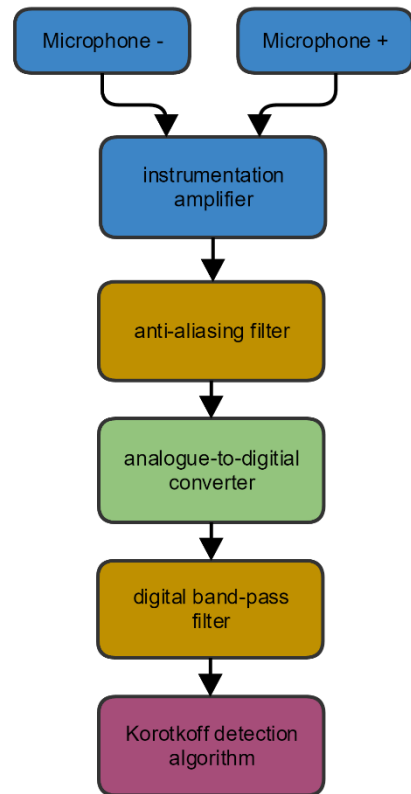


Figure 11: Dataflow of the designed non-invasive BP monitoring system

7.2 Signal acquisition

The purpose of the signal acquisition experiment was to obtain signals measured with the designed DAQ which contain K-sounds under increasing stress conditions. The paragraphs below describe the used materials and procedures.

7.2.1 Materials

To do so, the following materials were required:

- Corival ergometer [50] with Kadenz BP module [29]
- Lode cuff with contact microphone [51]
- Computer

The Lode cuff air hose was connected to the Kadenz DKA module of the Corival ergometer, however the piezo microphone was connected to the DAQ. Connect two channels of an oscilloscope to two input of the DAQ and set the scale to 5 s/div and the sampling rate to at least 2500 Hz. The DAQ was connected to the computer which a serial monitor running at the proper COM port and baud rate (230400 bits/s). Furthermore, the serial monitor was configured to log the data to a file. The serial monitoring software used was Putty [52]. On the Corival ergometer a custom test protocol was created that increased the load by 50 Watt every three minutes, with an initial load of 50 and a maximum load of 200 Watt. Afterward an unlimited recovery period was implemented of 50 Watt.

7.2.2 Procedure

The following two procedures describe the process used to obtain K-signals. The procedure described in paragraph 7.2.2.1 describes how a BP-measurement is done, which is needed in the procedure in paragraph 7.2.2.2.

7.2.2.1 Procedure BP-measurement

1. Open the serial monitor and send a command via serial to the DAQ, to start logging the microphone signal
2. Inflate the cuff and start deflating it at a rate of 3 mm Hg/s, as is default for the Kadenz DKA, by pressing the 'start BP-measurement' button on the Corival ergometer interface
3. Whilst the cuff is slowly being deflated, monitor the oscilloscope and check if the time between the pumping action of the Kadenz, indicated by large consecutive peaks, and the first K-sounds, indicated by periodic individual peaks, is at least 2 seconds. If not, skip step 4 and let the Kadenz DKA inflate the cuff again. This time the cuff will be inflated to 280 mm Hg making sure there is enough time between the pumping action and the first K-sounds
4. Once the cuff pressure is close to zero mm Hg, prevent the cuff from being inflated again by pressing the 'stop BP-measurement' button on the Corival interface. The stop button has to be pressed as the Kadenz has no contact microphone signal available
5. Send a command via serial to the DAQ, to stop the logging of the microphone signal and close the serial monitor

7.2.2.2 Procedure main experiment

1. Instruct the patient to take place on the ergometer
2. Locate the brachial artery with your index and middle finger
3. Place the cuff such that the contact microphone is located over the brachial artery
4. Instruct the patient to place its hand, palm up, on the handlebar and relax his arm
5. Conduct a BP-measurement, once the measurement is done instruct the patient that he can take hold of the handle again
6. Start the test protocol on the ergometer and instruct the patient to start cycling
7. After one minute, initiate a BP-measurement
8. Once the protocol reaches the next load repeat step 7
9. Repeat steps 7 and 8 until the protocol reaches recovery and perform one more BP-measurement

7.2.3 Obtained signals

In this paragraph the obtained signals from the above-mentioned experiment will be briefly explained. There are three clearly definable regions in the obtained signal, namely: pumps active, baseline and K-sounds. A signal obtained whilst the patient was cycling at a load of 50 Watt is depicted in Figure 12. All graphs, including Figure 12, were made in Matlab 2016b [53]. In this figure the three regions are roughly indicated by the red dotted lines.

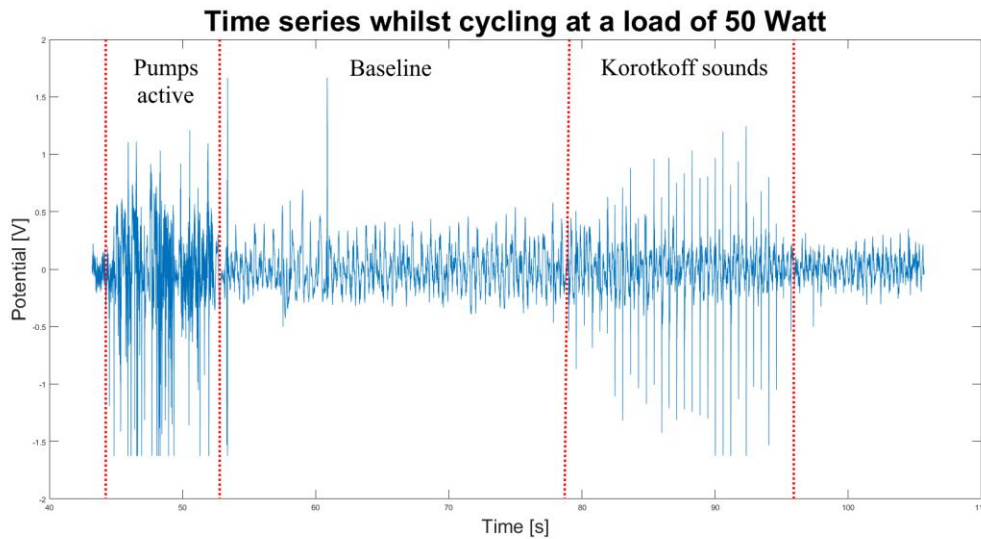


Figure 12: Time series of piezo microphone during BP-measurement whilst cycling at a load of 50 Watt for test person A

In the region where the pumps are inflating the cuff, labelled ‘pumps active’, the signal mainly consists of vibrations from the pump, motion artefacts and other sources of noise but also K-sounds. K-sounds will occur when the cuff pressure is between DBP and SBP. However, via visual inspections these K-sounds are hardly recognizable.

The region where the cuff is being slowly deflated but no K-sounds have yet occurred is labelled baseline. In the baseline, the signal mainly consists of motion artefacts and other sources of noise. In Figure 12 it can be seen that sometimes large peaks occur due to irregular movement.

The region labelled ‘K-sounds’ is the region of interest. The goal is to determine the start and end time of the K-sounds. The K-sounds region contains motion artefacts and other sources of noise but also K-sounds. In Appendix C more time series of signals can be found.

For the purpose of readability this report will only present three of the obtained signals: during rest conditions, whilst cycling at a load of 200 Watt and during recovery whilst cycling at a load of 50 Watt. These three scenarios were selected as they represent the ongoing change when measuring BP for the purpose of stress testing.

7.3 Filter cut-off frequencies

All filters were designed using the FIRPM function in Matlab 2016a. The FIRPM function utilizes the Parks-McClellan algorithm, also called the Equiripple design. These filters are optimized in such a way that the error between the desired and actually frequency response is minimized [53].

In order to determine the appropriate filter cut-off frequencies, the obtained signals were high-pass, low-pass and band-pass filtered. A procedure was formulated to obtain the optimal cut-off frequencies with respect to the developed peak detection algorithm. The procedure is designed to select filter coefficients which reduce the spread of the baseline maximally and K-sounds minimally.

7.3.1 Filter cut-off frequencies determination procedure

The following procedure was used to determine the filter cut-off frequencies:

1. Determine sensible regions for cut-off frequencies based on literature, previous testing and intuition
2. Design five filters with coefficients in this region
3. Select three signals that best represent the to be expected signals: rest, maximum load and recovery
4. Filter each signal with each filter, resulting in 15 filtered signals
5. Determine the start and end time of the baseline for each filtered signal manually via visual inspection
6. Run the Korotkoff detection algorithm, presented in chapter 0
7. Use the location of the detected peaks to cut out the K-sounds, store these in a new dataset
8. Determine the standard deviation of the cut out K-sounds with Equation 1
9. Create a new dataset with only the baseline using the manually determined start and end time
10. Calculate the standard deviation of the baseline with Equation 1
11. Calculate the percentage decrease in standard deviation between the unfiltered and filtered situations for each selected signal with Equation 2
12. Calculate the percentage decrease for each filter using Equation 3
13. Calculate the scaled decrease ratio using Equation 4
14. Select cut-off frequency with highest ratio

The equations used in this procedure are described on the next page.

Equations used in the filter cut-off frequencies determination procedure are the following:

Equation 1: Sample standard deviation

$$\text{standard deviation} = \sqrt{\frac{1}{N-1} \sum (x_i - \bar{x})^2}$$

Equation 2: Percentage decrease in standard deviation between filtered and unfiltered signals

$$\text{percentage decrease} = 100\% * \frac{SD(\text{NoFilter}) - SD(\text{Filter})}{SD(\text{NoFilter})}$$

Equation 3: Ratio of decrease in baseline over decrease in K-sounds

$$\text{decrease ratio} = \left(\frac{\text{percentage decrease baseline}}{\text{percentage decrease K - sounds}} \right)$$

Equation 4: Scaled ratio of decrease in baseline over decrease in K-sounds

$$\text{scaled decrease ratio} = \frac{\text{decrease ratio}}{\max(\text{decrease ratios})}$$

An example of resulting data from the above procedure for one signal is presented in Table 4 below. Here, it can be seen that during rest a cut-off frequency of 11 Hz provides the highest degree of reduction in spread of the baseline. However, a cut-off frequency of 7 Hz provides the lowest amount of reduction in spread of the cut out K-sounds, both of which are desired. However, when a ratio of decrease in baseline over cut out K-sounds is calculated, the highest ratio is obtained with a cut-off frequency of 10 Hz.

Table 4: Standard deviation decrease ratios for a high order high-pass filter with different cut-off frequencies, applied to a signal obtained during rest conditions

	SD baseline	Percentage decrease baseline	SD cut K-sounds	Percentage decrease K-sounds	K-Scaled decrease ratio
No Filter	0.027		0.171		
Fc = 11 Hz	0.019	26.641	0.116	32.301	0.173
Fc = 10 Hz	0.020	24.899	0.132	22.954	0.227
Fc = 9 Hz	0.021	21.127	0.134	21.846	0.202
Fc = 8 Hz	0.022	17.554	0.132	22.527	0.163
Fc = 7 Hz	0.023	13.543	0.135	20.783	0.136

7.3.2 High-pass filter results

As the calculated ratio has no unit, it is only useful for comparison. The resulting data for all three signals, high-pass filtered at different cut-off frequencies, is depicted in Figure 13. When the cut-off frequency increases, more of the lower frequencies are filtered. However, the ratio of decrease in baseline over K-sounds does not necessarily decrease. When the patient is in movement, as is the case in signals ‘load 200’ and ‘recovery’, the ratio becomes higher. The ratio becomes higher due to the fact that there are more motion artefacts present in the baseline and motion artefacts are low-frequent.

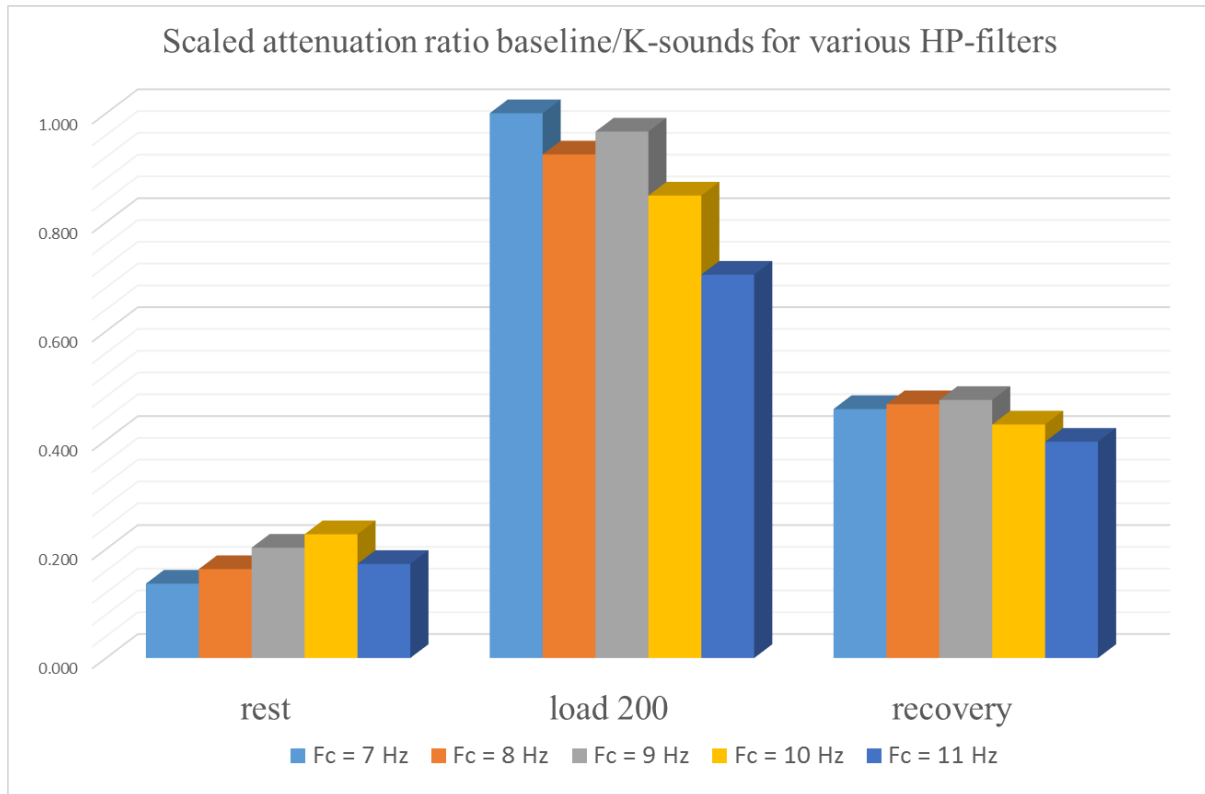


Figure 13: Scaled attenuation ratio of baseline over K-sounds for various HP-filters

Table 5 displays the average percentage decrease in baseline and cut K-sounds of all three signals for each cut-off frequency. Overall, a cut-off frequency of 9 Hz seems to give the best results with a decrease in baseline of 52% and a decrease in cut out K-sounds of 22%.

Table 5: Average decrease percentages for signals rest, load 200 and recovery of various HP-filters

	Average decrease baseline	average decrease cut K-sounds	ratio
Fc = 11 Hz	55.440	29.837	1.858
Fc = 10 Hz	54.043	24.309	2.223
Fc = 9 Hz	51.750	21.888	2.364
Fc = 8 Hz	49.275	22.089	2.231
Fc = 7 Hz	46.093	20.685	2.228

7.3.3 Low-pass filter results

When using the same method for low-pass filters, the decrease in spread is insignificant. The decrease is insignificant due to the fact that the signals obtained contain more low frequencies, as can be seen in the FFT of the K-sounds (note these are not cut out, so also contain baseline) in Figure 38, Figure 39 and Figure 40 in appendix D. Therefore, when only filtering high frequencies, the decrease in standard deviation compared to an unfiltered situation is insignificant. All filter data results are presented in appendix D.

7.3.4 Band-pass

The resulting data for all three signals, band-pass filtered at different cut-off frequencies, is depicted in Figure 14. For rest conditions, the band-pass filter with a passband from 10 to 275 Hz gives the highest ratio. However, during cycling at a load of 200, a passband of 9 to 275 gives the highest ratio. For cycling during recovery at a load of 50, a passband of 9 to 275 also gives the highest ratio.

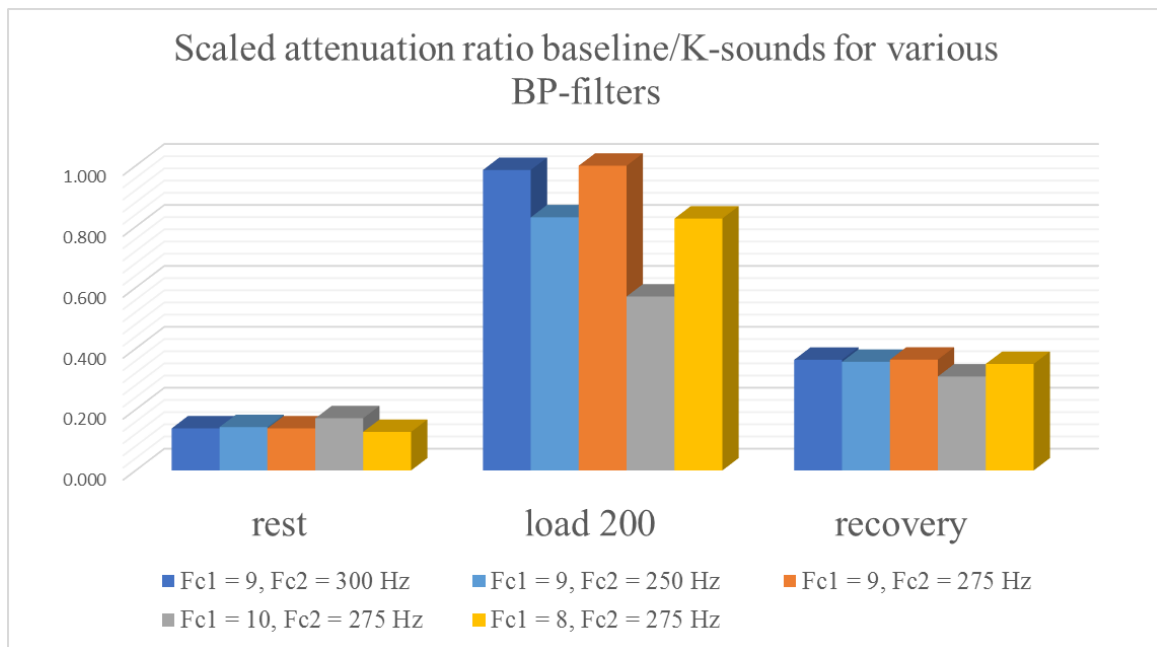


Figure 14: Scaled attenuation ratio of baseline over K-sound for various BP-filters

The average decreases of the baseline and K-sound for all three signals are shown in Table 6. A band-pass filter with a passband from 9 to 275 Hz gives the highest ratio with a ratio of about 2.6. For a passband from 9 to 275 Hz a decrease in baseline of about 52% and a decrease in baseline of 20% is observed.

Table 6: Average decrease percentages for signals rest, load 200 and recovery of various HP-filters

	Average decrease baseline	average decrease cut K-sounds	ratio
Fc1 = 9, Fc 2 = 300 Hz	51.894	19.933	2.603
Fc1 = 9, Fc 2 = 250 Hz	51.368	20.463	2.510
Fc1 = 9, Fc 2 = 275 Hz	51.896	19.677	2.637
Fc1 = 10, Fc 2 = 275 Hz	54.022	25.664	2.105
Fc1 = 8, Fc 2 = 275 Hz	49.356	19.843	2.487

7.4 Band-pass filter design with optimal passband

From the test results presented in paragraph 7.3.4 it can be concluded that the filter with a passband from 9 to 275 Hz provides the best results. The filters used in the experiment were of extreme high order, above 3000, to provide minimal transition band whilst having a flat passband and minimal ripple. However, these characteristics in the amplitude response have a tradeoff with the phase response. In the experiment case, a FIR filter of order 3163 yielded an average lead time of $0.5 \times 3163 \times (1/2500 \text{ Hz}) = 0.6326 \text{ s}$. As these tests are not influenced by an ultimately undesired phase response but a steep roll-off can help determine the optimal passband more accurately, these filters were used.

The main parameters defining the filter are:

- Sampling Frequency = 2500
- First Stopband Frequency = 9
- First Passband Frequency = 11
- Second Passband Frequency = 275
- Second Stopband Frequency = 277
- First Stopband Attenuation = 0.0001
- Passband Ripple = 0.057501127785
- Second Stopband Attenuation = 0.0001
- Density Factor = 20

Furthermore, the magnitude and phase response of the filter are depicted in Figure 15 below. Here the extreme steepness and minimal ripple of the passband become clearly visible.

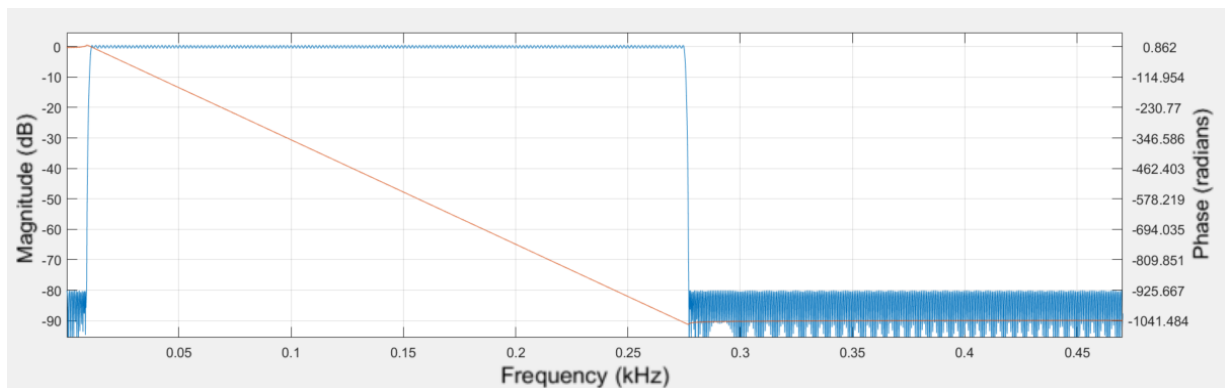


Figure 15: Band-pass filter design with optimal amplitude response

7.5 Final filter design

As stated in chapter 7.4, optimal cut-off frequencies were determined to be 9 and 275 Hz. However, these cut-off frequencies were determined for a filter with a transition band of only 2 Hz. As the final goal is to determine the start and end time of the k-sounds, the lead time of the filter will directly influence the error. As it is desired to have a smaller lead time than 0.6326 s, a lower order filter was designed. The order of the new filter is reduced to 253, meaning the lead time is reduced to $0.5 \times 253 \times (1/2500 \text{ Hz}) = 0.0506 \text{ s}$. The amplitude and phase response of the lower order filter are depicted in Figure 16.

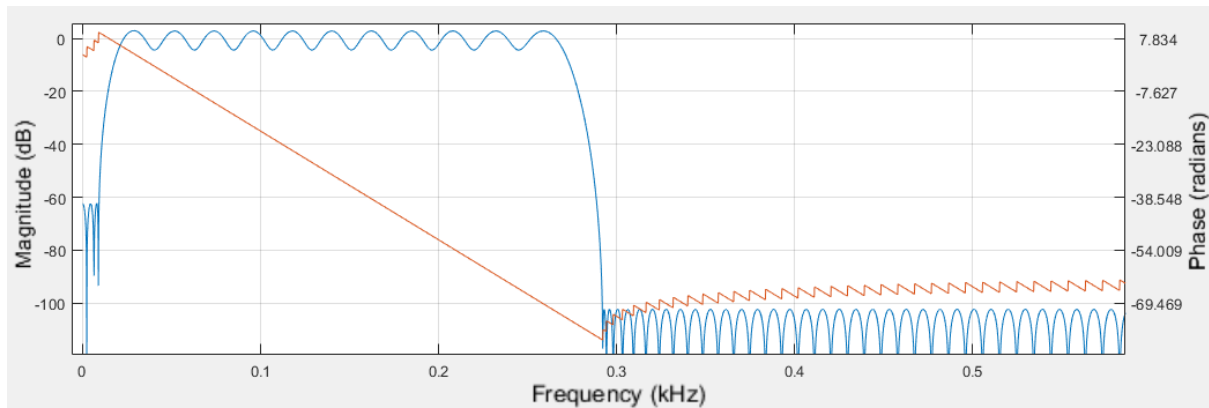


Figure 16: Band-pass filter design with balanced amplitude and phase response

When comparing the time series of the high and low order band-pass filters, depicted in Figure 17, a few things come to light. Firstly, most of the peaks of the k-sounds become less in amplitude. However, most of the peaks in the baseline also become less in amplitude. Most importantly, as the phase shift is linear, no significant shifts in time within each signal occurs.

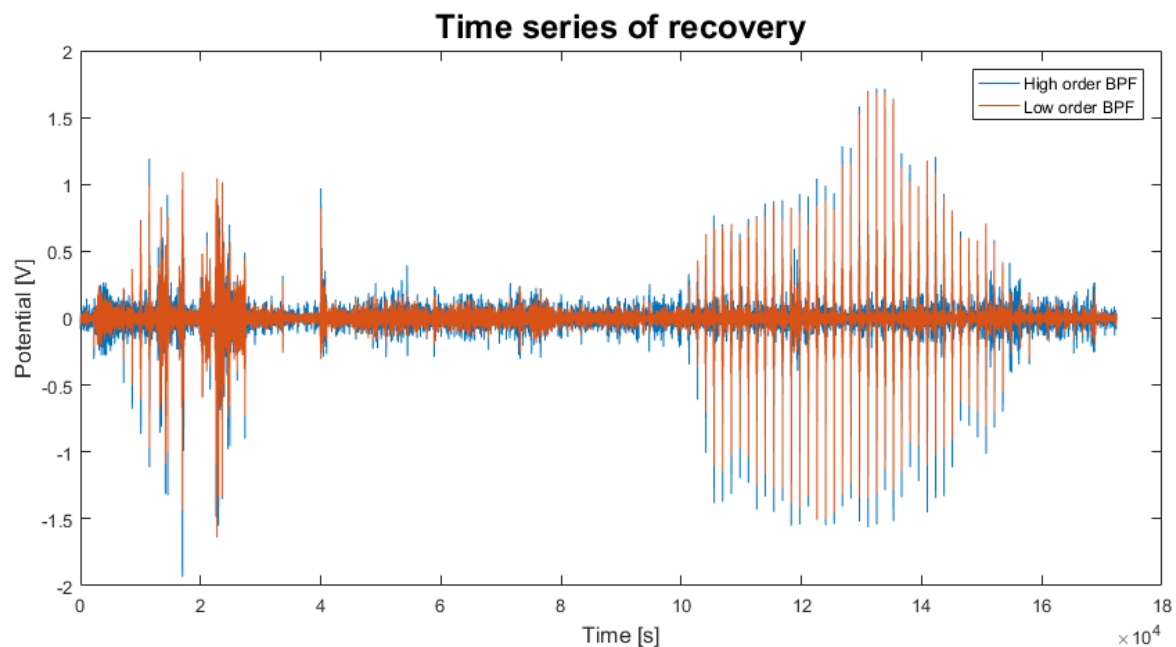


Figure 17: Time series of cycling at a load of 50 Watt filtered with the high and low order band-pass filters, adjusted for phase shift

The high order filter resulted in a maximum decrease is baseline over cut k-sounds of 2.6. The average decrease of the low order filter 2.4, as can be seen in Table 7. The group delay decreased of the high order and low order filter were 0.6 and 0.05 s respectively. The ratio decreased by 7.6% whilst the group delay decreased more than ten-fold.

Table 7: Average decrease percentages for signals rest, load200 and recovery for the low order BP-filter

	Average decrease baseline	Average decrease cut K-sounds	ratio
rest	40.977	39.878	1.028
load200	78.833	11.999	6.570
recovery	76.557	29.763	2.572
average	65.456	27.213	2.405

7.6 Korotkoff detection algorithm

The final goal is to detect the start and end time of K-sounds, indicating systolic and diastolic blood pressure. In order to achieve the detection of the start and end time of K-sounds, the developed algorithm has to be adaptive: it has to be able to adjust to the amount of noise, amplitude of the peaks of the K-sounds and select only the valid peaks. Adaptability to the amount of noise was realized by sampling the baseline and calculating the standard deviation of it. By sliding a window over the signal and calculating the standard deviation of the window, the spread of the signal could be evaluated locally. When the spread of the window is five times greater than the spread of the baseline, the local maximum is determined and stored. The selectivity of valid peaks was realized with a periodicity check. The time between peaks was calculated, after which an incrementing window ran forward and backward over the dataset. Over the window the standard deviation was calculated. Using some error margin, the standard deviation was only allowed to decrease. Once it increased, an indication was found for false detection of the peaks. Below each step will be explained in depth.

The main function of the peak detection algorithm is depicted in Figure 19. After starting, the program enters the initialize function, depicted in Figure 18. In initialize function the signal is being prepared for peak detection. Currently, the point in time where the pumps stop is determined manually because the mechanism used to inflate and deflate the cuff is outside of the scope of the project. However, once Lode B.V. develops inflation/deflation mechanism, the point in time where the pumps stop can be determined by monitoring the pump and valve controllers and registering the point in time where these turn off. The data from the DAQ is imported to Matlab from the putty generated log file. The mean of the dataset is calculated and subtracted from each sample to centre the signal around zero. The resulting signal is band-pass filtered with the filter design presented in Figure 16. The normalized and filtered dataset is stored as 'data in' and fed back to the main function.

Once in the main function, the dataset is split into timestamps labelled 'time', potentials generated by the microphone labelled 'signal' and the stop time of the pump. The baseline is sampled from the stop time of the pumps until the stop time plus 5 seconds. The standard deviation of the subset is calculated, multiplied by five, and stored as the threshold for peak detection.

The signal is looped through from start to end via a sliding window, over which the standard deviation is calculated. According to literature, the duration of K-sounds is between 37 and 98 ms [12]. The impulse response of the piezo microphone is roughly between 12 and 46 ms, as was determined from applied research. The experiment used to determine the impulse response can be found in Appendix B. Adding the impulse response to the duration of k-sound, an estimation of the minimal to be expected peak width is 49 ms and the maximum to be expected width is 144 ms. Therefore, to create a window over which the spread of the smallest peak is maximally large, a window size of 120 samples was selected as:

$$\begin{aligned} \text{window size} &= \text{sampling rate} * \text{min. peak width} \\ &= 2500 \text{ [Hz]} * 49 \text{ [ms]} \approx 123 \text{ [samples]} \end{aligned}$$

The maximum average HR for people under the age of 20 is considered to be 200 BPM and decreases with increasing age. [54] Therefore, the minimum distance between peaks is defined 750 samples, as:

$$\begin{aligned} \text{min. distance peak} &= \text{sampling rate} * \Delta t \text{ heartbeats} \\ &= 2500 \text{ [Hz]} * \frac{60 \text{ [s]}}{\text{maximum heart rate [BPM]}} \\ &= 750 \text{ [samples]} \end{aligned}$$

If the standard deviation of the window is larger than the threshold and no other peaks have been detected for 750 samples, the local maximum of the window is determined and stored and as a peak index. An example of a resulting dataset is depicted in Figure 20. However, there are three false detections at the start of the signal. Once the window is ran over the entire signal, the function ‘periodicity check’ is called.

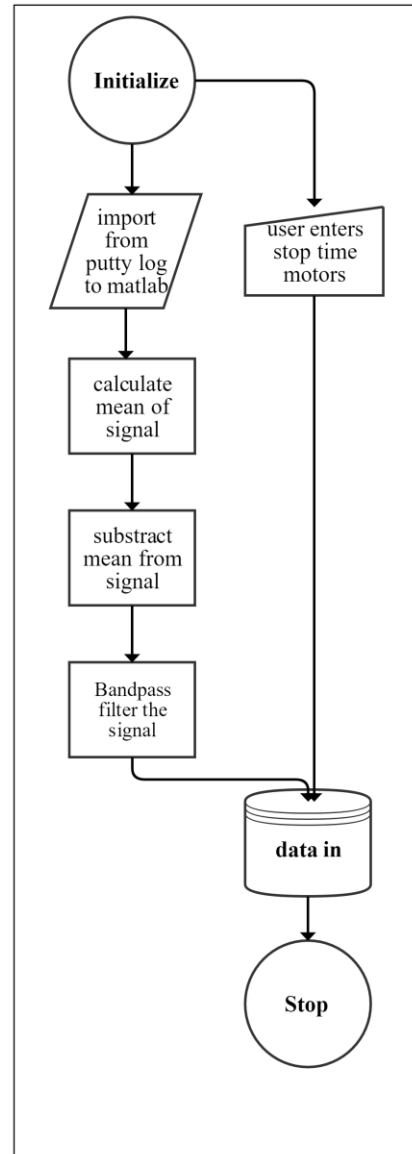


Figure 18: Initialize function of Korotkoff detection algorithm

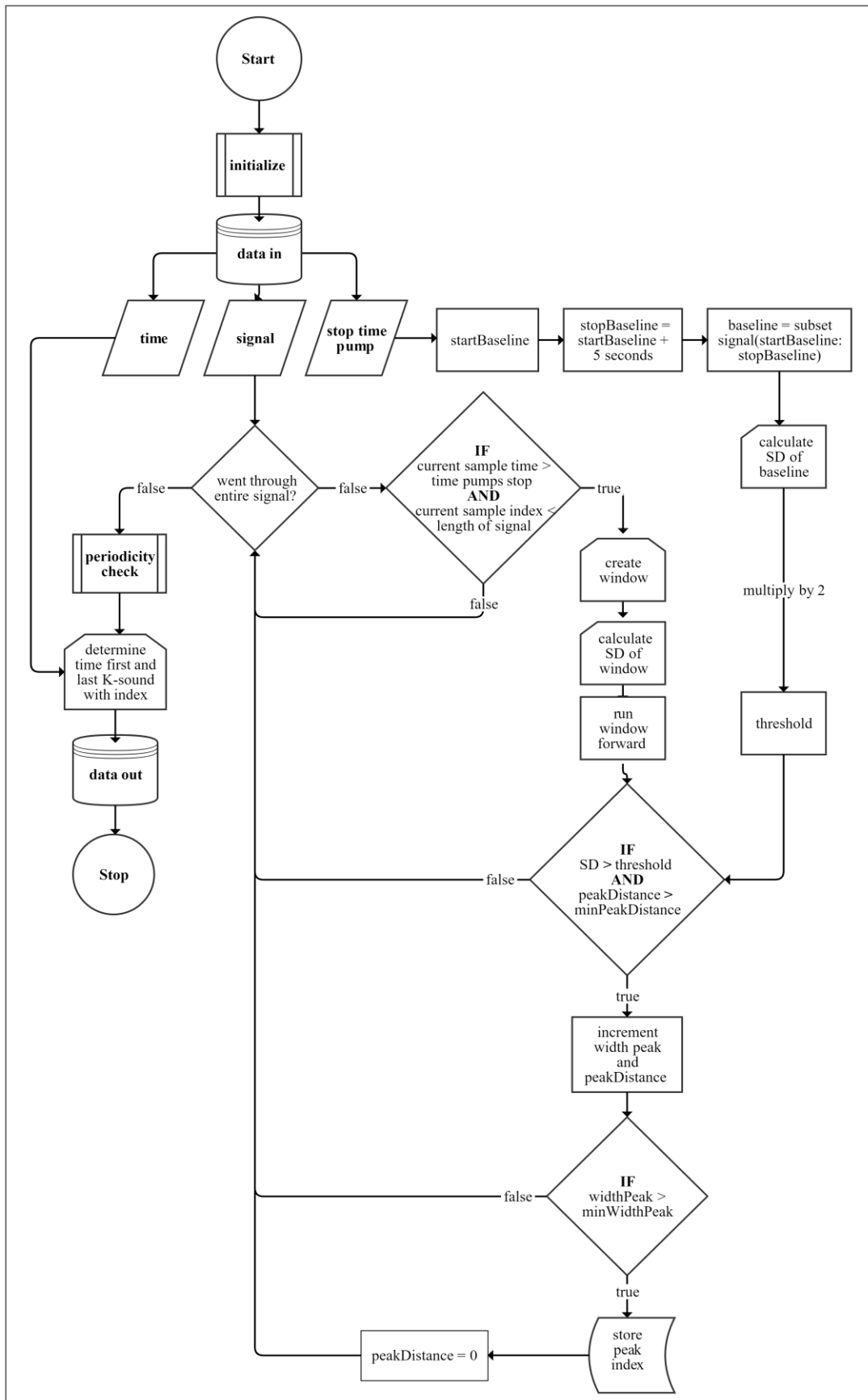


Figure 19: Main function of Korotkoff detection algorithm

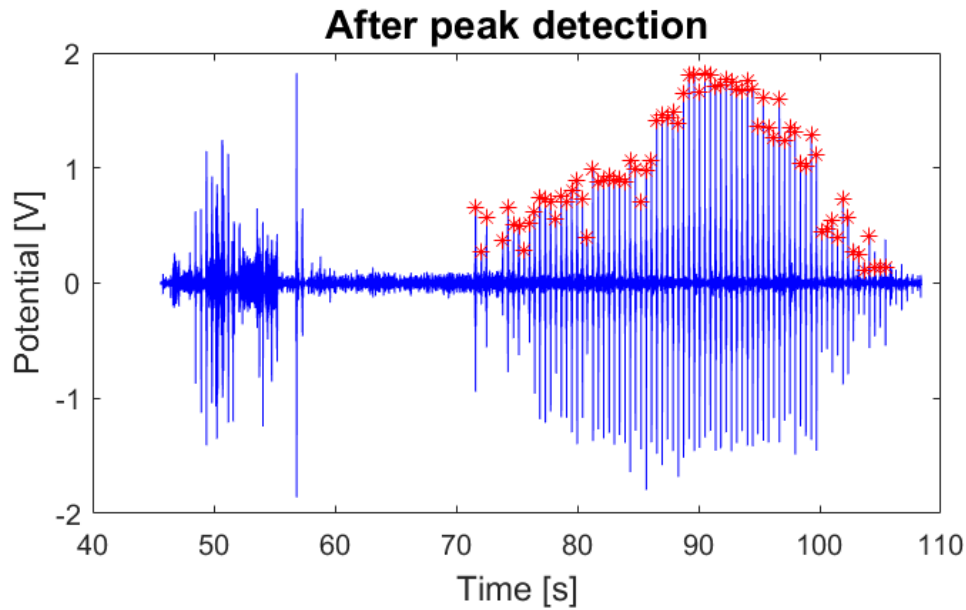


Figure 20: Filtered microphone signal after peak detection

A flow chart of the function ‘periodicity check’ is depicted in Figure 22. The periodicity check function accepts an array of peak indexes. From the array of peak indexes the distance between peaks, or delta peak index, is calculated. The delta peak index for the signal depicted in Figure 20 is plotted in Figure 21 as the blue striped line. The minimum to be expected HR and pulse pressure are 75 BPM and 22 mm Hg respectively [54] [55]. As the cuff pressure is deflated at 3 mm Hg/s, there will be K-sounds for at least 7.34 s. At an HR of 75 BPM, a single beat take 0.8 s on average, meaning that there will be at least 9 K-sounds present in the signal. Therefore, once the delta peak index array is calculated, a window is created of size $N = 8$ to prevent indexing problems. The standard deviation is calculated over the window after which the size is incremented. The same is done forwards and backwards, depicted by the orange and yellow dots in Figure 21.

Periodicity check via expanding SD window

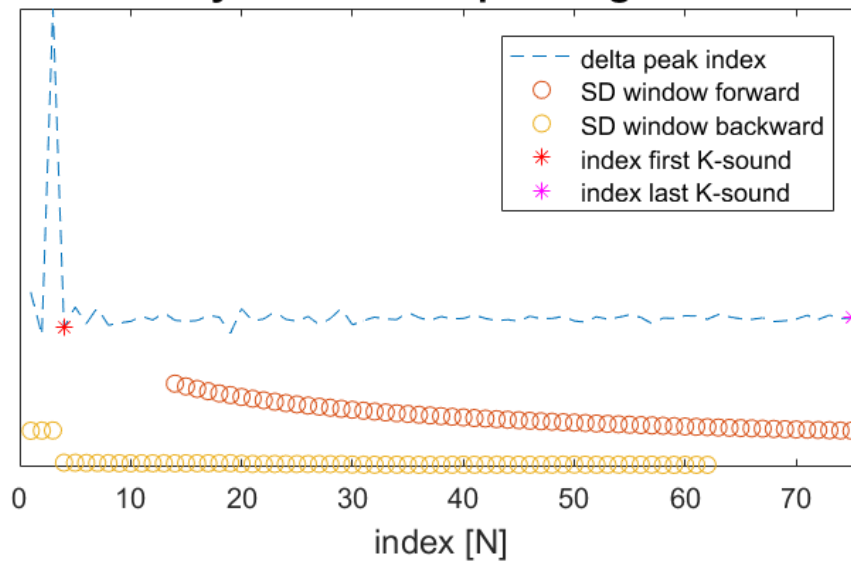


Figure 21: Periodicity check via a forward and backward expanding window, over which the standard deviation is calculated and only allow to decrease

When the peak distance is constant, the standard deviation will decrease as the amount of samples increase:

$$standard\ deviation = \sqrt{\frac{1}{N-1} \sum (x_i - \bar{x})^2}$$

The decrease in standard deviation can be clearly seen in the window incrementing forward in Figure 21. As the standard deviation keeps decreasing, the last peak index is stored as the last valid peak index. However, the backwards incrementing window encounters a steep increase in delta peak index. The steep increase in delta peak index causes the standard deviation over the entire window to increase, making the algorithm select the fourth peak index as the first valid peak index.

However, when the peak distance is irregular, the standard deviation increases, indicating false detections. As it is only desired to determine the start and end time of the K-sounds, false detection after the first or before the last K-sounds does not influence the accuracy of the outcome. However, these false detection will cause variations in the standard deviation of the increasing window. Furthermore, conditions like arrhythmia can also cause variation in the calculated standard deviation [56]. Therefore, an error margin, or max. step size has to be implemented.

The values of delta peak index vary with HR and false detections. The standard deviation varies with delta peak index and decreases with sample size. As these numbers vary greatly for dataset to dataset, the max. step size has to scale with these variations. Therefore, the max. step size was experimentally determined to be:

$$max.\ step\ size = mean(delta\ peak\ index) * \frac{1.5}{N}$$

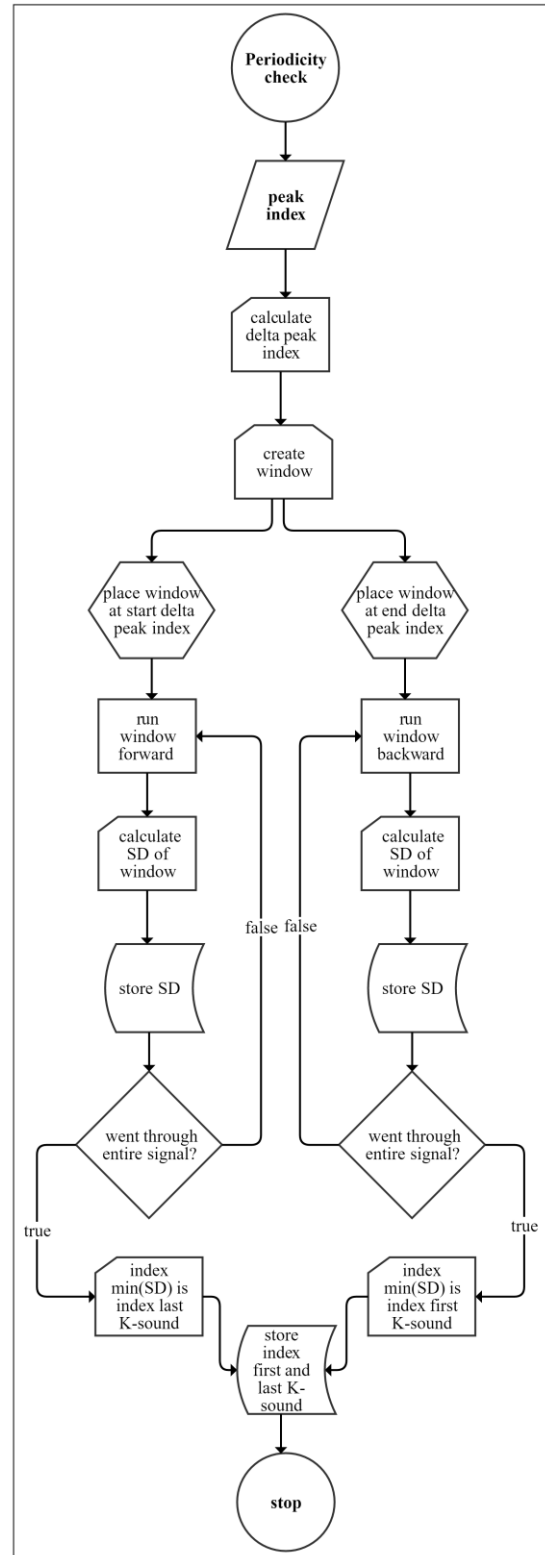


Figure 22: Periodicity check of Korotkoff detection algorithm

8

CONCLUSIONS

The auscultatory method was selected as a basis for the to be designed BP monitoring system. The selection of the auscultatory method was justified with data from literature research on currently used and experimental methods for measuring BP. Literature research indicated that the auscultatory method scored best on each evaluated property except motion tolerance. The evaluated properties were rated according to their correspondence to the formulated requirements and the central research question.

8.1 Sub-questions answered

The sub-questions formulated to aid in answering the central research question are the following:

- Q What methods can be applied to monitor blood pressure?
A *Multiple methods can be used to monitor BP under stress conditions, however few can do this for SBP and DBP with medical grade accuracy. The auscultatory method approximates systemic arterial pressure accurately due to its physical properties such as measurement location and method.*
- Q How resilient to motion artefacts are these methods compared to the mostly used oscillometric methods?
A *The methods used in popular BP monitors and their advertised purpose indicate that the oscillometric method is not used in stress testing. Some used methods are auscultatory and finger cuff.*
- Q Can these methods be used to obtain medical grade precision according to ANSI/AAMI standards?
A *In order to reach medical grade precision according to ANSI/AAMI standards, the developed system has to be validated on all population groups and conditions. Validation is done using an auscultatory reference sphygmomanometer [30]. What methods are possible to be used under stress condition will have to be determined in future applied research.*
- Q What causes motion artefacts to induce noise in auscultatory NIBP monitoring?
A *BP monitors based on the auscultatory method mostly use a piezo microphone to detect k-sounds. Piezo elements convert mechanical stress to electric potential. The piezo elements used in the microphone are maximally flat. The flatness is to maximize potential from k-sounds and minimize potential from motion artefacts. By being maximally flat, sideways vibrations are picked up less by the microphone. However, motion will still induce onto the obtained signal. I suspect a large quantity of the noise induced by motion is caused by the movement of the cables and varying muscle tension.*

- Q How can artefacts be filtered in an auscultatory NIBP monitoring system?
- What type of filters are able to do so? *Both analogue and digital filters.*
 - What type of filters are used by existing products? *Analogue and digital filters such as anti-aliasing and ECG-gating.*
 - How can this filter be implemented into an embedded system? *Via a digital signal processor optimized for digital filtering.*
- A *The main advantages of analogue filters are easy implementation and minimal components. The main advantages of digital filters are their adaptability and wide variety of possibilities. ECG-gating is used in NIBP monitor signal processing as it can be used to indicate the location of the K-sounds, resulting in a more selective K-sound detection algorithm. The implementation of a digital filter into an embedded system can be done with a separate digital signal processor or a processor with integrated DSP functionality.*

8.2 Research question answered

The central research question was formulated as follows:

How can blood pressure be monitored automatically whilst the patient is under stress conditions on a bicycle ergometer using non-invasive techniques?

To which the answer is:

Automate the auscultatory method using a piezo microphone, electronic pumps and valves. Filter the microphone data and use a peak detection algorithm to detect the start and end time of the K-sounds. Cross reference the start and end time of the K-sounds with cuff pressure on a time scale to arrive at SBP and DBP.

8.3 Developed system

The developed system comprises of a DAQ, a digital filter and a peak detection algorithm with periodicity check. The DAQ was proven to function correctly on component level and yielded signals with a 16-bit resolution and a sampling speed of 2500 Hz. The system was optimized for functioning under constantly changing conditions by being adaptive.

False positive detections between the beginning and ending of K-sounds were allowed, as the goal was to detect the start and stop time of the K-sounds. In order to filter out false positively detected K-sounds, a periodicity check was implemented. The fundamental principle of the periodicity check algorithm is the physical property that, even as the HR of the patient changes over the duration of a stress test, during a single measurement the HR is more or less periodic. As no strict bounds can be laid on HR, due to the possibility of many false detections or a slightly changing HR, an adaptive algorithm was developed.

8.4 Success factors

In this paragraph the work presented will be evaluated by reflecting on the success factors formulated in chapter 1.1.

Success factor: extensive analysis of motion artefacts using an existing NIBP monitoring system

Evaluation: the cuff with microphone from Lode B.V. and Kadenz OEM module from SunTech were used in combination with the designed DAQ to obtain signals during rest and stress conditions. These were thoroughly analysed to develop a filter and detection algorithm. The most important time-frequency analyses used are presented in appendix C and include the Fast Fourier Transform and Wavelet Transform

Success factor: development of a filter which is able to filter measured signals

Evaluation: the digital filter is able to reduce the spread of the noise and cut k-sounds by 65% and 27% respectively and is able to filter measured signals

Success factor: development of a detection algorithm capable of determining the start and end time of K-sounds

Evaluation: the algorithm developed was able to detect K-sounds and in most cases filter out only the valid K-sounds

Optional success factors were the following:

Success factor: implementation of an embedded system capable of filtering BP signals real-time

Evaluation: the implementation an embedded system was not achieved, however advice on the development of one is included into the future recommendations

8.5 Meeting the requirements

In order to verify that the requirements are fulfilled, a complete BP monitoring system is required. As only part of a complete BP monitoring system was developed, a reflection based on my insight about the probability of a future system meeting these requirements is given in chapter 10.

8.6 Final conclusion

The work presented here is a solid first step towards the development of a non-invasive BP monitoring system for usage under stress conditions. The most challenging topics have been addressed. Literature research provided a clear outcome: the auscultatory method was the most viable method. The applied research conducted was extensive, providing insight into the complexity of the task. An effective digital filter was realized via time-frequency analysis of measured signals. Furthermore, the basis of a robust peak detection algorithm is ready for testing on a larger dataset.

9

DISCUSSION

The work presented here addresses the most complex parts of an auscultatory based, non-invasive BP monitor: the signal processing and data interpretation. The development of control circuitry, embedded architecture and firmware are areas Lode B.V. is already familiar with. The viability of Lode B.V. developing a BP monitor has increased by addressing the signal processing and data interpretation required in an auscultatory BP monitor. Moreover, opportunities provided by an in-house BP monitor have become more realistic. A larger profit margin on bicycle ergometers, increased company knowledge and independency of SunTech have become more attainable.

9.1 Literature & Applied research

Based on literature research the auscultatory method was selected as a basis for the to be developed BP monitor. The method was selected because of its excellent usability during stress testing. Applied research indicated that with proper filtering and adaptive detection algorithms, it is possible to detect the start and end time of K-sounds. This confirms the predicted usability during stress testing.

9.2 Method of collecting data

Testing indicated that when patients undergo stress their K-sounds contain more high frequencies. As these K-sounds become higher frequent they also increase in amplitude. A set of signals demonstrating this with time-frequency analysis can be found in appendix C. The static gain used in the DAQ was 30 V/V and resulted in low amplitude K-sounds in rest and clipping whilst under stress conditions. Although the clipping did not present major issues, the clipping peaks will contain more high frequencies as they are sharply cut off. This might have influenced time-frequency analysis used.

Although the procedure for obtaining first hand data was carefully thought out the usage of an external system for pumping and deflating the cuff proved to be clumsy. The starting time of the baseline, which is a required input for the peak detection algorithm, had to be determined manually. Furthermore, at the start of an experiment the Kadenz and DAQ had to be started around the same time.

9.3 Calibration of peak detection parameters

The amount of usable signals was small due to an unstable DAQ. This resulted in the peak detection algorithm being tested on a small dataset. The dataset consists of three persons in rest, maximal load and recovery conditions. The main parameters defining the peak detecting algorithm will have to be fine-tuned during future testing. The most important parameters which will have to be fine-tuned are the following:

- Minimum peak distance, currently 0.3 s
- Minimum amount of K-sounds in a signal, currently 9 peaks
- The amount of standard deviations K-sounds are greater than the baseline, currently 5 standard deviations

9.4 Digital filter

I am confident that the cut-off frequencies determined are close to optimal. However, the low order filter design might not be optimal. As stated before, the low order filter design was realized experimentally based on insight and thorough testing. It was validated to approximate the high order filter, however a more optimal design might be possible.

10

FUTURE RECOMMENDATIONS

Recommendations on how to proceed towards the development of a complete BP monitor will be presented here. First, I will discuss potential improvements on the work presented followed by chronologically ordered steps on how to proceed. A possible configuration of a finalized system will also be given. Finally, I will discuss what should be taken into account to reach the requirements with a complete BP monitor.

10.1 Improvements

To prevent clipping, an adaptive gain which scales based on the incoming signal should be implemented. Adaptiveness in the gain can be achieved by monitoring the peak-to-peak amplitude of the incoming signal and using a programmable gain that adjust accordingly. However, as the baseline has a low peak-to-peak amplitude compared to the K-sounds, the implementation will result in the baseline becoming maximally amplified. Therefore the maximum gain should be such that a maximum amplitude K-sound utilizes the rail-to-rail voltage as much as possible. Testing on a large dataset will be necessary to determine the optimal gain. However, this should be done to prevent the baseline becoming amplified unnecessarily much. Even though the baseline will usually get amplified more than the K-sounds, digital filtering will counteract this by attenuating the baseline more than the K-sounds.

If testing indicates that the baseline becomes amplified too much with respect to the K-sounds, a digital filter can be considered with a higher gain for certain frequencies instead of the currently flat passband. Furthermore, it might be useful to shift the frequencies amplified linearly with the increase in programmable gain. However, more research into the frequency shift in K-sounds under stress conditions will have to be conducted.

Furthermore, functionality should be implemented to reduce the period in which the cuff is inflated. During a stress test the cuff will get inflated many times, which can be an uncomfortable process. Reducing the period in which the cuff is inflated will increase patient comfort. The inflated period can be reduced in two ways:

1. Inflate the cuff to a pressure just above SBP
2. Deflate the cuff when the pressure reaches just below DBP

To inflate the cuff to a pressure just above SBP, the system has to detect K-sounds during the inflation of the cuff. A complexity here is the generation of vibrations by the pump which are carried through the wires and tube to the microphone. However, I believe it can be done as the vibrations of the pump comprise of higher frequencies than K-sounds.

To be able to deflate the cuff when the pressure reaches just below DBP, the designed peak detection algorithm has to run real-time. This means that the signal has to be processed shortly after it is sampled. The peak detection and periodicity check algorithms will have to be adjusted to do so. Real-time peak detection can be achieved by letting incoming signal slide through the window over which the standard deviation is calculated instead of the other way around. The periodicity check can be made to run real-time by incrementing the window with each detected peak. Once the peak detection algorithm has detected a peak, it should directly feed its index to the periodicity check. When the periodicity check has found the last K-sound, the cuff can be deflated. During the time it takes to deflate the cuff, the backwards periodicity check can run to determine the first K-sound. If the process proves to be too demanding in computational power, a system in which the two are done in parallel can be considered.

The implementation of the following points should lead to an improvement over the design presented in this report:

- Programmable gain
- Filter with higher gain for certain frequencies
- Detection of K-sounds during inflation of the cuff
- Real-time filtering and peak detection

10.2 Proceedings

In this paragraph I will provide a provisional procedure of steps required to develop a complete BP monitor. First, a database of K-sounds should be created with as many population groups as possible and a large spread in ages, under rest and stress conditions. To do so, I recommend the following steps:

1. Develop the inflation mechanism of the cuff
2. Develop a stable DAQ with the improvements mentioned in chapter 10.1
3. Validate the DAQ
4. Obtain signals with the improved DAQ and inflation mechanism to create a database of K-sound signals

After the above procedure has been completed, the algorithms should be adjusted to run real-time and be integrated into an embedded environment. Furthermore, the embedded architecture has to be designed whilst taking medical safety regulation into account. Afterwards, the whole system has to be validated.

1. Research into the possibilities and limitations of implementing the peak detection and periodicity check algorithms into an embedded system
2. Adjust the peak detection and periodicity check algorithms so that they can function real-time. Simulate the found requirements using Matlab or similar software and confirm its proper functioning
3. Develop an algorithm that automatically determines the optimal parameters of the peak detection and periodicity check algorithms. To do so, first manually determine the correct amount and location of the K-sounds of every signal in the database. Feed the amount of K-sounds and their location together with the signal into the algorithm
4. Create an embedded version of peak detection where signals can be filtered real-time
5. Create a test setup where signals from the database can be fed into the embedded system using a high precision digital-to-analogue converter. I think this test setup will be worth the effort as the embedded system can be tested quickly and easily after making adjustments
6. Validate the embedded system using measured signals
7. Design the architecture of the whole embedded environment, including all safety regulations
8. Test and validate the system carefully
9. Outsource the actual validation according to ANSI/AAMI SP10 standards

After these steps are completed the BP monitor should be market ready. In the next chapter I will elaborate more on my ideas of a final product design.

10.3 Final product design

A possible architecture for the complete BP monitor is depicted in Figure 23. The inflatable cuff with microphone are already developed and validated by Lode B.V. [51]. The DAQ, consisting of an instrumentation amplifier, anti-aliasing filter and ADC have been developed but are unvalidated. Other blocks, coloured red, still have to be developed and validated.

Signals from the microphone are passed through the DAQ and are fed into a DSP. In the DSP the signal is band-pass filtered after which the signal is fed to the main processor. In the main processor the peak detection and periodicity check are implemented. The main processor sends commands to a pump controller which is responsible for inflating the cuff. The cuff pressure is monitored by transducers which feed pressure data to the pumps and valves controllers for a closed control loop. Furthermore, the transducers send data to the main processor used in the determination of SBP and DBP. Moreover, the data is send to the safety processor for monitoring. The safety processor contains a watchdog timer monitoring the main processor. It also monitors cuff pressure, inflation time and is able to control the valves. The safety processor is implemented to increase patient safety which is required meet medical legislation.

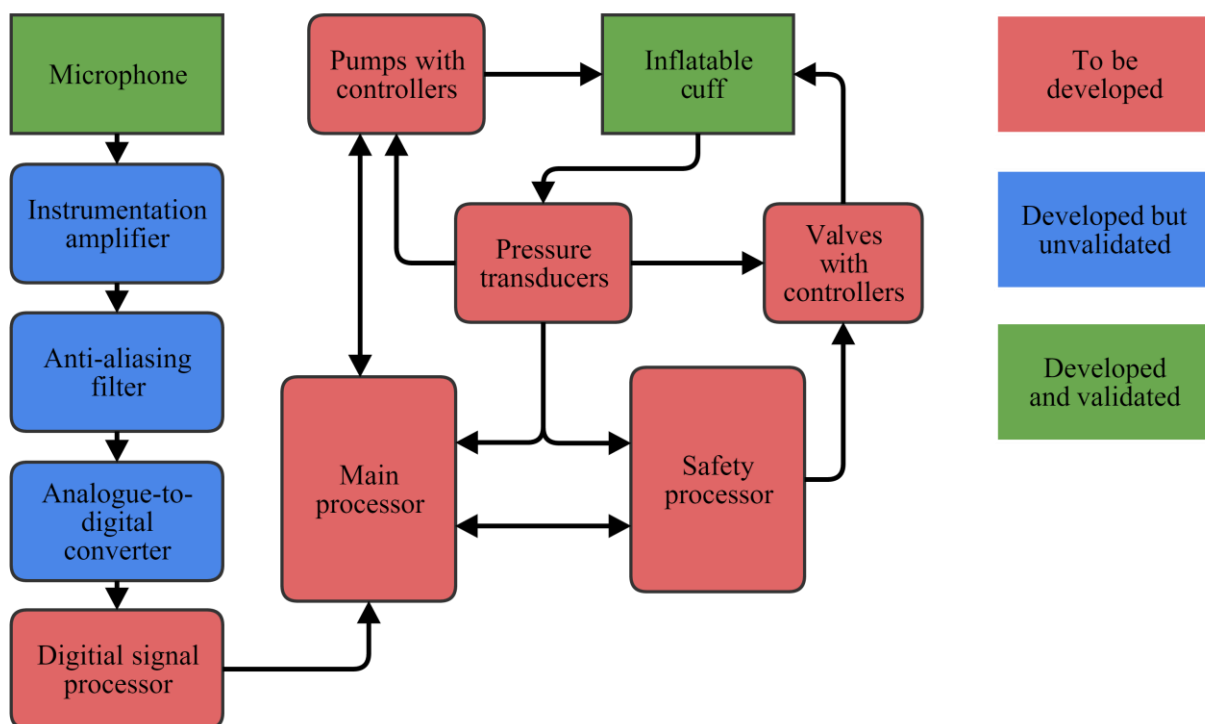


Figure 23: Possible configuration of the finalized BP monitor

10.4 Requirements

The system described in paragraph 10.3 should be capable of meeting the requirements presented in Table 8. To reach requirements 1 and 2, the cuff should be able to hold a pressure of 250 mm Hg and the pumps should be able to reach a pressure higher than 250 mm Hg, taking the resistance of tubing and valves into account. Furthermore, the microphone should be able to detect K-sounds under a high pressure of 250 mm Hg and a low pressure of 20 mm Hg. However, these capabilities have already been validated by Lode B.V.

To reach requirement 3, a cuff inflation time that is limited to 50 seconds, I recommend making the deflation rate scale with the final inflation pressure. By doing so the cuff will deflate in about the same time for a measurement in rest and at maximum load. However, first the relationship between increasing SBP and increase in HR during stress testing should be investigated. At a higher HR K-sounds are more closely together, meaning the cuff can deflate faster without losing precision. If an HR is available it can simply be used to scale with the deflation rate. A faster deflation rate will also help in reaching requirement 4, a maximum measurement duration of 160 seconds.

To obtain clinical accuracy the system has to be validated on all population groups and ages. Testing under extreme conditions have to be considered, such as high blood pressure and stiff arteries, resulting in very high BP. To reach requirement 5 the system has to be adaptive, robust and have excellent repeatability. Steps towards achieving this have been described but applied research will have to point if these steps are sufficient.

Table 8: Requirements of the to be developed non-invasive BP monitoring system

#	Property	Requirement	Reasoning
1	SBP Range (mm Hg)	40 - 250	Minimum to be expected is 40, maximum to be expected is 250
2	DBP Range (mm Hg)	20 - 150	Diastolic readings can continue to around zero mm Hg
3	Patient Safety	Cuff inflation limited to less than 50 seconds	Preventing prolonged blocking of blood stream
4	Measurement time	Duration of BP reading limited to 160 seconds	Able to take frequent readings during stress test
5	Clinical Accuracy	ANSI/AAMI SP10:2002 (mean difference (SD) ≤ 5 (8) mm Hg)	Reliable output for research, medical procedures and rehabilitation

The above-mentioned points are not excluded by the work presented here. However, improvements will have to be made on the developed system to reach the requirements. Requirement 5, clinical accuracy, was taken as a leading factor during the development process. The main finding was that in order to reach clinical accuracy, the system has to be adaptive to the incoming signal.

BIBLIOGRAPHY

- [1] Institute for health metrics and evaluation, "Deaths from cardiovascular disease increase globally while mortality rates decrease," IHME, [Online]. Available: <http://www.healthdata.org/news-release/deaths-cardiovascular-disease-increase-globally-while-mortality-rates-decrease>. [Accessed 28 5 2016].
- [2] J. Choquel, "The history of blood pressure monitoring," Health Boosters, [Online]. Available: <http://blog.withings.com/2014/05/21/the-history-of-blood-pressure/>. [Accessed 18 6 2016].
- [3] SunTech, "Tango M2," 2016. [Online]. Available: <http://www.suntechmed.com/bp-devices-and-cuffs/stress-bp-monitors/tango-m2>. [Accessed 16 02 2016].
- [4] Finapres, "Finapres Medical Systems | Portapres," Finapres, [Online]. Available: <http://www.finapres.com/Products/Portapres>. [Accessed 23 02 2016].
- [5] E. britannica, "Pascal's principle," [Online]. Available: <http://www.britannica.com/science/Pascals-principle>. [Accessed 16 02 2016].
- [6] C. & Brown, Introduction to Biomedical Equipment Technology, Noida: Pearson Education, Inc., 2007.
- [7] M. & Hoehn, Human Anatomy & Physiology, Pearson Education, Inc., 2013.
- [8] S. Medical, "An Introduction to Automated Blood Pressure Monitoring," 31 08 2009. [Online]. Available: <http://blog.suntechmed.com/blog/32-bp-measurement/261-an-introduction-to-automated-blood-pressure-monitoring>. [Accessed 18 02 2016].
- [9] M. F. Matthew Ward, "Blood Pressure Measurement," Medscape, 4 7 2007. [Online]. Available: http://www.medscape.com/viewarticle/563819_5. [Accessed 6 7 2016].
- [10] K.-G. NG, "Survey of automated noninvasive blood pressure monitors," Journal of clinical engineering, Ontario, 1994.
- [11] Y. David, W. W. v. Maltzahn, M. R. Neuman and J. D. Bronzino, 15: Noninvasive Arterial Blood Pressure and Mechanics, 2003.
- [12] J. Allen, "Characterization of the Korotkoff sounds using joint time–frequency analysis," 8 12 2003. [Online]. Available: <http://iopscience.iop.org/article/10.1088/0967-3334/25/1/010/meta;jsessionid=0164AE905B7BBB09B4F4230B593247FE.c4.iopscience.cld.iop.org>. [Accessed 5 4 2016].
- [13] HARTMANN, "Tensoval," 2016. [Online]. Available: <http://tensoval.com/oscillometric-measurement-devices.php>. [Accessed 16\ 02 2016].
- [14] D. N. Townsend, "Oscillometry," 2001. [Online]. Available: http://www.robots.ox.ac.uk/~neil/teaching/lectures/med_elec/notes8.pdf.

- [15] CB, "BioMed Central," 2012. [Online]. Available: <http://biomedical-engineering-online.biomedcentral.com/articles/10.1186/1475-925X-11-56>. [Accessed 16 02 2016].
- [16] C. Clinic, "Cardiac MRI Adenosine Stress Test," [Online]. Available: <http://my.clevelandclinic.org/services/heart/diagnostics-testing/radiographic-tests/cardiac-mri-adenosine-stress-test>. [Accessed 8 3 2016].
- [17] M. S. Kurl, M. J.A. Laukkanen, M. P. M. R. Rauramaa, M. P. T.A. Lakka, M. P. J. Sivenius and M. P. M. J.T. Salonen, "Systolic Blood Pressure Response to Exercise Stress Test and Risk of Stroke," 11 2000. [Online]. Available: <http://stroke.ahajournals.org/content/32/9/2036.full>. [Accessed 18 2 2016].
- [18] MedScape, "Treadmill Stress Testing," WebMD LLC, 22 11 2015. [Online]. Available: <http://emedicine.medscape.com/article/1827089-overview>. [Accessed 11 2 2016].
- [19] T. Pickering, J. Hall, L. Appel, B. Falkner, J. Graves, MN, Jones, K. T, S. SG and E. Roccella, "Recommendations for Blood Pressure Measurement in Humans and Experimental Animals: Part 1: Blood Pressure Measurements in Humans: A Statement for Professionals From the Subcommittee of Professional and Public Education of the American Heart Association Co," 2005.
- [20] K. C. Manning DM and K. J. Miscuffing, "inappropriate blood pressure cuff application," 1983.
- [21] M. A. Chen, "Exercise stress test," MedlinePlus, 02 02 2016. [Online]. Available: <https://www.nlm.nih.gov/medlineplus/ency/article/003878.htm>. [Accessed 11 02 2016].
- [22] SunTech, "Advantages of Automated Blood Pressure Measurement during Cardiac Stress Testing," SunTech, 30 11 2009. [Online]. Available: <http://blog.suntechmed.com/blog/30-cardiac-stress-bp/273-advantages-of-automated-blood-pressure-measurement-during-cardiac-stress-testing>. [Accessed 16 02 2016].
- [23] SunTech, "SunTechMed Tang+ stress BP," 11 10 2008. [Online]. Available: <http://www.suntechmed.com/pricing-support/customer-support/download-library/finish/36-tango-user-guide/171-tangomanualenglish>. [Accessed 16 02 2016].
- [24] S. Medical, "Exercise Stress Testing- The Importance of The Importance of," 2007. [Online]. Available: http://www.suntechmed.com/downloads/Tangoplus/white_papers/82-0084-00-MD-RevA.pdf. [Accessed 29 02 2016].
- [25] J. Villeneuve, Artist, *Blood pressure during exercise*. [Art].
- [26] SunTech medical MDD, "Classification," 2015.
- [27] Health, European Union Public, "Sphygmomanometers," 2009. [Online]. Available: http://ec.europa.eu/health/scientific_committees/opinions_layman/sphygmomanometers/en/1-3/7.htm. [Accessed 8 3 2016].
- [28] Blood pressure UK, "The facts about blood pressure," 2008. [Online]. Available: <http://www.bloodpressureuk.org/microsites/u40/Home/facts/Whatisnormal>. [Accessed 9 6 2016].
- [29] SunTech Medical, "OEM BP Kadenz Module," 2005.

- [30] A. N. Standard, "ANSI/AAMI/ISO 81060-2:2013," 2013. [Online]. Available: http://my.aami.org/aamiresources/previewfiles/8106002_1306_preview.pdf. [Accessed 7 6 2016].
- [31] E. W. Weisstein, "Doppler Effect," science world wolfram, 2007. [Online]. Available: <http://scienceworld.wolfram.com/physics/DopplerEffect.html>. [Accessed 22 3 2016].
- [32] S.-S. Chio, "Korotkoff sound versus oscillometric cuff sphygmomanometers: comparison between auscultatory and DynaPulse blood pressure measurements," 1 1 2011. [Online]. Available: <http://www.sciencedirect.com.proxy.hanze.nl/science/article/pii/S1933171110002159>. [Accessed 22 02 2016].
- [33] SunTech Medical, "Cycle stress BP," [Online]. Available: <http://www.suntechmed.com/support/document-library/send/25-instructions-and-manuals/127-cyclemanualenglish>. [Accessed 17 5 2016].
- [34] C. Liu, "Comparison of Repeatability of Blood Pressure Measurements between Oscillometric and Auscultatory Methods," 11 2015. [Online]. Available: https://www.researchgate.net/publication/281649386_Comparison_of_Repeatability_of_Blood_Pressure_Measurements_between_Oscillometric_and_Auscultatory_Methods. [Accessed 22 02 2016].
- [35] S. Healthcare, "Oscillometric vs Calculated MAP: Why doesn't it always," 2015. [Online]. Available: <http://www.spacelabshealthcare.com/wp-content/uploads/2015/06/850-0490-00-Rev-A-MAP-ABP-Case-Study-1.pdf>. [Accessed 23 02 2016].
- [36] J. Johansson, P. Puukka and A. Jula, "Oscillometric and auscultatory blood pressure measurement in the assessment of blood pressure and target organ damage.," 19 02 2014. [Online]. Available: <http://www.ncbi.nlm.nih.gov/pubmed/24247364>. [Accessed 23 02 2016].
- [37] D. J. Turney., "Sphygmomanometers," Public health Europa, 2009. [Online]. Available: http://ec.europa.eu/health/scientific_committees/opinions_layman/sphygmomanometers/en/1-3/4.htm. [Accessed 22 3 2016].
- [38] SunTech Medical, "Advantage A+," SunTech Medical, [Online]. Available: <http://www.suntechmed.com/oem-nibp-solutions/modules/advantage-a>. [Accessed 17 05 2016].
- [39] S. Healthcare, Artist, *Oscillometric vs Calculated MAP: Why doesn't it always*. [Art].
- [40] U. o. Leicester, "Ground-breaking technology will revolutionise blood pressure measurement for first time for over a century," 21 02 2011. [Online]. Available: <http://www2.le.ac.uk/offices/press/press-releases/2011/february/ground-breaking-technology-will-revolutionise-blood-pressure-measurement-for-first-time-for-over-a-century>. [Accessed 16 02 2016].
- [41] T. Keulen, "Continuous blood pressure monitoring," Groningen, 2012.
- [42] Maisense, "Freescan Technology," [Online]. Available: <http://maisense.com/index.php/en/freescan/technology.html>. [Accessed 16 02 2016].

- [43] M. Sheldon G. Sheps, "How accurate are wrist blood pressure monitors?," 5 6 2015. [Online]. Available: <http://www.mayoclinic.org/diseases-conditions/high-blood-pressure/expert-answers/wrist-blood-pressure-monitors/faq-20057802>. [Accessed 23 02 2016].
- [44] Healthstats, "A-PULSE CASPro® Specifications," [Online]. Available: http://www.healthstats.com/index3.php?page=product_apulsepro_spec. [Accessed 23 02 2016].
- [45] B. W. Beulen, N. Bijmens, G. G. Koutsouridis, P. J. Brands, M. C. Rutten and F. N. v. d. Vosse, "Toward Noninvasive Blood Pressure Assessment in Arteries by Using Ultrasound," 31 01 2011. [Online]. Available: [http://www.umbjournal.org/article/S0301-5629\(11\)00080-9/abstract](http://www.umbjournal.org/article/S0301-5629(11)00080-9/abstract). [Accessed 21 3 2016].
- [46] T. G. Pickering, D. Phil, J. E. Hall, L. J. Appel, B. E. Falkner, J. Graves, M. N. Hill, D. W. Jones, T. Kurtz, S. G. Sheps and E. J. Roccella, "Recommendations for Blood Pressure Measurement in Humans and Experimental Animals," CrossMark, 20 12 2004. [Online]. Available: <http://hyper.ahajournals.org/content/45/1/142.full>. [Accessed 23 02 2016].
- [47] M. Golparvar, "Evaluating the Relationship Between Arterial Blood Pressure Changes and Indices of Pulse Oximetric Plethysmography," 2002. [Online]. Available: https://www.researchgate.net/publication/11014450_Evaluating_the_Relationship_Between_Arterial_Blood_Pressure_Changes_and_Indices_of_Pulse_Oximetric_Plethysmography?enrichId=rgreq-03054f20-eea5-4f13-89c5-836de5f92c9b&enrichSource=Y292ZXJQYWdlOzExMDE0NDUwO. [Accessed 17 02 2016].
- [48] M. Nitzan, Y. Adar, E. Hoffman, E. Shalom, S. Engelberg, I. Z. Ben-Dov and M. Bursztyn, "Comparison of Systolic Blood Pressure Values Obtained by Photoplethysmography and by Korotkoff Sounds," 2 9 2013. [Online]. Available: <http://www.mdpi.com/1424-8220/13/11/14797/htm>. [Accessed 21 3 2016].
- [49] Gliffy, "Make Diagramming a Team Sport," [Online]. Available: <https://www.gliffy.com/>. [Accessed 17 5 2016].
- [50] Lode B.V., "Corival cpet," [Online]. Available: <http://www.lode.nl/en/product/corival-cpet/567>. [Accessed 8 6 2016].
- [51] Lode B.V., "Cuff Complete 2.25 m," [Online]. Available: http://www.lode.nl/en/product/cuff-complete-2-25-m/65/id_p_product/183. [Accessed 8 6 2016].
- [52] PuTTY, "Download PuTTY," [Online]. Available: <http://www.putty.org/>. [Accessed 18 6 2016].
- [53] MathWorks, "Parks-McClellan optimal FIR filter design," [Online]. Available: <http://nl.mathworks.com/help/signal/ref/firpm.html>. [Accessed 26 5 2016].
- [54] A. h. association, "Target Heart Rates," 1 2015. [Online]. Available: http://www.heart.org/HEARTORG/HealthyLiving/PhysicalActivity/FitnessBasics/Target-Heart-Rates_UCM_434341_Article.jsp#.V0bNmGgrKUI. [Accessed 26 5 2016].
- [55] M. Tansel Yildiran and M. Mevlut Koc, "Clinical, Laboratory, and Echocardiographic Variables of the Study Population According to NYHA Quartile," 2010. [Online]. Available: <http://www.ncbi.nlm.nih.gov/pmc/articles/PMC2879196/table/t1-5/>. [Accessed 25 5 2016].

- [56] American heart association , "Arrhythmia," [Online]. Available: http://www.heart.org/HEARTORG/Conditions/Arrhythmia/Arrhythmia_UCM_002013_SubHomePage.jsp. [Accessed 12 06 2016].
- [57] *Major factors enhancing CO*. [Art]. Pearson Education Inc..
- [58] R. G. O'Regan, h. Nolan, D. S. McQueen and D. J. Paterson, *Arterial chemoreceptors*, Springer science + business media, LCC, 2012.
- [59] muRata, "Piezoelectric Sound Components," 1 2 2012. [Online]. Available: <http://www.farnell.com/datasheets/1722738.pdf>. [Accessed 24 5 2016].
- [60] Microchip, "MCP6041/2/3/4," 3 2013. [Online]. Available: <http://ww1.microchip.com/downloads/en/DeviceDoc/21669D.pdf>. [Accessed 24 5 2016].
- [61] Freescale, "K20P64M72SF1," 11 2012. [Online]. Available: <https://www.pjrc.com/teensy/K20P64M72SF1.pdf>. [Accessed 24 5 2016].
- [62] PJRC, "Teensyduino," [Online]. Available: <https://www.pjrc.com/teensy/teensyduino.html>. [Accessed 24 05 2016].
- [63] Microchip, "Anti-aliasing, analog filters for data acquisition systems," 2002.
- [64] A. Devices, "Analog filter wizard," [Online]. Available: <http://www.analog.com/designtools/en/filterwizard/>. [Accessed 24 5 2016].
- [65] *Blood pressure in various blood vessels of the systemic circulation*. [Art].
- [66] *Auscultatory method of blood pressure measurement*. [Art].
- [67] S-Media, Artist, *Summary of blood vessel anatomy*. [Art].
- [68] MidLandsTech, Artist, *Baroreceptor reflexes that help maintain blood pressure homeostasis*. [Art].
- [69] AcuNeeds, Artist, *Mercury column sphygmomanometer*. [Art].
- [70] Healthstats, Artist, *Bpro*. [Art].
- [71] J. Wiley, Artist, *A Doppler flow meter measures the speed of red blood cells*. [Art]. John Wiley & Sons, 2003.

APPENDIX A

BLOOD VESSELS AND PRESSURE REGULATION

Blood vessels

A blood vessel is a tubular structure carrying blood through the body. Blood vessels can be categorized as; a vein, artery or capillary. Arteries can be further subdivided into elastic arteries, muscular arteries or arterioles. Veins can be further subdivided into venules or veins. Figure 24 depicts the structure of these categories [7].

Maintaining blood pressure

Maintaining an adequate amount of blood throughout the body is vital for organs to function properly. This process is supervised by the brain, which ensures a finely tuned cooperation between the heart, blood vessels and kidneys. Changes in blood pressure are registered by baroreceptors, which are present in blood vessels and are integrated by the cardiovascular centre of the medulla. The homeostatic mechanisms that regulate BP are CO, PR and blood volume. BP varies directly with CO and PR. Furthermore, CO varies directly with blood volume. An overview of how the body reacts to a change in BP is depicted in Figure 25 [7].

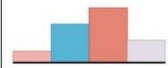
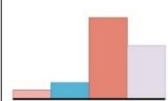
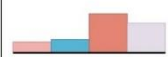
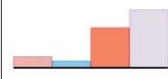
VESSEL TYPE/ ILLUSTRATION*	AVERAGE LUMEN DIAMETER (D) AND WALL THICKNESS (T)	RELATIVE TISSUE MAKEUP			
		Endothelium	Elastic Tissues	Smooth Muscles	Fibrous (Collagenous) Tissues
 Elastic artery	D: 1.5 cm T: 1.0 mm				
 Muscular artery	D: 6.0 mm T: 1.0 mm				
 Arteriole	D: 37.0 μm T: 6.0 μm				
 Capillary	D: 9.0 μm T: 0.5 μm				
 Venule	D: 20.0 μm T: 1.0 μm				
 Vein	D: 5.0 mm T: 0.5 mm				

Figure 24: Summary of blood vessel anatomy [64]

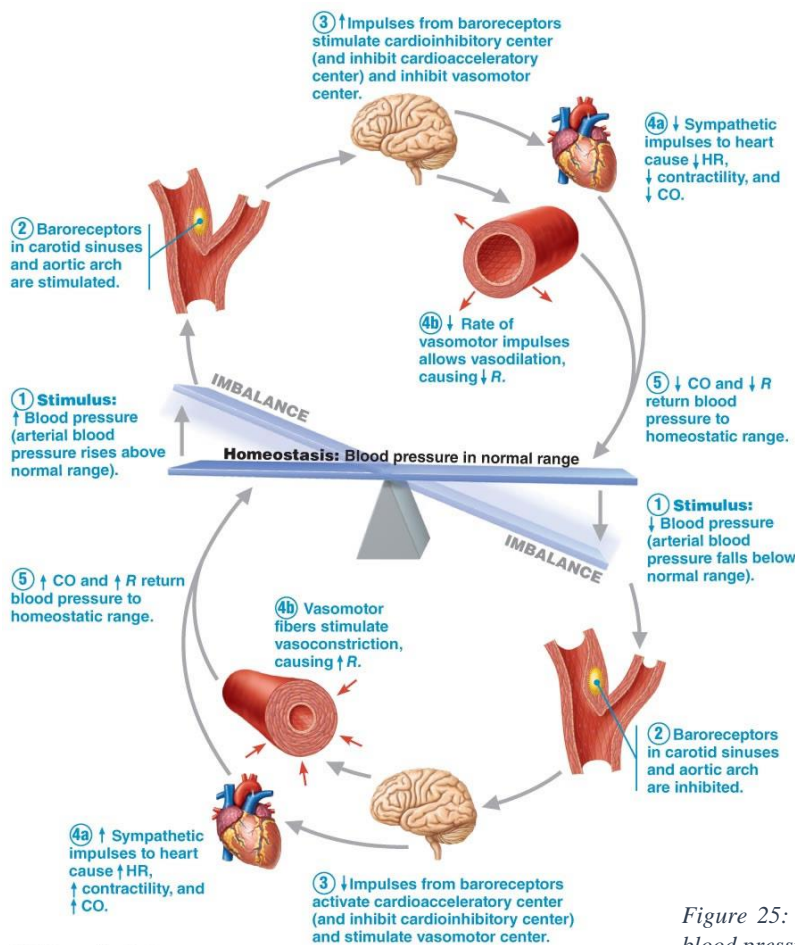


Figure 25: Baroreceptor reflexes that help maintain blood pressure homeostasis [65]

Changes in one of these variables are quickly compensated by adjusting one of the other variables accordingly. Short-term regulation is done via neural controls by changing the total peripheral resistance (TPR) and (CO). Neural control of the TPR serves two main goals, maintaining adequate mean arterial pressure (MAP) and altering blood distribution. An adequate level of MAP is maintained by altering vessel diameter on a moment-to-moment basis. The altering of blood distribution is done during exercise or digestion. An overview of how the processes mention above interact is depicted in Figure 26 [7].

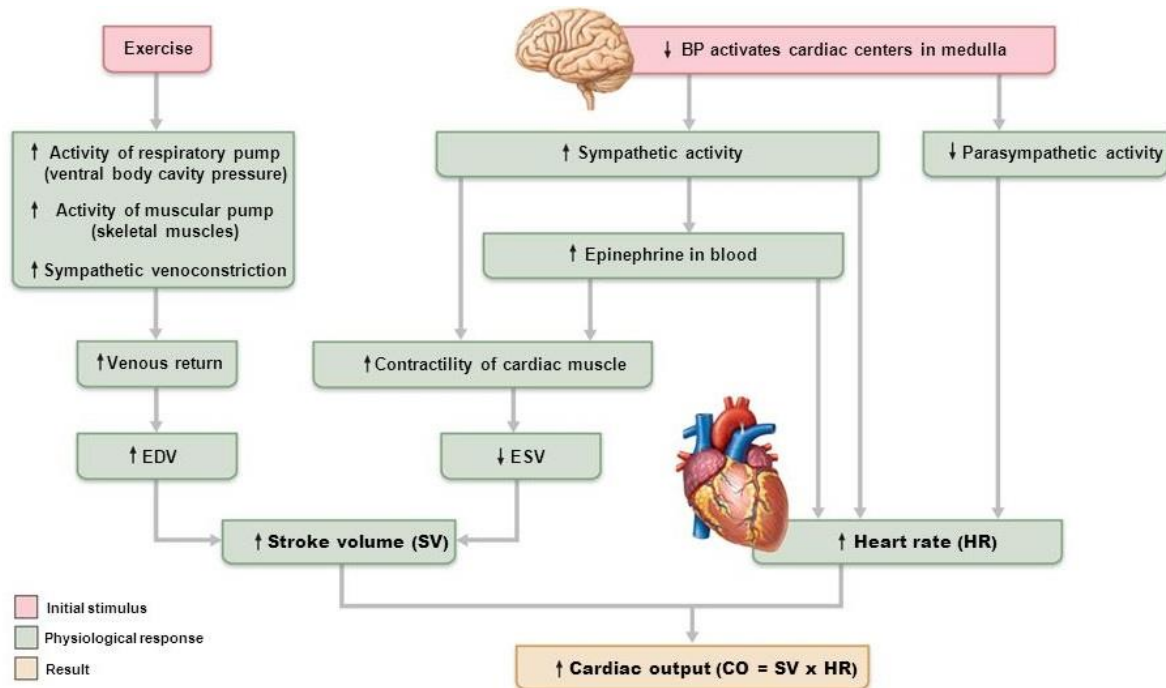


Figure 26: Major factors enhancing CO [57]

Apart from baroreceptors, chemoreceptors also transmit pulses to the cardiovascular center, which in turn can cause a change in CO and vasoconstriction. These receptors play a larger role in respiratory rate than in blood pressure. However, during stress conditions they become more influential, for instance when adrenaline is released [7]. Oxygen saturation in blood is also picked up by these chemoreceptors, which can cause a chemoreflex. For instance, arterial chemoreflex rapidly activates lowering of heart rate (HR) and more slowly inhibits vasoconstriction [58]. Some brain centers that influence blood pressure, apart from the cardiovascular center, are the cerebral cortex and hypothalamus. The hypothalamus is not involved in routine controls of blood pressure, however during the fight-or-flight response it has profound effects on blood pressure [7].

APPENDIX B

COMPONENT VALIDATION

Piezo microphone

The sensor used to detect K-sounds is a piezo microphone, or contact microphone, developed by Lode B.V. The design of this microphone is depicted in Figure 27. The electronic part of the microphone is enclosed in an insulation cover. The sound transducers consist of a brass plate with a maximally thin piezo crystal mounted onto it and are placed in such a way that their piezo crystals are facing inward [59]. The piezo crystals are maximally flat to ensure that the transduced sound it coming from the axis to which the microphone is faced.

The microphone utilizes two piezo crystals for multiple reasons. Firstly, it makes the microphone bidirectional. Secondly, it makes for a better signal quality. Once the microphone is placed inside an inflatable cuff such that is in close contact with the skin, one of the sound transducers will be closer to the skin than the other. Therefore, the K-sounds will be picked up more strongly by this sound transducer.

However, the portion of the signal caused by unwanted artefacts, like cable movement, will be picked up by both sound transducers equally. Therefore, once the signals of both transducers fed into a differential amplifier setup the noise artefacts will mostly be cancelled out whereas the K-sounds will be amplified.

There is another advantage to this placement of the sound transducers. By placing both such that the piezo crystals are facing inwards, an incoming vibration will cause one crystal to be bent inwards whereas the other will be bent outwards. This will result in one becoming more positively charged whereas the other will become more negatively charged.

In order to visualize this phenomena the microphone was placed inside a test setup where an iron rod was dropped from a certain height onto the table nearby the microphone. The resulting data is plotted in Figure 29, Figure 30 and Figure 31. What can be observed from this figure is that when the microphone is flipped from size A under to size B under, the shape of the signal also flips from Mic- to Mic+. The third graph shows the resulting output from the instrumentation amplifier, it can be seen that the baseline become less noisy.

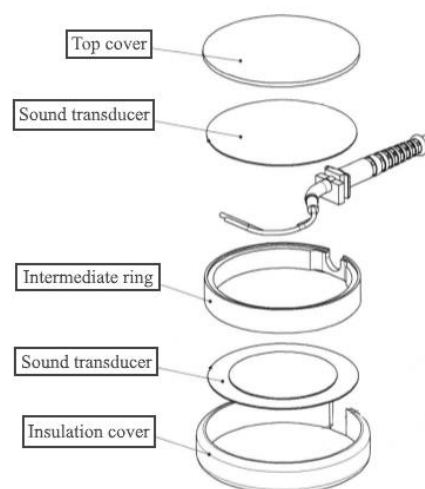


Figure 27: Exploded view of piezo microphone developed by Lode B.V.

Test setup

The microphone was placed inside a modified cardboard box. In this box a hole was cut out to ensure a fixed position of the microphone. A metal rod was dropped from 3, 5 and 10 mm height onto the table, as can be seen in Figure 28.

For data acquisition the Yokogawa dlm2024 oscilloscope was used at 5 ms/div and 12.5 kS, meaning the sampling frequency was 25 kHz. The data was exported to as a text file and loaded into Matlab for evaluation. In Matlab the data was smoothed with a Savitzky-Golay filter with a polynomial of order 3 and frame size 9.

Procedure

1. Lift the rod **till to** certain height, ensure by tape
2. Start oscilloscope
3. Let go of the rod
4. Stop oscilloscope
5. Flip microphone
6. Repeat steps 1 - 4
7. Load data into Matlab
8. Smooth with Savitzky-Golay filter
9. Align impact at $t = 0$



Figure 28: Test setup impulse response piezo microphone, configuration B under

Results

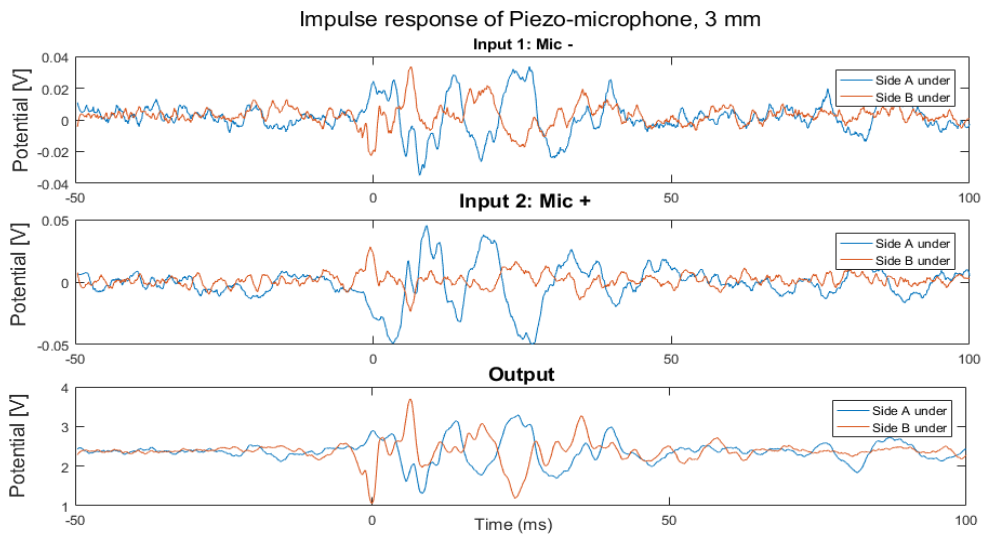


Figure 29: Impulse response of a piezo microphone for a drop height of 3 mm

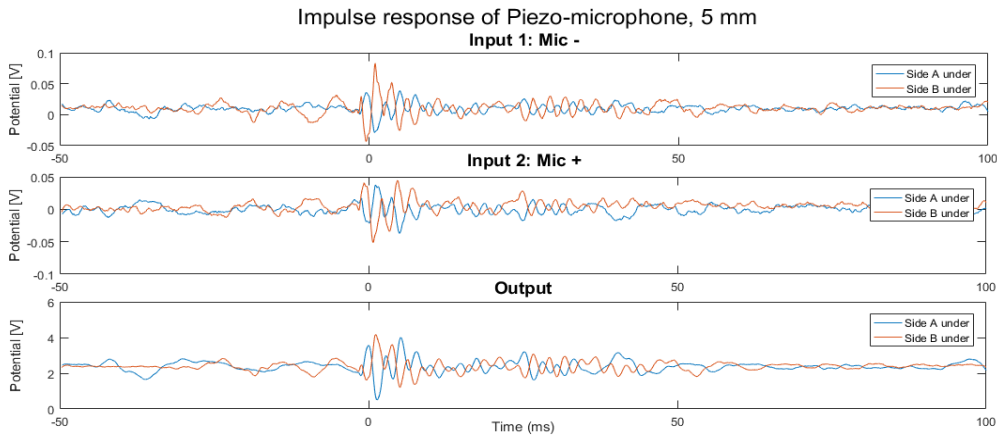


Figure 30: Impulse response of a piezo microphone for a drop height of 5 mm

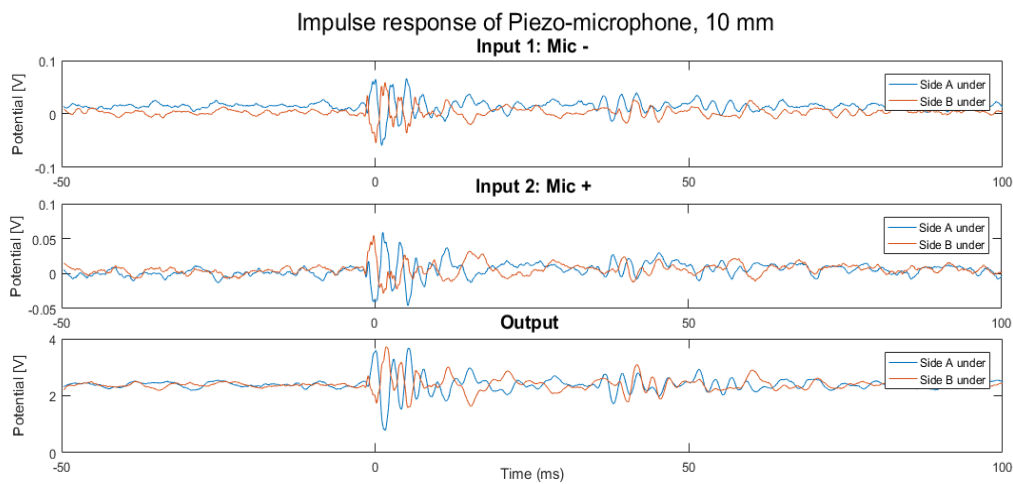


Figure 31: Impulse response of a piezo microphone for a drop height of 10 mm

Instrumentation amplifier

The instrumentation amplifier used to differentially amplify the two microphone signals is depicted in Figure 32. The amplifier first removes any DC component with C1 and C2. Afterward, it gives the signal a DC offset. This is done as the MCP6044 OpAmp is powered from 0 to 3.3V [60]. These signals are fed into the first 2 OpAmps of the MCP6044, a quad configuration OpAmp. Here the signal is amplified with a gain of 30. After C2 and C4, placed for stability, the signals is fed through resistors to U3. The signal from U2 is given an offset of half the supply voltage. The last OpAmp, U3, removes the common mode in these signals.

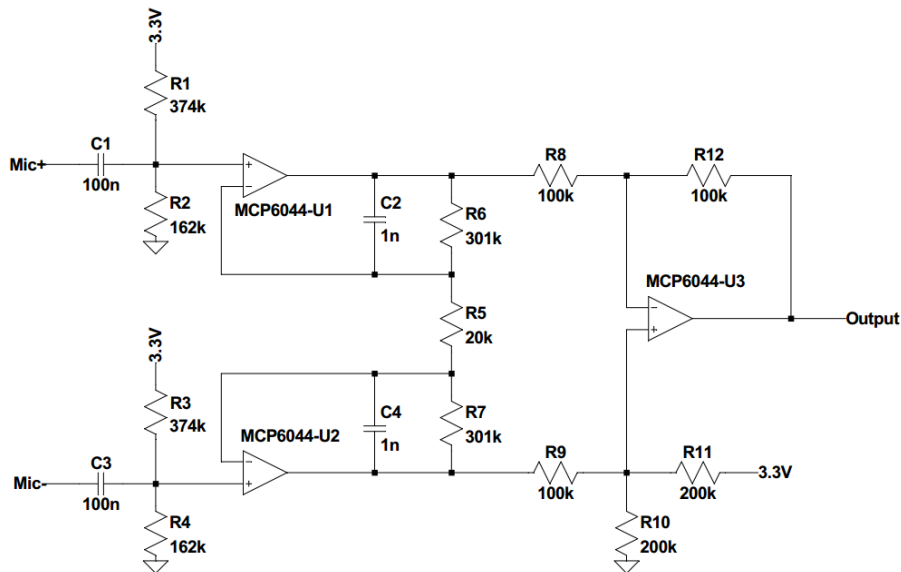


Figure 32: Schematic instrumentation amplifier

In order to validate the functionality of this instrumentation amplifier configuration, the circuit was tested by connecting it to function generator. Two scenarios were created, one where two sinusoids of equal phase and amplitude were fed into the circuit, another where the one of the sinusoids was inverted, or shifted by half its period. This was done using an inverting amplifier. The data acquisition was done with a Yokogawa dlm2024 oscilloscope at 100 ms/div and 12.5 kS, or a sampling frequency of 12.5 kHz. The resulting data is depicted in Figure 33. In the top three graphs, the two sinusoid with equal phase and amplitude with the resulting signal from the instrumentation amplifier are depicted. In the last three graphs the two sinusoids with unequal phase but equal amplitude and the resulting signal from the instrumentation amplifier are depicted.

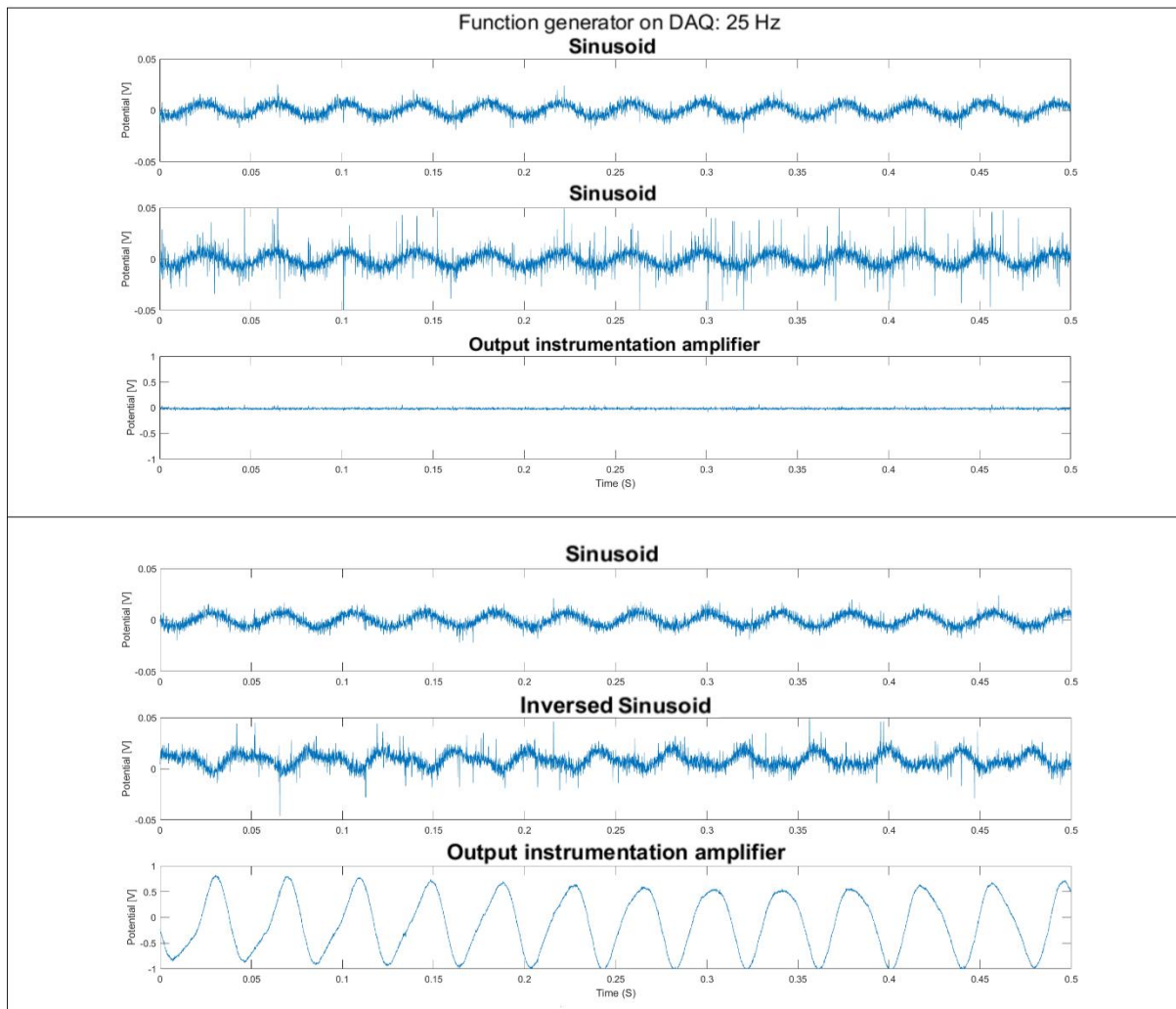


Figure 33: Function generator on instrumentation amplifier

Analogue-to-Digital converter

To log the incoming signal, a 16-bit successive approximation ADC was used. This ADC was controlled by the K20P64M72SF1 Freescale chip [61]. This chip was programmed using the Teensy 3.2 development board with the TeensyDuino add-on of the Arduino IDE [62]. The ADC was programmed to run at a minimum sampling speed of 2500 Hz. A flow chart of this algorithm is depicted in Figure 45 through Figure 48 in appendix E.

To validate the proper functioning of the ADC, a signal created with a HAMEG HM8030 function generator. The function generator was directly connected to an analogue input pin of the Teensy. The frequency was driven up from 10 to 1500 Hz. The resulting sampled signals are depicted in Figure 34. What can be seen is that as the frequency of the input sinusoid becomes higher, the samples start to cut into each other frequency band. At a frequency of 1250 Hz, half the sampling frequency also called the Nyquist frequency, a phenomena called aliasing starts to occur. At this frequency, or higher, the signal will not be able to be reconstructed after sampling whilst sampling at a rate of 2500 Hz.

Although the signal of interest should be no higher than 275 Hz according to literature, noise artifact can be of higher frequencies [12]. If these higher frequencies are not filtered out before sampling, they will not be able to be filtered out as they are aliased into the other frequencies. This shows the need of an anti-aliasing filter.

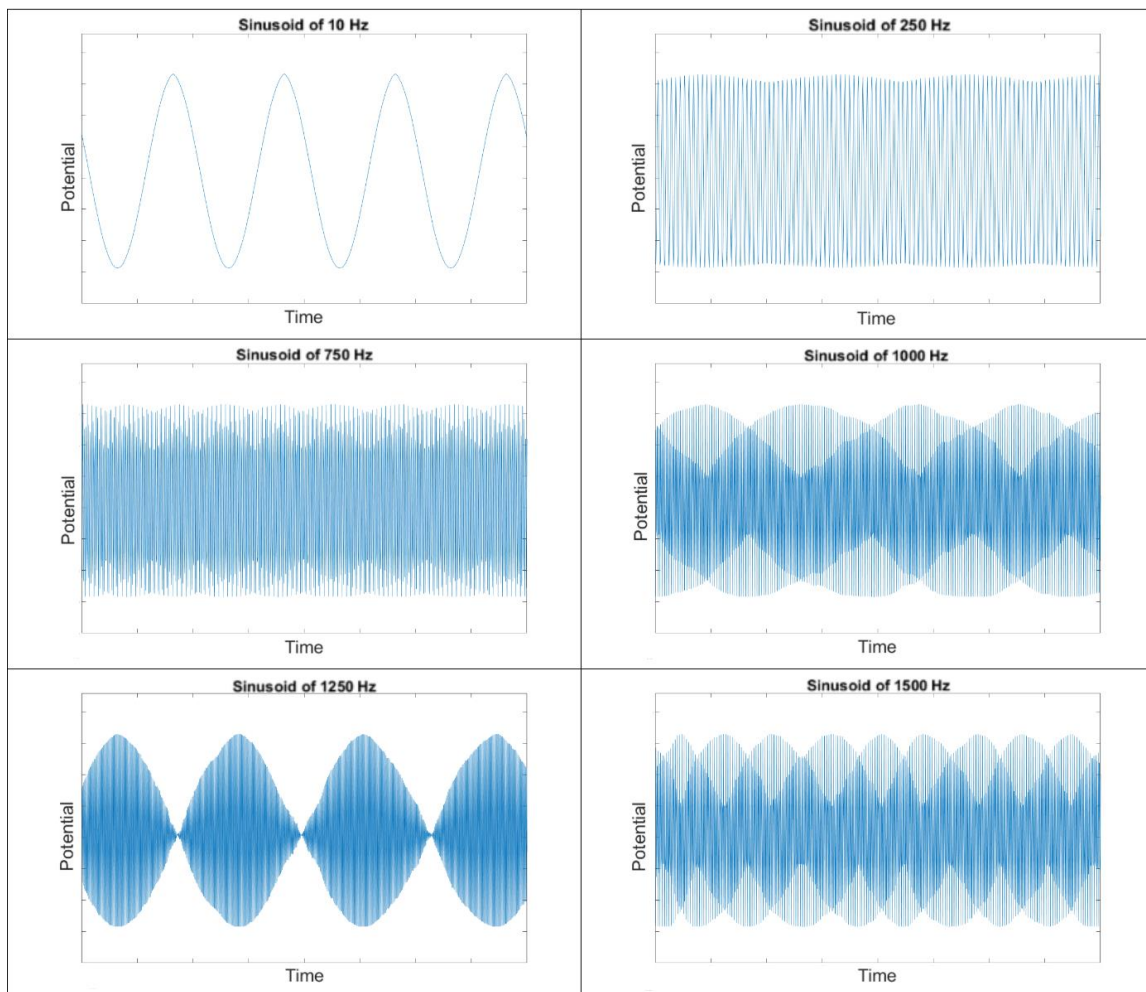


Figure 34: Function generator at different frequencies sampled with Teensy ADC

Butterworth anti-aliasing filter

For the determination of the low-pass anti-aliasing filter design the most important features were a flat pass band and low ringing. This was to ensure the integrity of the peaks in the signal. There was no need for an extremely high rate of attenuation as the filter is just designed to cut-off high frequencies to prevent aliasing. This is why, despite having some overshoot, the Butterworth design was selected. The considered design and their rated properties are presented in Table 9.

Table 9: Most important characteristics of popular anti-aliasing filter designs rated according to the requirements [63]

Filter \ Characteristic	Biggest advantage	Rate of attenuation	Flat pass band	Overshoot	Ringing
Butterworth	Maximally flat pass band	+	++	+/-	+
Bessel	Constant time delay	--	+	++	++
Chebyshev	Minimize transition bandwidth	++	+/-	+/-	--

As an anti-aliasing filter an analogue Butterworth design was used. The filter was designed using the Analog Devices filter wizard [64]. The most important design criteria were low noise, 0-5 V supply voltage and a stopband of -40 dB at 2.4 kHz. The circuit of the filter is depicted in Figure 49, appendix B. This filter has a maximum phase delay of 900 us, however at the bandwidth of interest (~10-300 Hz) the phase delay is 730 us, as can be seen in Figure 51 also in appendix B. The attenuation at the Nyquist frequency of the ADC is about -27 dB or about 0.05 V/V.

To validate the proper functioning of the anti-aliasing filter, the input of the circuit was connected to a function generator, the HM 8030-4 by HAMEG. The output was logged using the Picoscope 3205 at 100 ms/div and 12.5 kS, or a sampling frequency of 12.5 kHz. The frequency of the sinusoid generated by the function generator was increase from 2.5 to 2500 Hz. The resulting signal is depicted by Figure 35. As can be seen in the first three graphs the lower frequencies, 2.5 to 500 Hz, are barely attenuated. However, from frequencies higher than 1000 Hz the attenuation becomes more clearly visible.

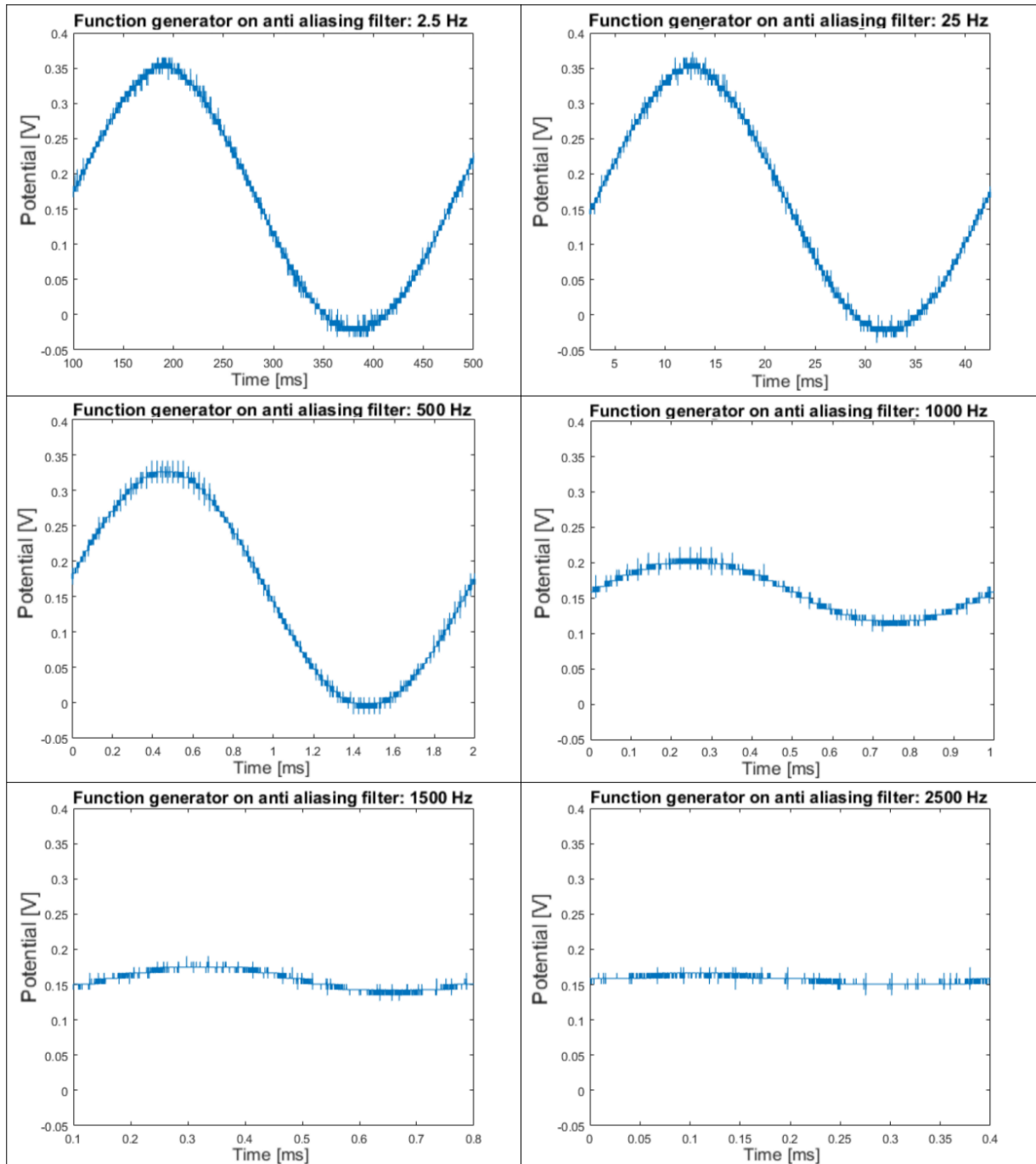


Figure 35: Function generator at different frequencies on anti-aliasing filter

APPENDIX C

KOROTKOFF SIGNALS

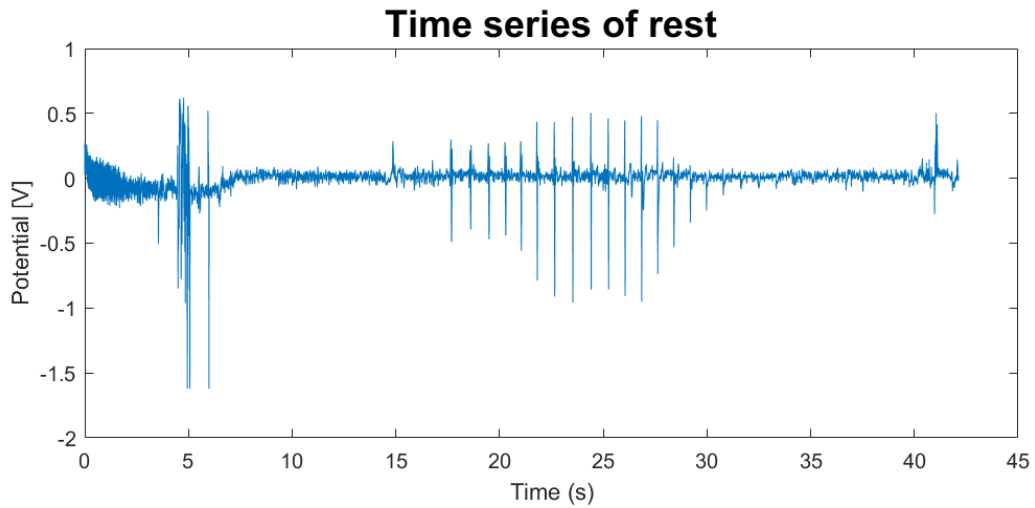


Figure 36: Time series of piezo microphone during BP-measurement whilst in rest for test person A

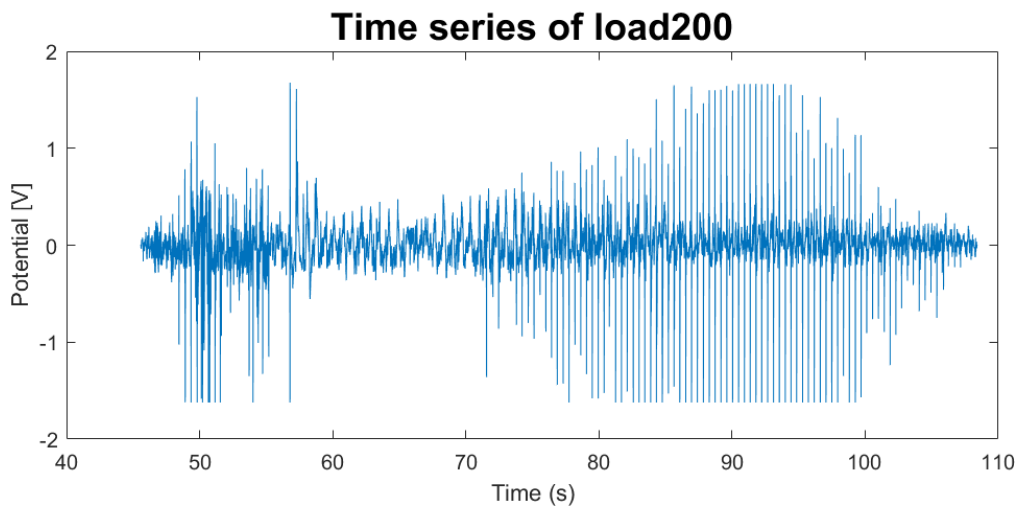


Figure 37: Time series of piezo microphone during BP-measurement whilst cycling at a load of 200 Watt for test person A

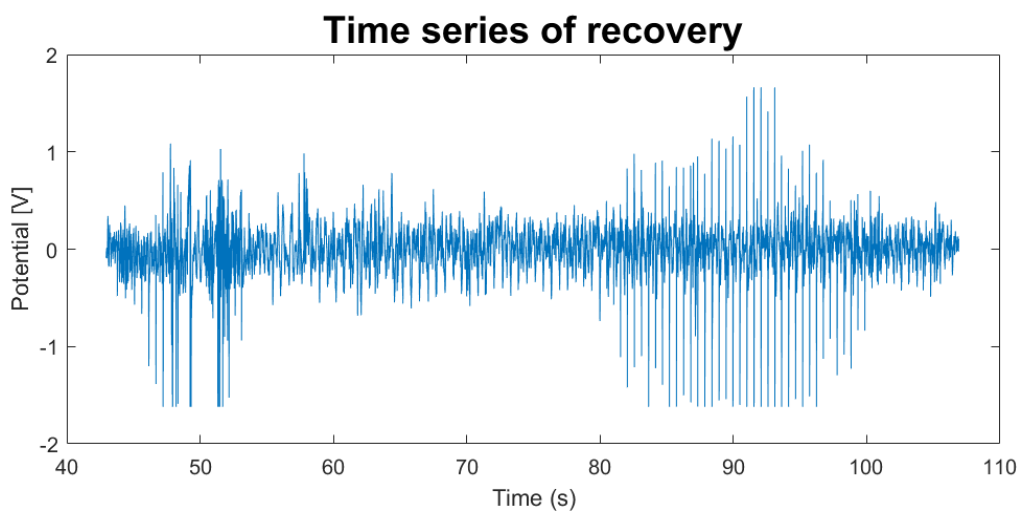


Figure 38: Time series of piezo microphone during BP-measurement whilst cycling during recovery at a load of 50 Watt for test person A

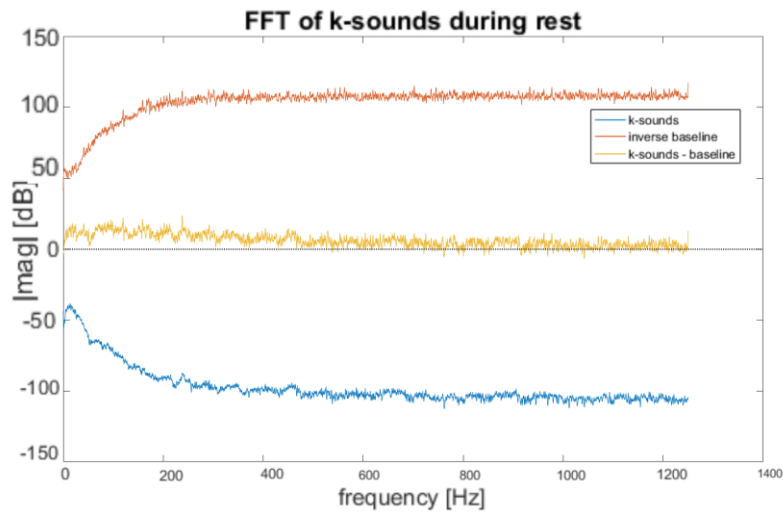


Figure 39: Smoothed FFT on K-sounds, inversed baseline and the K-sounds–baseline during rest

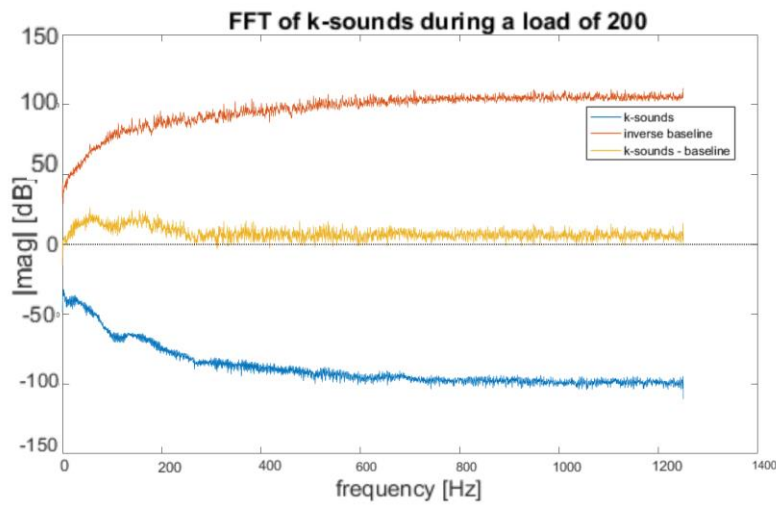


Figure 40: Smoothed FFT on K-sounds, inversed baseline and the K-sounds–baseline whilst cycling at a load of 200 Watt

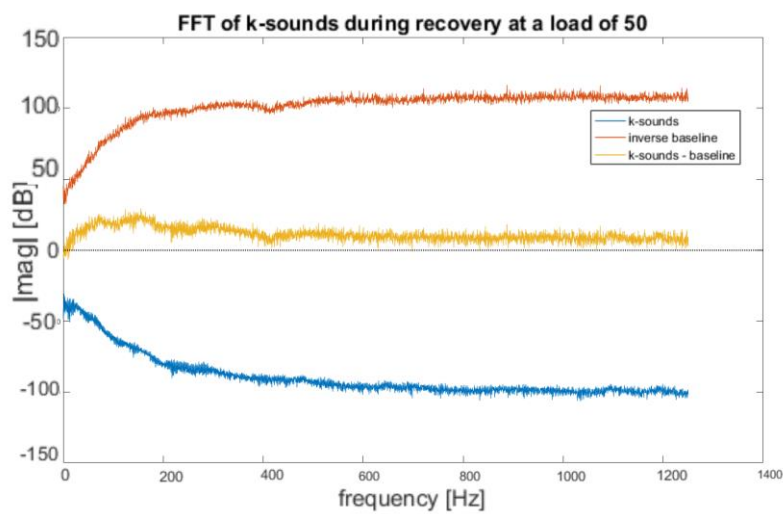


Figure 41: Smoothed FFT on K-sounds, inversed baseline and the K-sounds–baseline during recovery whilst cycling at a load of 50 Watt

Time-frequency representation

The motion artefacts become clearly visible when looking at the difference between Figure 42 and Figure 43 in appendix D. During rest conditions, the lower frequencies are so low in power they fall under the power threshold and are not displayed, as can be seen in Figure 42. However, during cycling at a load of 200 Watt, the lower frequencies are have a much higher power and are well above the threshold, as can be seen in Figure 42, Figure 43, and Figure 44.

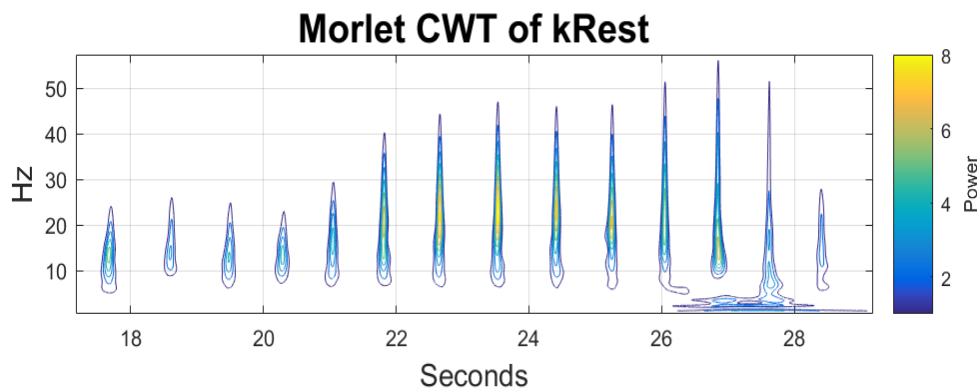


Figure 42: Interpolated continuous wavelet transform with Morlet wavelet of K-sounds during rest

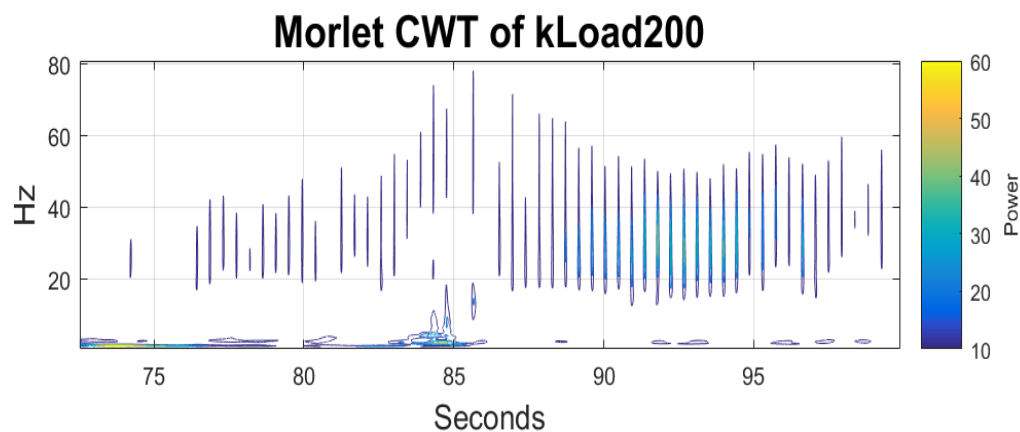


Figure 43: Interpolated continuous wavelet transform with Morlet wavelet of K-sounds whilst cycling at a load 200

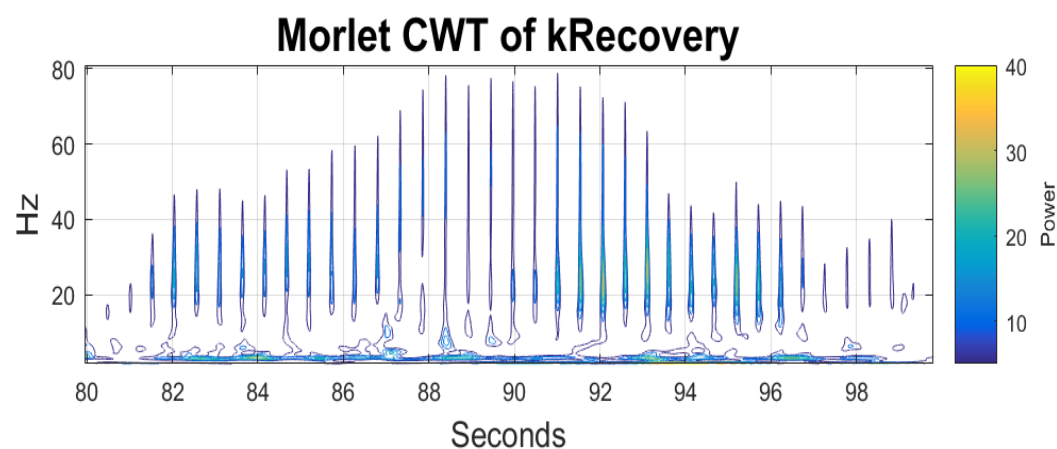


Figure 44: Interpolated continuous wavelet transform with Morlet wavelet of K-sounds during recovery whilst cycling at a load 50

APPENDIX D

FILTER COEFFICIENTS STANDARD DEVIATION TEST RESULTS

Table 10: Standard deviation decrease ratios for a high order high-pass filter with different cut-off frequencies, applied to a signal obtained during rest

	SD baseline	Percentage decrease baseline	SD cut K-sounds	Percentage decrease sounds	K-	Scaled decrease ratio
No Filter	0.027		0.171			
Fc = 11 Hz	0.019	26.641	0.116	32.301		0.173
Fc = 10 Hz	0.020	24.899	0.132	22.954		0.227
Fc = 9 Hz	0.021	21.127	0.134	21.846		0.202
Fc = 8 Hz	0.022	17.554	0.132	22.527		0.163
Fc = 7 Hz	0.023	13.543	0.135	20.783		0.136

Table 11: Standard deviation decrease ratios for a high order high-pass filter with different cut-off frequencies, applied to a signal obtained during cycling at a load of 200 Watt

	SD baseline	Percentage decrease baseline	SD cut K-sounds	Percentage decrease sounds	K-	Scaled decrease ratio
No Filter	0.156		0.567			
Fc = 11 Hz	0.044	71.565	0.446	21.292		0.704
Fc = 10 Hz	0.046	70.518	0.468	17.392		0.849
Fc = 9 Hz	0.049	68.604	0.483	14.862		0.966
Fc = 8 Hz	0.052	66.433	0.482	15.047		0.924
Fc = 7 Hz	0.056	63.790	0.491	13.354		1.000

Table 12: Standard deviation decrease ratios for a high order high-pass filter with different cut-off frequencies, applied to a signal obtained during recovery whilst cycling at a load of 50 Watt

	SD baseline	Percentage decrease baseline	SD cut K-sounds	Percentage decrease sounds	K-	Scaled decrease ratio
No Filter	0.204		0.727			
Fc = 11 Hz	0.065	68.112	0.466	35.918		0.397
Fc = 10 Hz	0.068	66.712	0.490	32.579		0.429
Fc = 9 Hz	0.070	65.518	0.516	28.957		0.474
Fc = 8 Hz	0.074	63.836	0.518	28.693		0.466
Fc = 7 Hz	0.080	60.947	0.524	27.919		0.457

Table 13: Standard deviation decrease ratios for a high order low-pass filter with different cut-off frequencies, applied to a signal obtained during rest

	SD baseline	Percentage decrease baseline	SD cut K-sounds	Percentage decrease K-sounds	Scaled decrease ratio
NoFilter	0.027		0.171		
Fc = 350 Hz	0.026	0.524	0.156	8.671	0.100
Fc = 300 Hz	0.026	0.585	0.156	8.610	0.112
Fc = 275 Hz	0.026	0.539	0.156	8.656	0.103
Fc = 225 Hz	0.026	0.683	0.156	8.992	0.125
Fc = 200 Hz	0.026	0.573	0.156	8.625	0.110

Table 14: Standard deviation decrease ratios for a high order low-pass filter with different cut-off frequencies, applied to a signal obtained during cycling at a load of 200 Watt

	SD baseline	Percentage decrease baseline	SD cut K-sounds	Percentage decrease K-sounds	Scaled decrease ratio
NoFilter	0.156		0.567		
Fc = 350 Hz	0.153	1.616	0.552	2.665	1.000
Fc = 300 Hz	0.153	1.635	0.545	3.828	0.705
Fc = 275 Hz	0.153	1.630	0.550	3.029	0.887
Fc = 225 Hz	0.154	1.299	0.543	4.268	0.502
Fc = 200 Hz	0.153	1.652	0.546	3.683	0.740

Table 15: Standard deviation decrease ratios for a high order low-pass filter with different cut-off frequencies, applied to a signal obtained during recovery whilst cycling at a load of 50 Watt

	SD baseline	Percentage decrease baseline	SD cut K-sounds	Percentage decrease K-sounds	Scaled decrease ratio
NoFilter	0.204	0.000	0.727	0.000	0.000
Fc = 350 Hz	0.204	0.098	0.692	4.793	0.034
Fc = 300 Hz	0.204	0.152	0.687	5.517	0.045
Fc = 275 Hz	0.204	0.113	0.690	5.052	0.037
Fc = 225 Hz	0.203	0.657	0.681	6.343	0.171
Fc = 200 Hz	0.204	0.147	0.687	5.500	0.044

Table 16: Standard deviation decrease ratios for a high order band-pass filter with different cut-off frequencies, applied to a signal obtained during rest

	SD baseline	Percentage decrease baseline	SD cut K-sounds	Percentage decrease K-sounds	Scaled decrease ratio
NoFilter	0.027		0.171		
Fc ₁ = 9, Fc ₂ = 300 Hz	0.021	21.384	0.131	23.428	0.138
Fc ₁ = 9, Fc ₂ = 250 Hz	0.021	20.671	0.133	21.963	0.142
Fc ₁ = 9, Fc ₂ = 275 Hz	0.021	21.379	0.131	23.412	0.138
Fc ₁ = 10, Fc ₂ = 275 Hz	0.020	24.885	0.133	21.972	0.171
Fc ₁ = 8, Fc ₂ = 275 Hz	0.022	17.890	0.134	21.374	0.127

Table 17: Standard deviation decrease ratios for a high order band-pass filter with different cut-off frequencies, applied to a signal obtained whilst cycling at a load of 200 Watt

	SD baseline	Percentage decrease baseline	SD cut K-sounds	Percentage decrease K-sounds	Scaled decrease ratio
NoFilter	0.156		0.567		
Fc ₁ = 9, Fc ₂ = 300 Hz	0.049	68.677	0.507	10.529	0.986
Fc ₁ = 9, Fc ₂ = 250 Hz	0.049	68.389	0.496	12.442	0.831
Fc ₁ = 9, Fc ₂ = 275 Hz	0.049	68.687	0.508	10.382	1.000
Fc ₁ = 10, Fc ₂ = 275 Hz	0.046	70.577	0.461	18.689	0.571
Fc ₁ = 8, Fc ₂ = 275 Hz	0.052	66.536	0.498	12.166	0.827

Table 18: Standard deviation decrease ratios for a high order band-pass filter with different cut-off frequencies, applied to a signal obtained during recovery whilst cycling at a load of 50 Watt

	SD baseline	Percentage decrease baseline	SD cut K-sounds	Percentage decrease K-sounds	Scaled decrease ratio
NoFilter	0.204		0.727		
BP9-300	0.070	65.620	0.528	27.299	0.363
BP9-250	0.071	65.043	0.526	27.575	0.357
BP9-275	0.070	65.622	0.528	27.276	0.364
BP10-275	0.068	66.605	0.489	32.640	0.308
BP8-275	0.074	63.641	0.527	27.520	0.350

APPENDIX E

ADC SOFTWARE FLOW CHARTS

ADC software

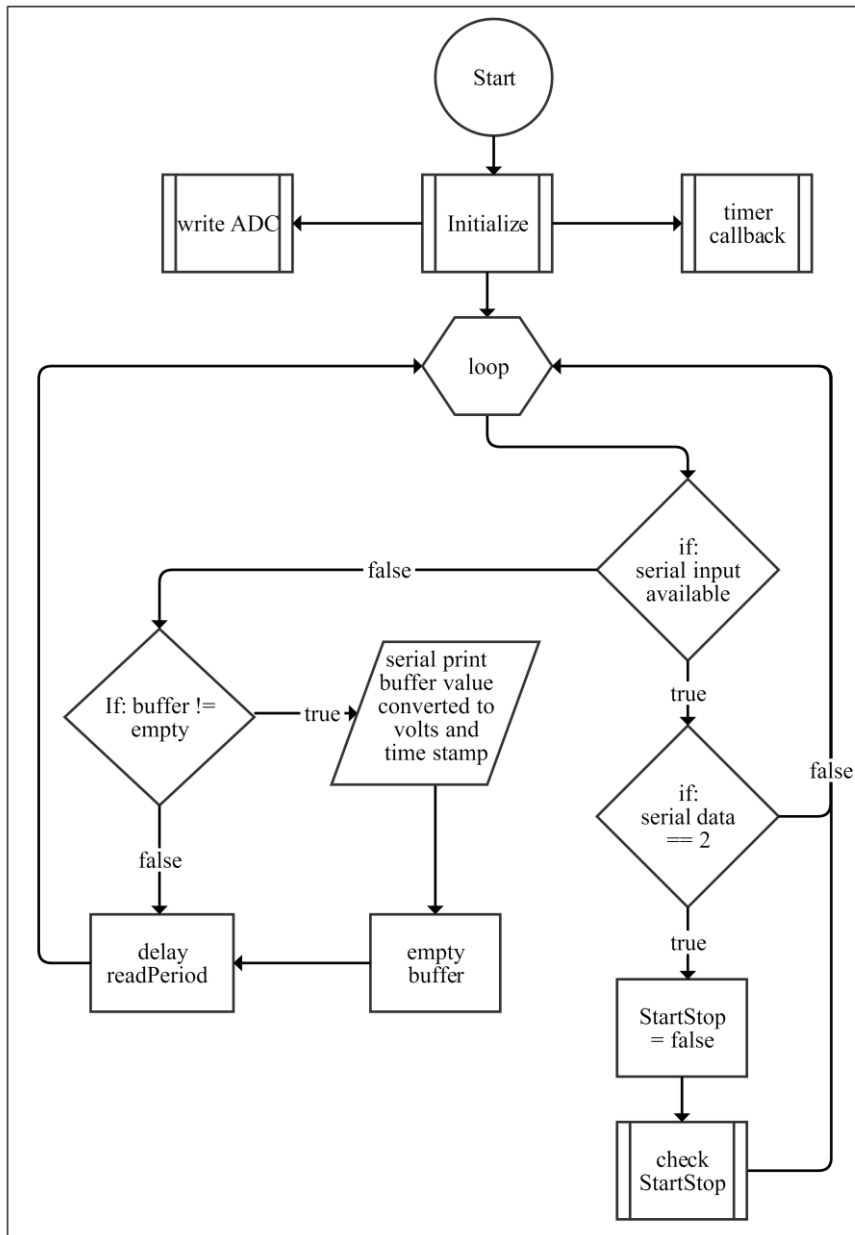


Figure 45: Main function of ADC algorithm

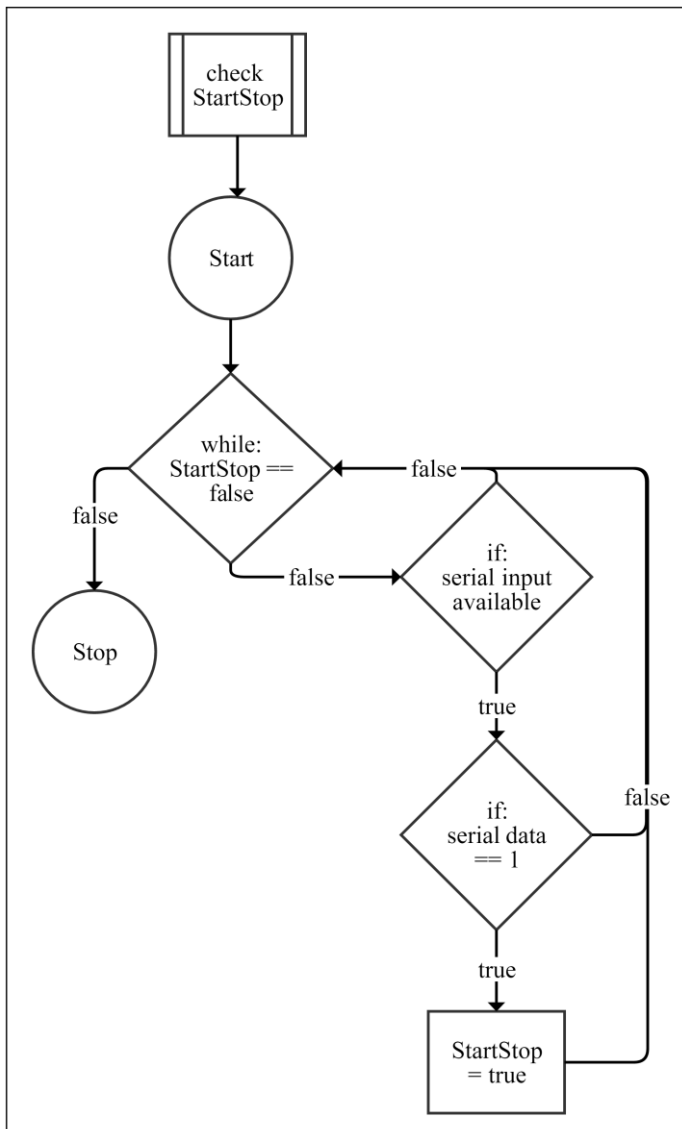


Figure 48: Check StartStop function of the ADC algorithm

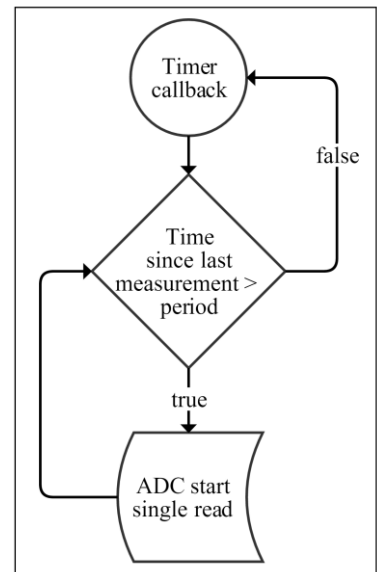


Figure 46: timer callback function of ADC algorithm

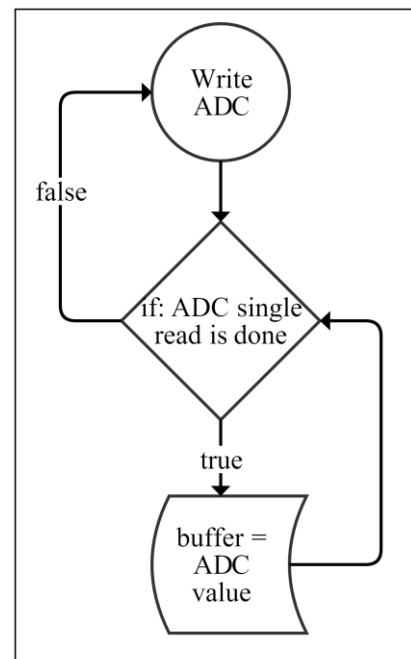


Figure 47: Write ADC function of teensy algorithm

APPENDIX F

ANTI-ALIASING FILTER DESIGN

Filter Wizard Design Report Filter Requirements for

Low-Pass, 3rd order Butterworth

- Specifications: Optimize for Noise, +Vs= 5, -Vs= 0
- Gain: 0 dB
- Passband: -1dB at 350Hz
- Stopband: -40dB at 2.4kHz
- Component Tolerances: Capacitor = 5%; Resistor = 1%; Inductor = 5%; Op Amp GBW = 20

Circuit

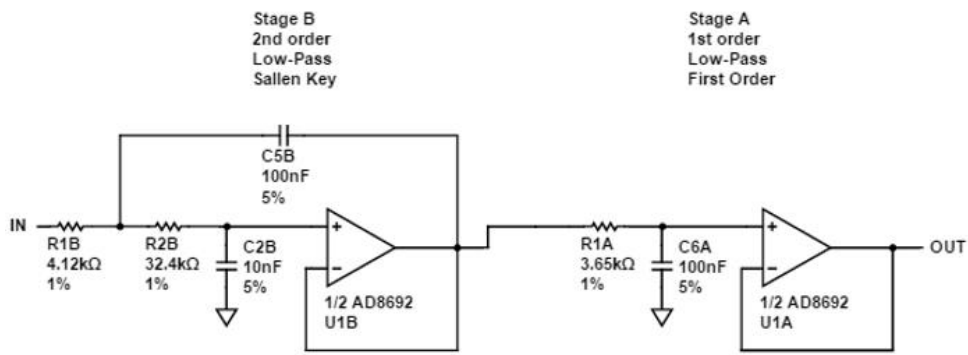


Figure 49: Circuit design of 3rd order Butterworth filter

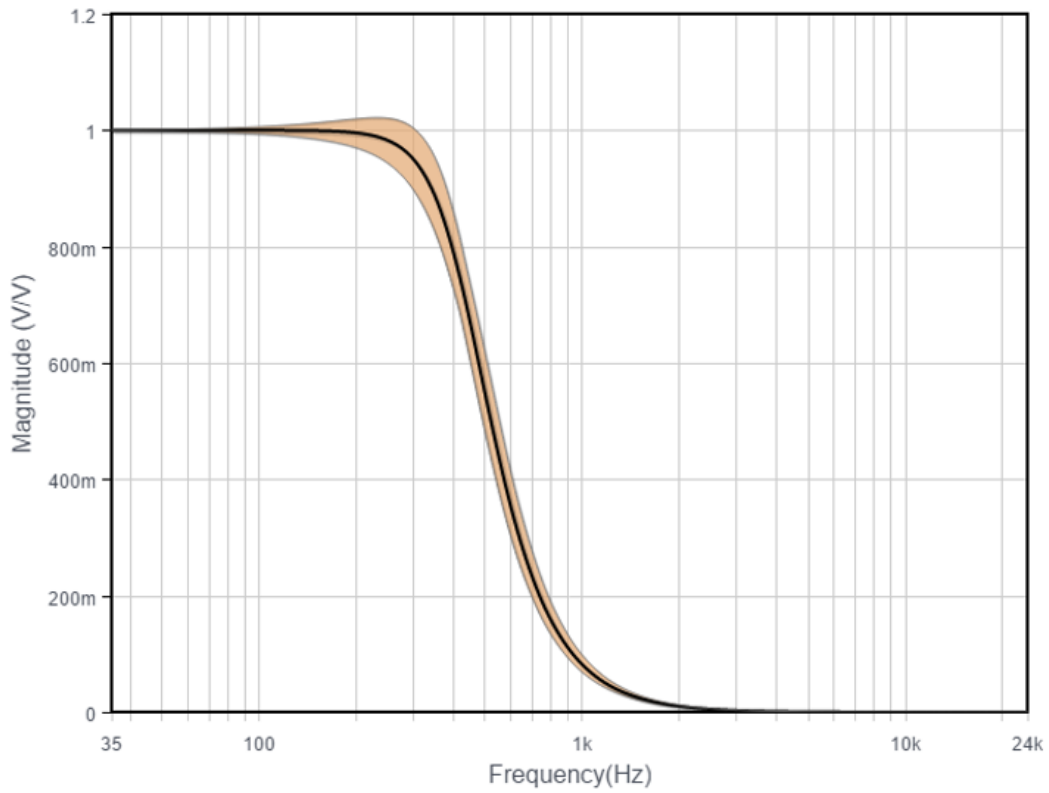


Figure 50: Magnitude response of 3rd order Butterworth filter

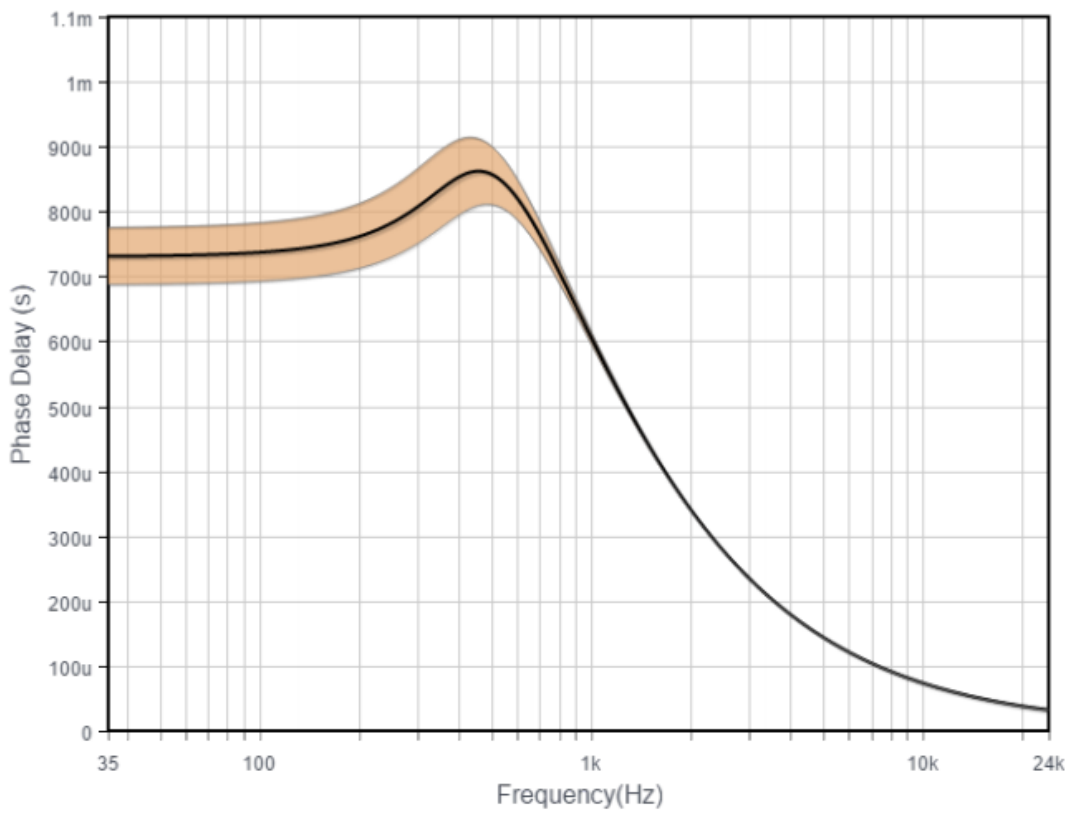


Figure 51: Phase delay of 3rd order Butterworth filter

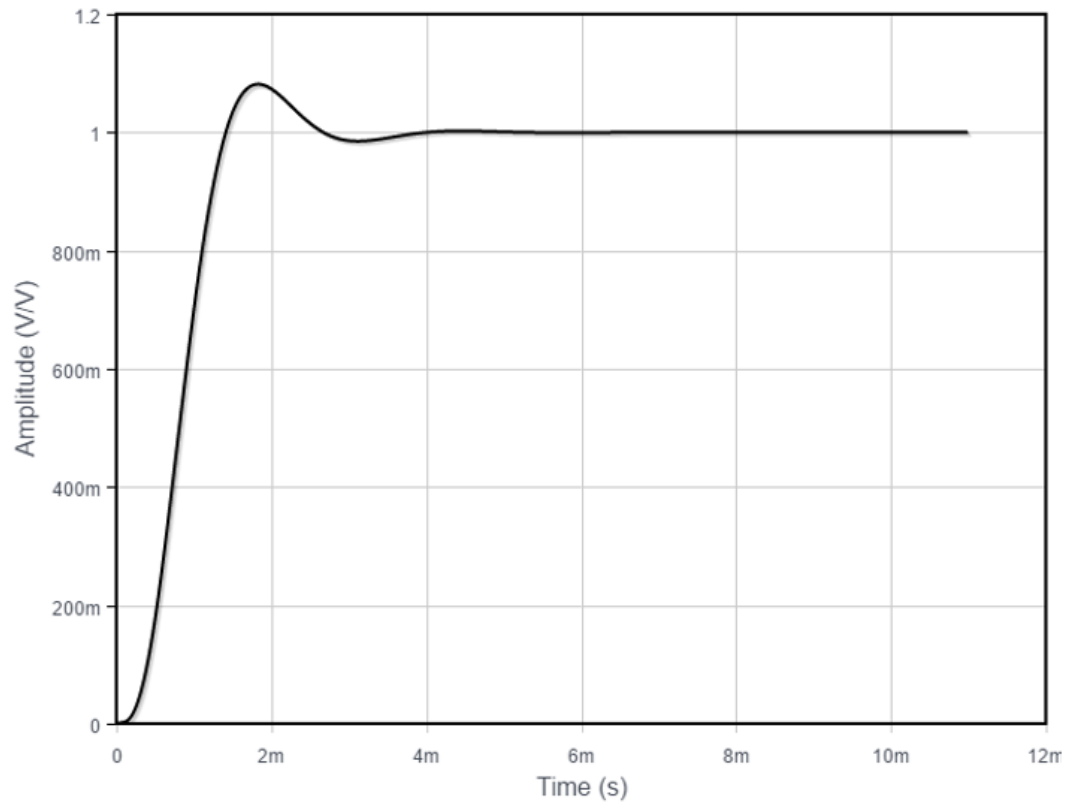


Figure 52: Step response of 3rd order Butterworth filter

APPENDIX G

RESULTING SIGNALS

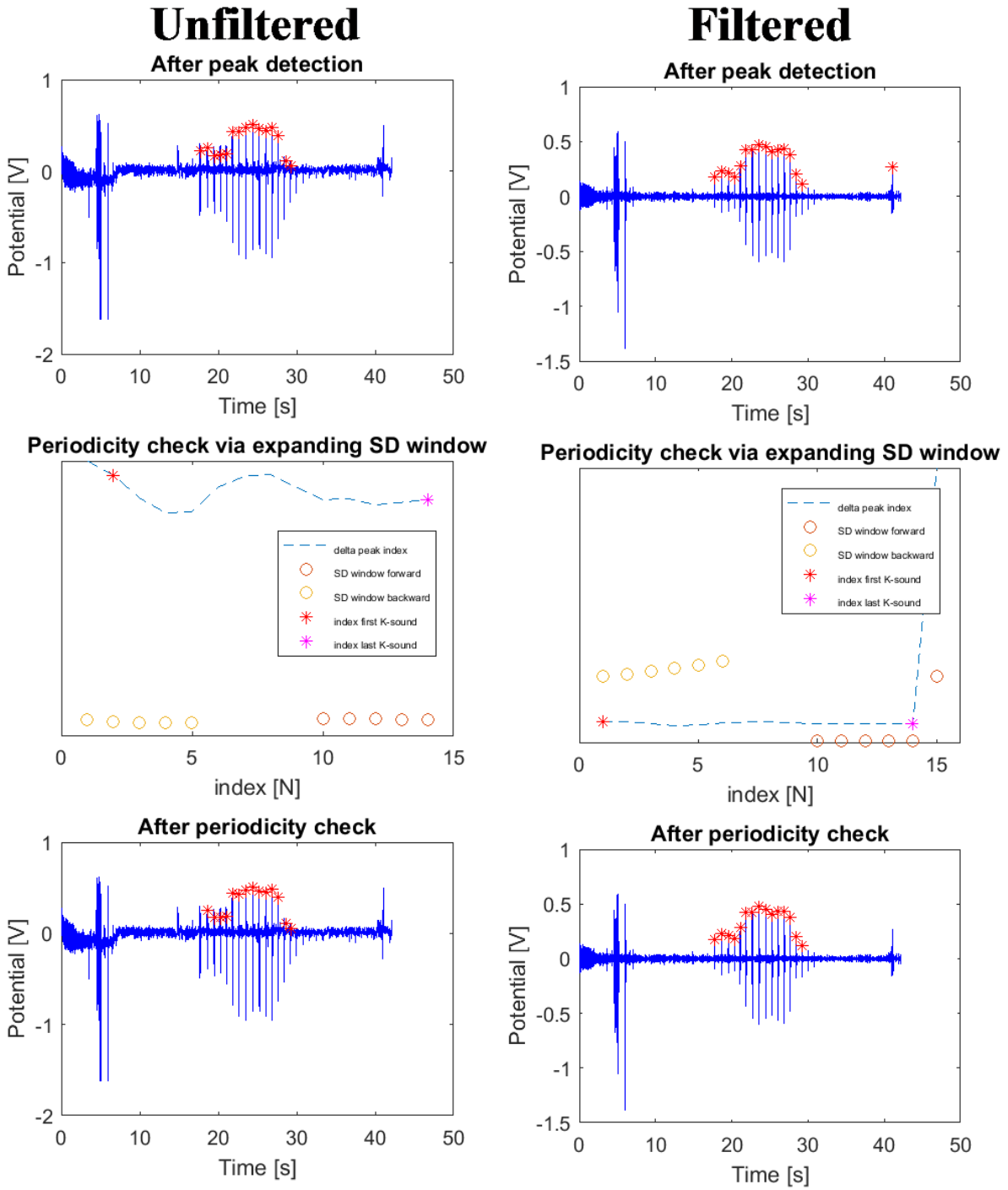


Figure 53: Unfiltered and filtered signals before and after peak detection and periodicity check, obtained whilst test person A was in rest conditions

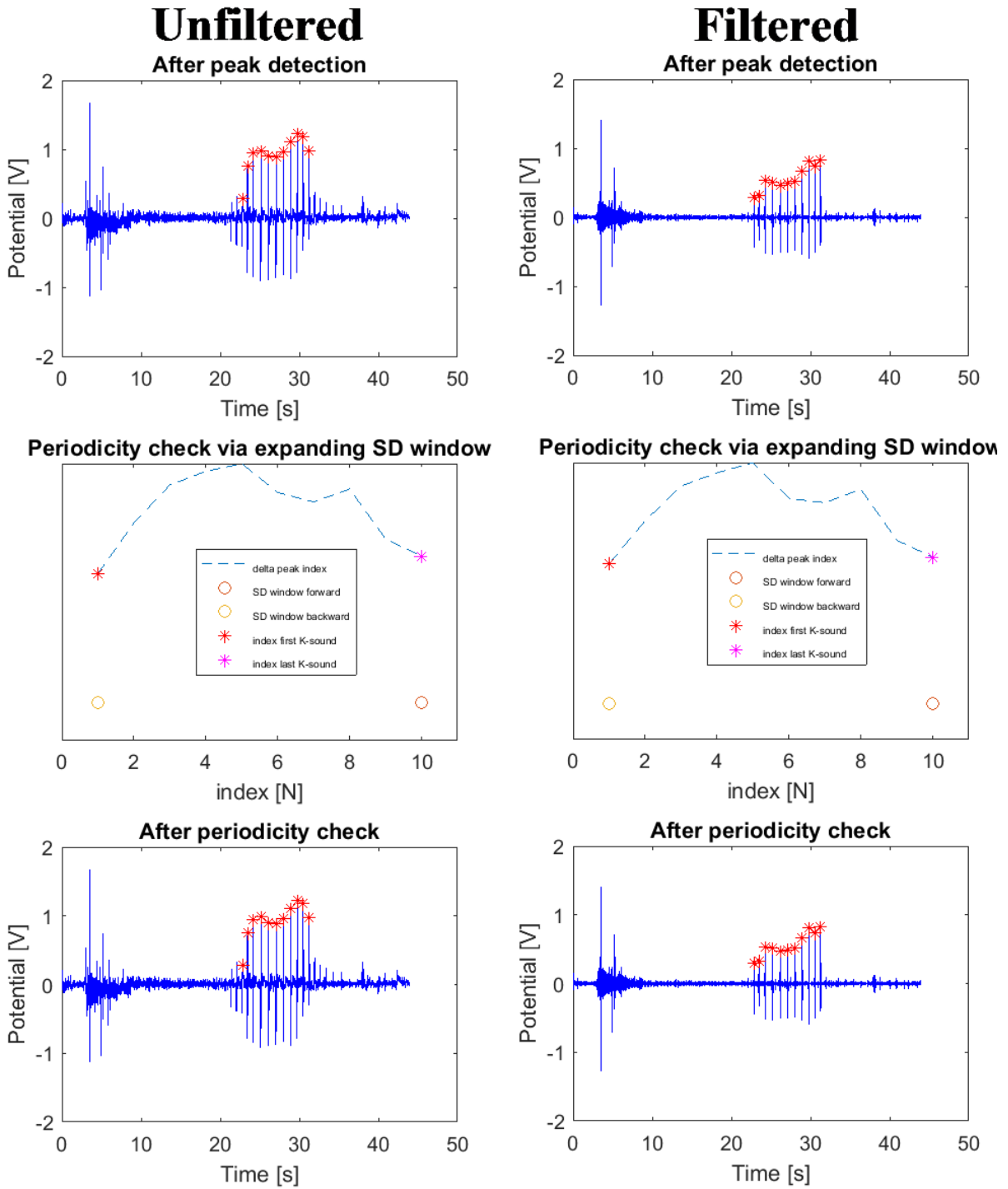


Figure 54: Unfiltered and filtered signals before and after peak detection and periodicity check, obtained whilst test person B was in rest conditions

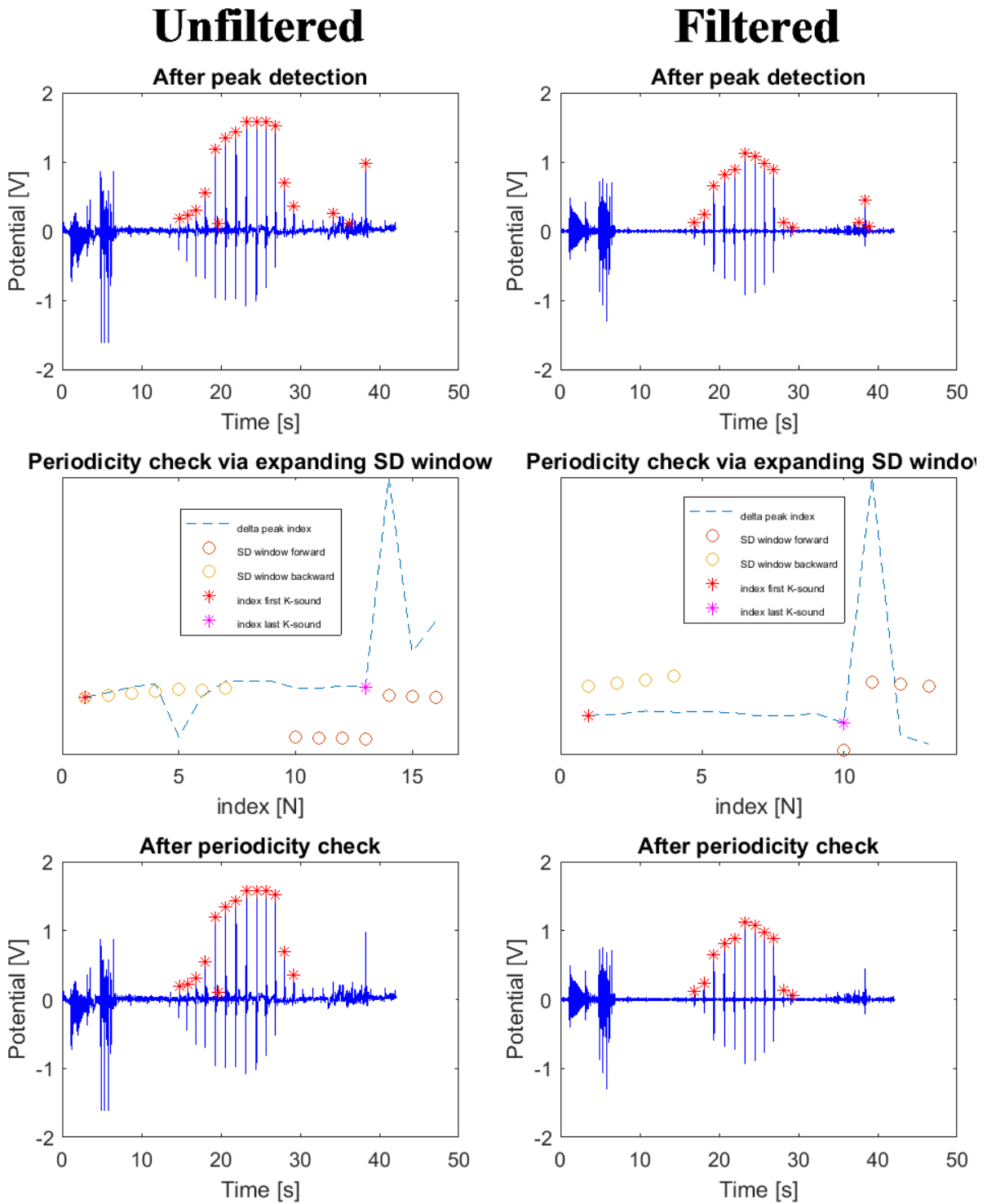


Figure 55: Unfiltered and filtered signals before and after peak detection and periodicity check, obtained whilst test person C was in rest conditions

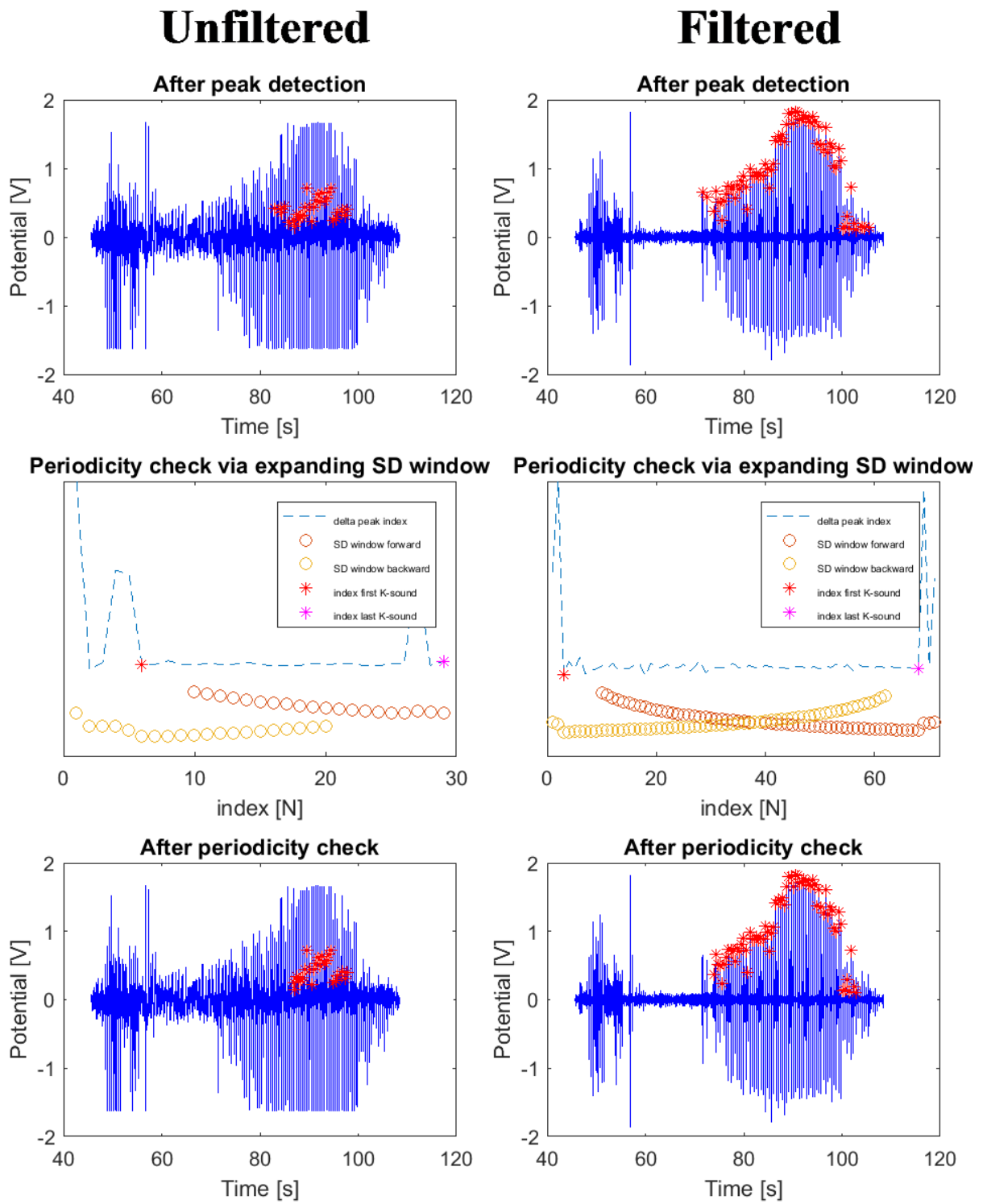


Figure 56: Unfiltered and filtered signals before and after peak detection and periodicity check, obtained whilst test person A cycling at a load of 200 Watt

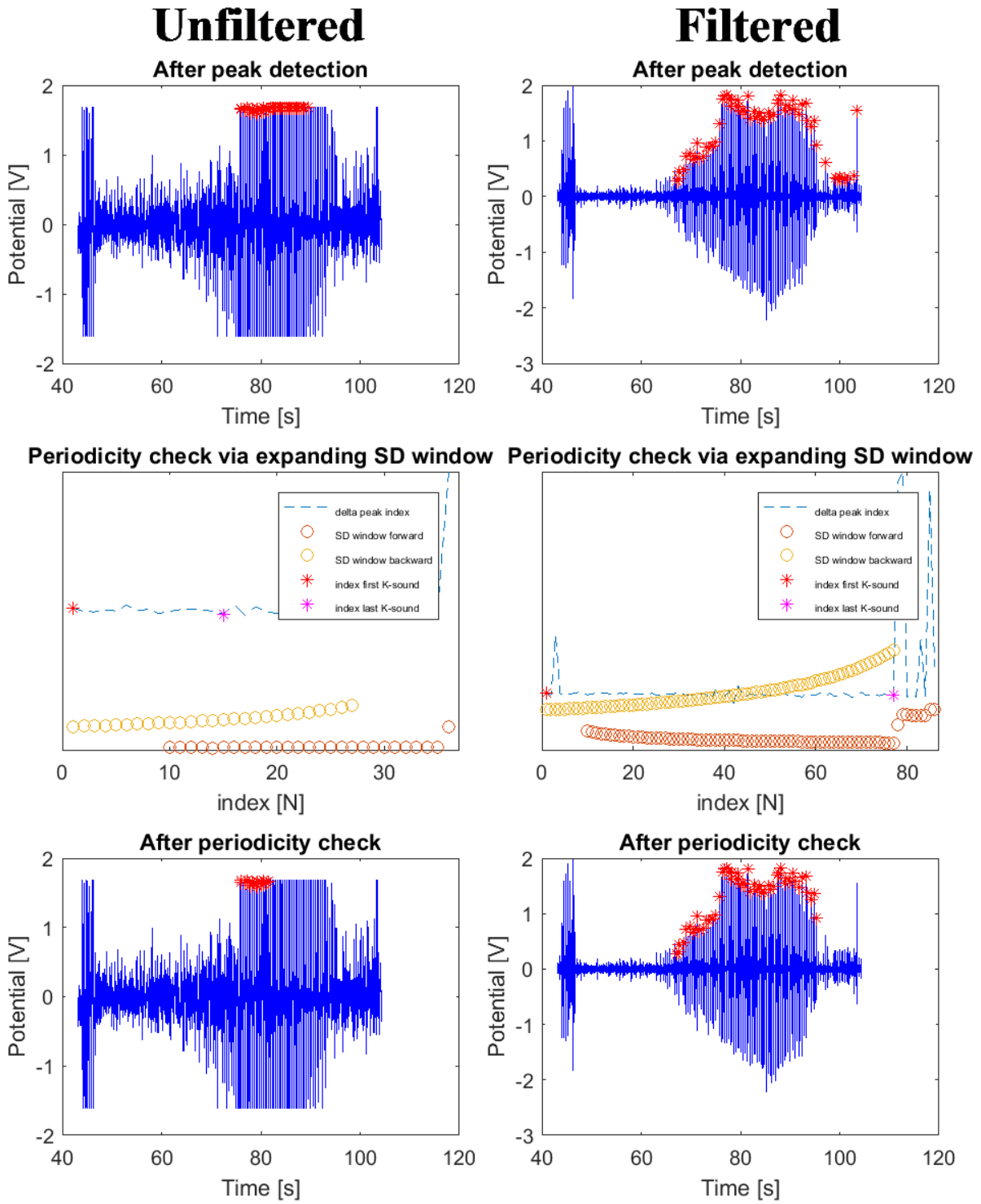


Figure 57: Unfiltered and filtered signals before and after peak detection and periodicity check, obtained whilst test person B was cycling at a load of 200 Watt

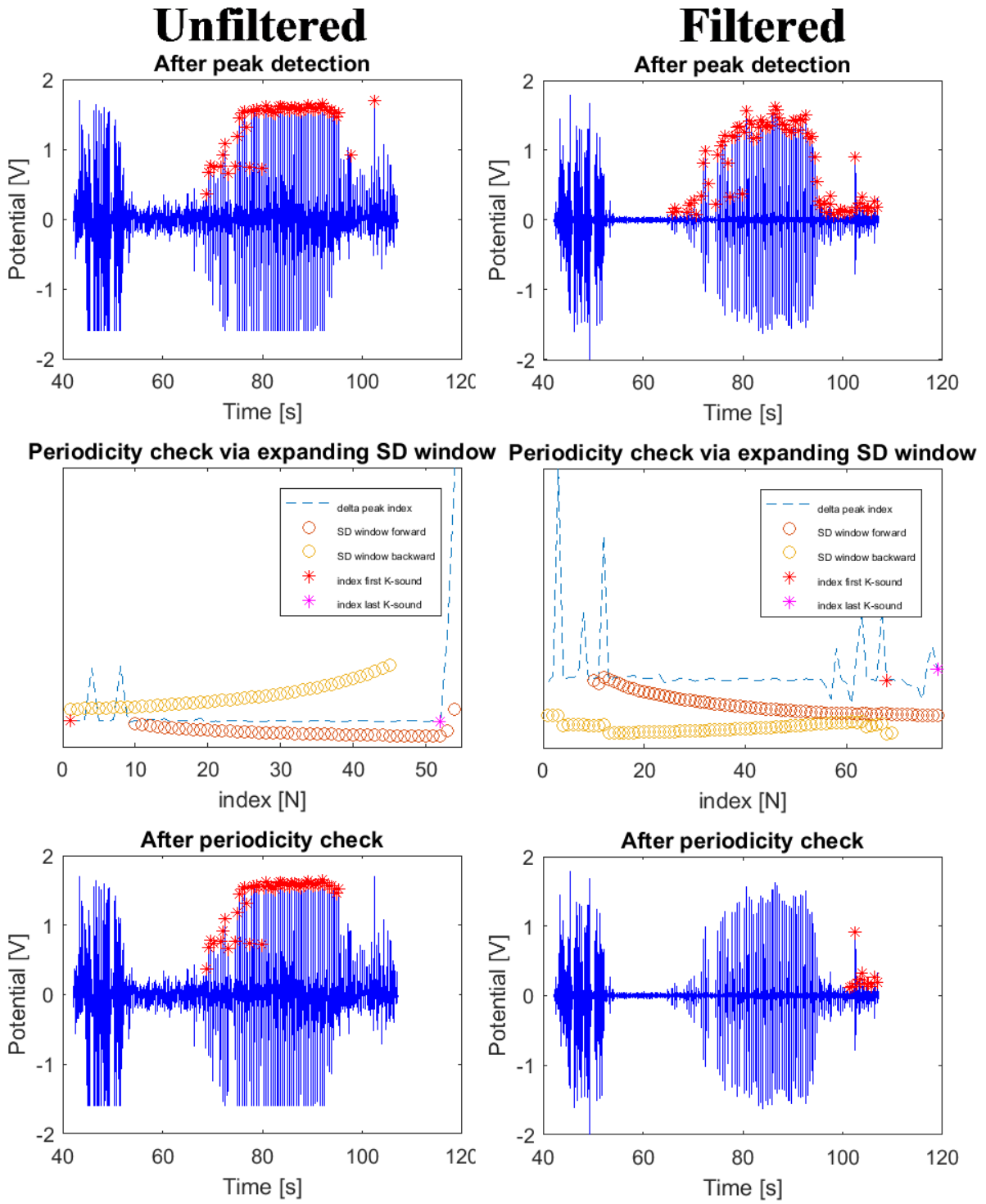


Figure 58: Unfiltered and filtered signals before and after peak detection and periodicity check, obtained whilst test person C was cycling at a load of 200 Watt

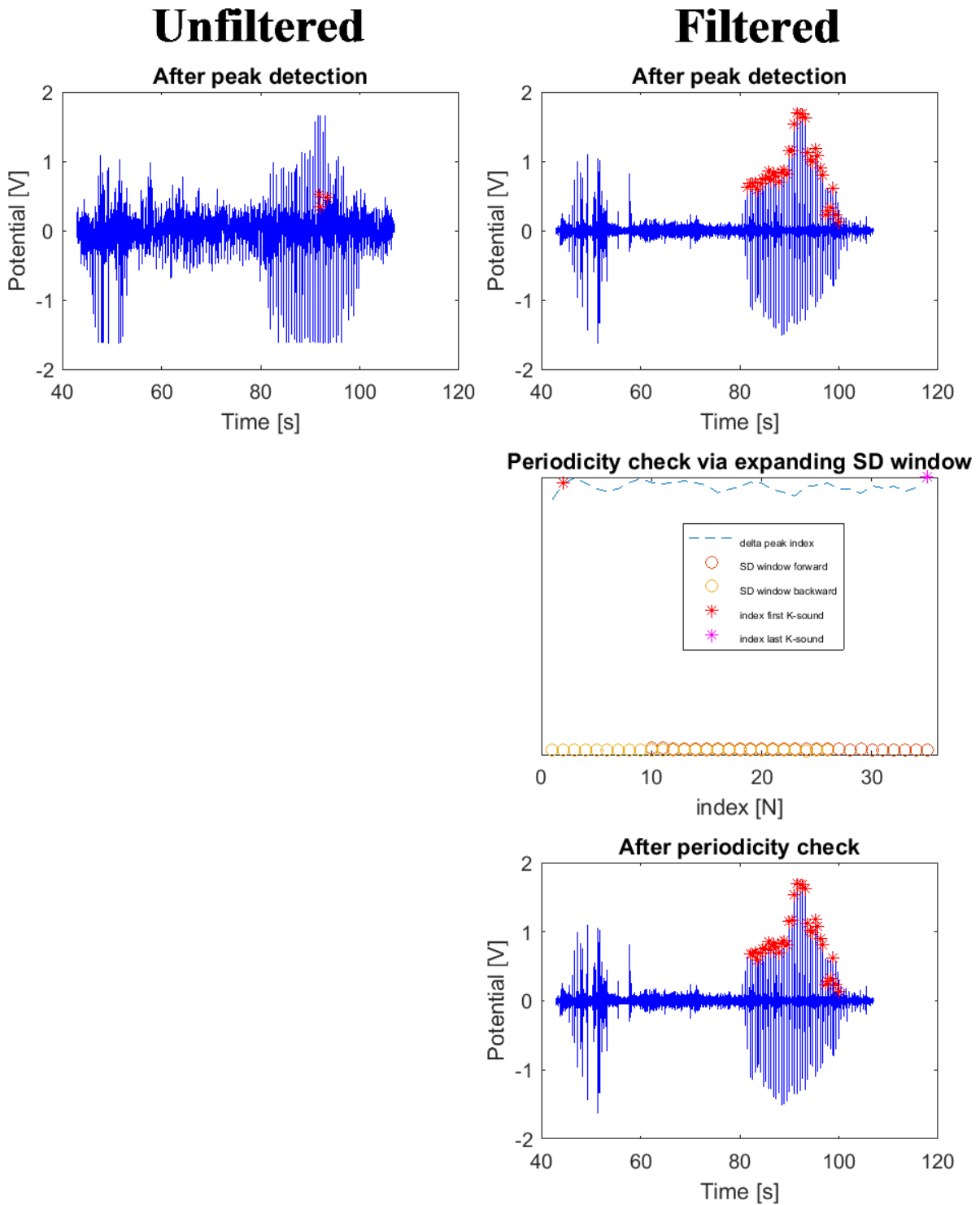


Figure 59: Unfiltered and filtered signals before and after peak detection and periodicity check, obtained whilst test person A was cycling at a load of 50 during recovery. Note that in the unfiltered situation only three peaks are detected, which make the periodicity check fail due to the assumption that the minimum amount of K-sounds is 9.

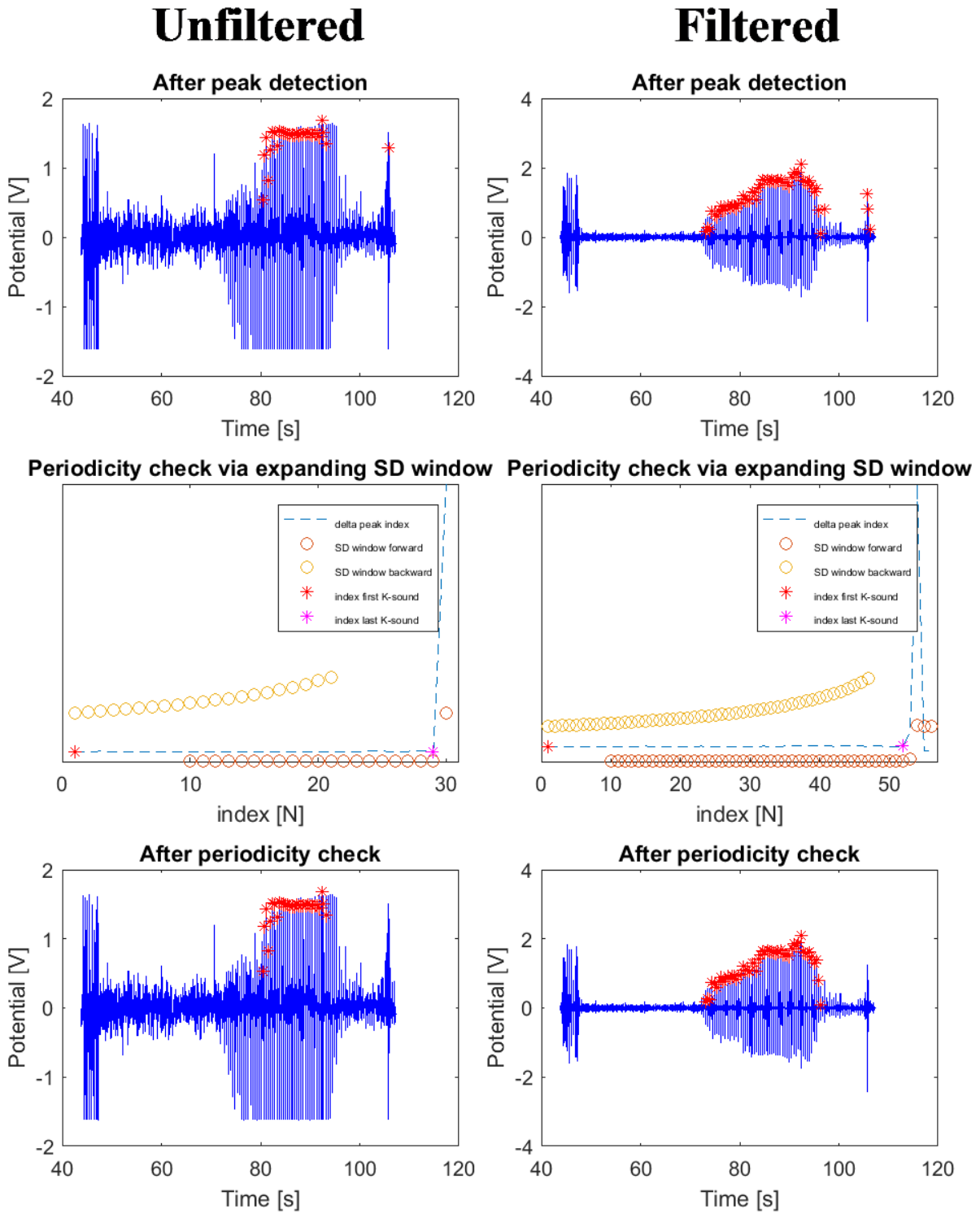


Figure 60: Unfiltered and filtered signals before and after peak detection and periodicity check, obtained whilst test person B cycling at a load of 50 Watt during recovery

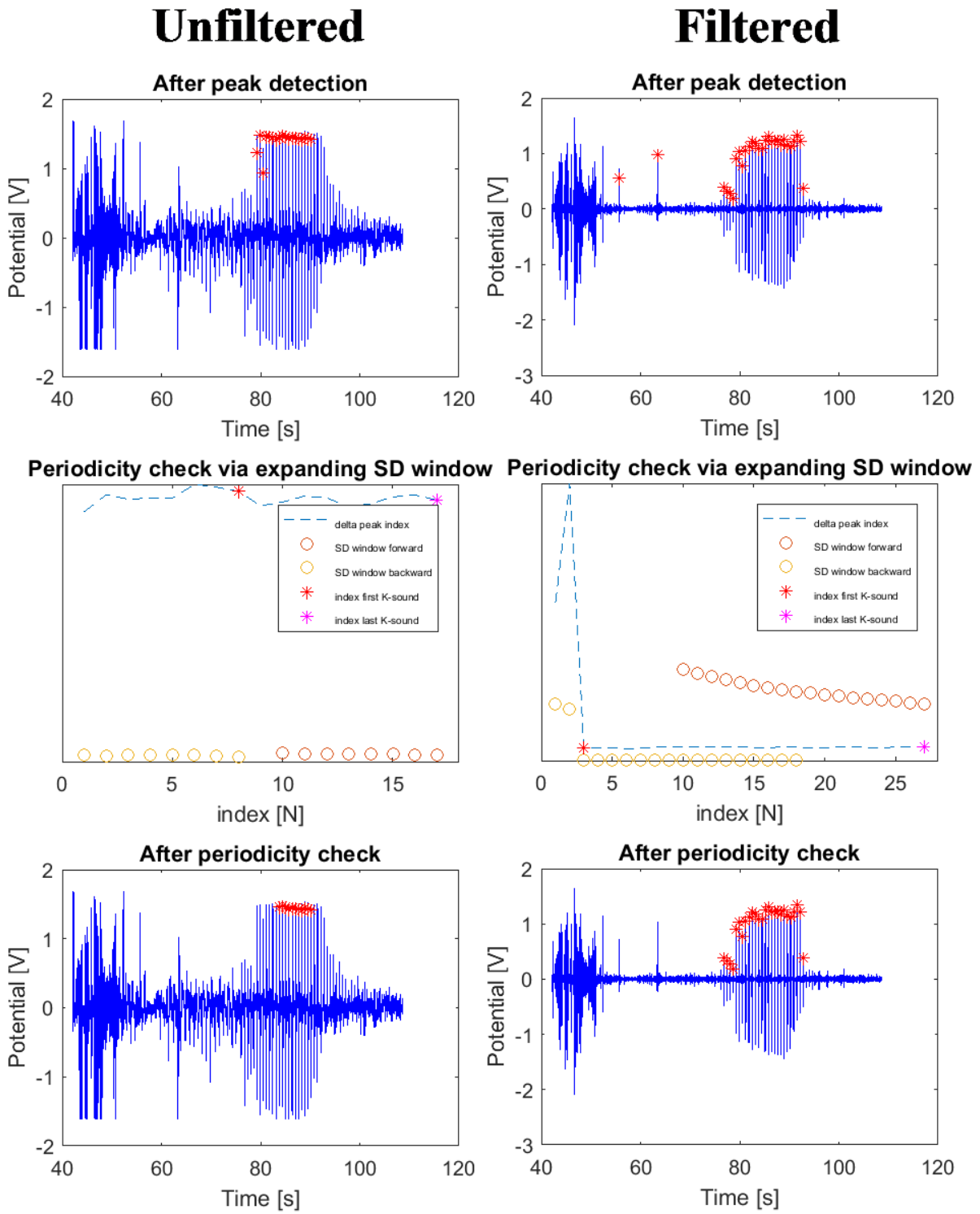


Figure 61: Unfiltered and filtered signals before and after peak detection and periodicity check, obtained whilst test person C was cycling at a load of 50 Watt during recovery

APPENDIX H

DAQ SIGNALS

Although the DAQ was validated on a component level, the system as a whole was unstable. The first problem encountered was the skipping of data, depicted in Figure 62. The cause was determined to be an interrupt from the library used on the Teensy microcontroller which controlled the onboard ADC [62]. The problem was solved by writing an interrupt based program for controlling the ADC so that no interrupts from the library could stop the data logging.

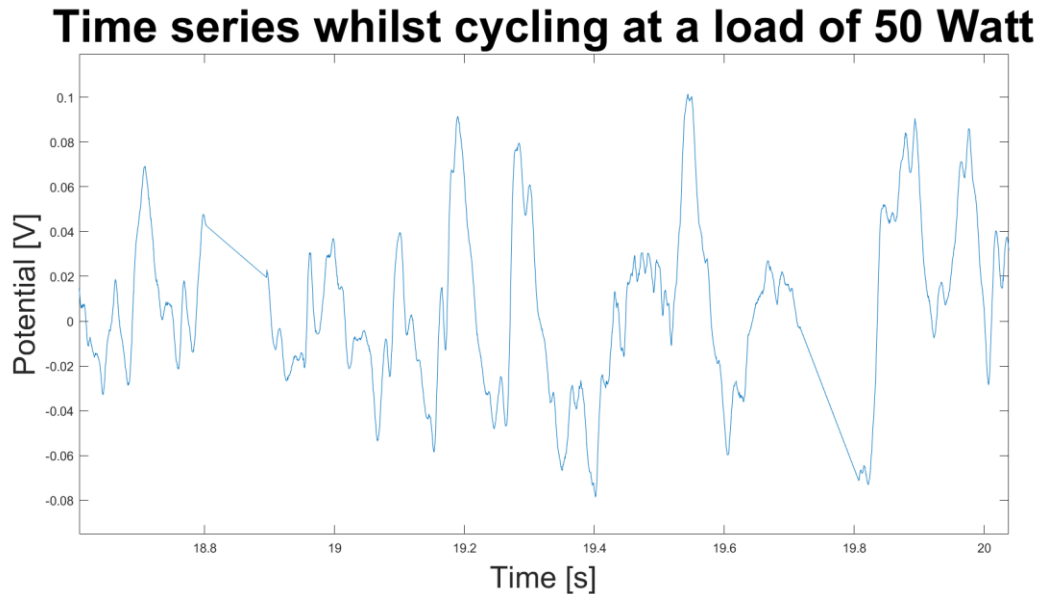


Figure 62: Time series whilst cycling at a load of 50 Watt with data skipping

A second problem encountered with the DAQ was a high frequent signal appearing in some measurements. This phenomenon is depicted in Figure 63 and observed appeared as random intervals and periods. The high frequent noise was determined comprise mostly of frequencies in the range between 830 and 1015 Hz. However, I was unable to reproduce the phenomenon, making it difficult to find a cause. The problem occurred less frequent than the previous problem, in some stress tests it did not occur at al. Due to time restrictions, only datasets were used that did not contain this high frequency, leading to a small sample size.

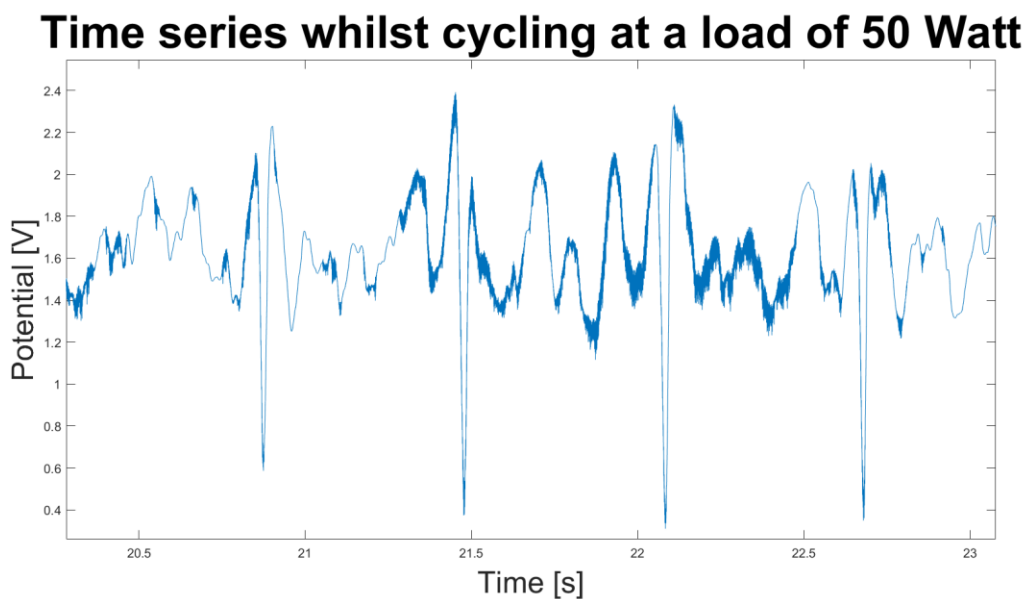


Figure 63: Time series whilst cycling at a load of 50 Watt with high frequent noise